

Universidade do Minho

Escola de Engenharia

João Ricardo Cerqueira Pinto

**Production of Cellulose-Binding Domains by
Proteolysis; Studies on the Adsorption and
Modification of Cellulose Fibres**

Tese de Doutoramento
Doutoramento em Engenharia Química e Biológica

Trabalho efectuado sob a orientação dos
Doutor Miguel Gama
Professor Doutor Manuel Mota

Autor João Ricardo Cerqueira Pinto

e-mail joaoricardo@yahoo.com

Telf. +351 253604400

BI 10399488

Título da tese

Production of Cellulose-Binding Domains by Proteolysis; Studies on the Adsorption and Modification of Cellulose Fibres

Orientadores

Doutor Miguel Gama

Professor Doutor Manuel Mota

Ano de conclusão 2006

Doutoramento em Engenharia Química e Biológica

É AUTORIZADA A REPRODUÇÃO PARCIAL DESTA TESE, APENAS PARA EFEITOS DE INVESTIGAÇÃO, MEDIANTE DECLARAÇÃO ESCRITA DO INTERESSADO, QUE A TAL SE COMPROMETE.

Universidade do Minho, 3 de Novembro de 2006

Agradecimentos

Gostaria de agradecer em primeiro lugar ao meu orientador, Doutor Miguel Gama, por todo o apoio e paciência durante a execução experimental deste trabalho, assim como durante as diversas correcções dos artigos e desta tese.

Ao Professor Doutor Manuel Mota pelo apoio e correcções pertinentes do texto dos diversos artigos.

A todas as pessoas do Departamento de Ciências e Tecnologias do Papel, em particular à Professora Ana Paula Duarte, por toda a ajuda e apoio disponibilizados durante as minhas estadias na Covilhã.

À Eng^a Teresa Ferrete e aos técnicos do laboratório de análise da Portucel Viana, pela disponibilidade e apoio dados ao trabalho aí efectuado.

A todos os meus amigos que, de uma forma ou de outra, contribuíram para a realização desta tese.

A la Jacqueline que, con todo su apoyo, cariño y amor, me ayudó a realizar más esta etapa de mi vida.

À Fundação para a Ciência e Tecnologia (FCT) pelo apoio financeiro através da bolsa de investigação SFRH/BD/6934/2001.

Abstract

Most cellulose degrading enzymes are composed of modular structures. In the case of fungi, cellulases are formed by a catalytic domain (CD) and by a cellulose-binding domain (CBD), interconnected through a highly glycosylated protein linker. These enzymes are used for paper production, either to allow a more efficient refinement or to improve the paper sheet production.

This work aimed at implementing a procedure to produce significant amounts of purified CBDs. The purified CBDs coating of the fibers surface was assessed by a method based on fluorescence microscopy. Finally, the application of CBDs in paper production was evaluated.

The CBDs production was achieved by proteolysis, with papain, of the commercial preparation Celluclast[®] (cellulases from *Trichoderma reesei*). Afterwards, the CBDs were separated by ultrafiltration and further purified by ion exchange chromatography. The obtained CBDs is part of cellobiohydrolase I, as demonstrated by N-terminal peptide sequencing and MALDI-TOF. The isolated proteins kept the highly glycosylated peptide linker, as verified by sugar analysis, that demonstrated the existence of 30% (w/w) of carbohydrates, most of which mannose (85%). It was shown that these CBDs, as expected, have a high cellulose affinity, desorbing very slowly. Using CBDs conjugated with fluorescein isothiocyanate (FITC), it was verified that the adsorption is not uniform, being higher on the fibre extremities and defects, due either to a higher specific surface area (amorphous regions) or to a higher affinity of CBDs to these regions.

To quantify the CBDs coating of the fibres' surface, a MATLAB program was developed. This program allows for the correlation between the fluorescence signal intensity produced by the adsorbed CBD-FITC, and its surface concentration. The FITC photobleaching was verified to be only significant for CBD-FITC in solution, being negligible for the protein adsorbed on cellulose. The adsorption of CBDs to cellulose films (made from cellulose acetate), in saturation concentrations, resulted in the equivalent to 1.6 to 2 layer of protein. In the case of cellulose fibres (Whatman CF11), this value increased to the equivalent of roughly 4 layers. These high values are due to the protein penetration into the fibers, as was demonstrated by confocal microscopy and immunolabelling with colloidal gold and transmission electron microscopy, but also to the increased surface irregularities of Whatman CF11 that would increase the surface area.

The CBD adsorption onto primary and secondary fibres implied a reduction of the Schopper-Riegler index (increase in water flow between the fibres) and an increase of both the water retention value (WRV) and air permeability of the handsheets. The strength properties did not suffer a significant variation with adsorbed CBDs, except for the non-refined virgin fibres. In this case, a slight improvement was observed, probably due to the lower surface area. The effect of CBDs on the surface properties was analysed by measuring the ZETA-potencial and contact angles. The adsorption of CBDs chemically conjugated to lysozyme (protein with a positive charge) did not significantly change the papersheet properties. The ZETA-potencial was only significantly altered in the case of low surface area fibres (non-refined virgin fibres), as noticed by the reduction of the fibres negative charge. As expected, the variation was more significant with lysozyme conjugated CBD. This higher variation was also confirmed by contact angles measurement. The presence of conjugates made the cellulose film hydrophobic, due to the reduction of the negative polar component of the fibres.

Resumo

As enzimas que degradam a celulose são maioritariamente constituídas por estruturas modulares. No caso dos fungos, as celulasas são constituídas por um domínio catalítico (CD) e um domínio de ligação à celulose (CBD), interligados por uma cadeia proteica altamente glicosilada. As enzimas têm sido amplamente utilizadas na produção de papel, para permitir uma mais eficiente refinação, e melhorar a formação das folhas de papel.

Neste trabalho pretendeu-se inicialmente implementar um processo laboratorial de produção de CBDs, em larga escala (grama). Para quantificar a taxa de cobertura dos CBDs sobre a superfície das fibras de celulose, foi desenvolvido um método baseado em microscopia de fluorescência. Posteriormente, avaliou-se o potencial de aplicação dos CBDs na produção de papel.

A produção de CBDs foi realizada por hidrólise, usando proteases (papaina), do preparado comercial Celluclast[®] (celulasas do fungo *Trichoderma reesei*). Posteriormente, os CBDs foram separados por ultrafiltração e posteriormente purificados numa coluna de troca iónica. Os CBDs isolados pertencem à enzima celobiohidrolase I, como foi demonstrado por sequenciação peptídica N-terminal e MALDI-TOF. A proteína purificada inclui a região de ligação altamente glicosilada, como foi verificado pela análise dos açúcares totais, que demonstrou a existência de 30% (m/m) de carboidratos nas proteínas, em particular de manose (85%). Verificou-se que estes CBDs possuem, como esperado, uma elevada afinidade por celulose. A adsorção a fibras de celulose pura (Whatman CF11) não é irreversível, sendo a desorção muito lenta. Recorrendo à conjugação dos CBDs com isotiocianato de fluoresceína (FITC) verificou-se que a adsorção nas fibras não é uniforme, sendo superior nas extremidades e irregularidades das fibras, devido a um aumento da área superficial disponível para os CBDs (regiões amorfas) ou a uma maior afinidade para estes locais.

Para quantificar a taxa de cobertura das fibras pelos CBDs, foi desenvolvido um método baseado em microscopia de fluorescência. Este método passou pelo desenvolvimento de um programa em MATLAB para calibrar o sinal produzido pelos CBDs, permitindo efectuar uma correspondência entre o sinal produzido por fibras com CBD-FITC e a densidade de proteína na superfície das fibras. No desenvolvimento do método tomou-se em consideração a fotoinstabilidade (*photobleaching*) do FITC, tendo-se verificado que este apenas é significativo para CBD-FITC em solução, mas negligenciável quando adsorvido em celulose. Os CBDs adsorvidos em filmes de celulose (preparados a partir de acetato de celulose), em concentrações

saturantes, corresponderam a um revestimento equivalente a 1.6 a 2 camadas de proteína. No caso das fibras de celulose, estes valores aumentaram para o equivalente a cerca de 4 camadas, no caso da Whatman CF11. Estes valores elevados resultam da penetração das proteínas no interior das fibras, como pôde ser demonstrado tanto por microscopia confocal como por microscopia electrónica de transmissão (por imunomarcção com ouro coloidal). A irregularidade da superfície das fibras poderá também aumentar a taxa de cobertura dos CBDs.

A adsorção de CBD a fibras de papel, primárias e secundárias, implica uma diminuição do índice de Shopper-Riegler (aumento do escoamento de água das fibras), assim como um aumento do índice de retenção de água (WRV) e da permeabilidade à passagem de ar nas folhas de papel produzidas no laboratório. As propriedades físicas das folhas não sofreram alterações significativas com a adsorção dos CBDs, excepto no caso das fibras virgens não refinadas. Neste caso, os parâmetros mecânicos aumentaram ligeiramente, devido muito provavelmente à menor área superficial destas fibras e logo a uma maior influência dos CBDs adsorvidos. A adsorção de CBDs conjugados com lisozima (proteína com carga positiva) não modificou significativamente as propriedades das folhas. O efeito dos CBDs nas propriedades de superfície das fibras foi analisado através da medição do potencial ZETA e dos ângulos de contacto. O potencial ZETA só variou significativamente no caso das fibras com menor área superficial (fibras virgens não refinadas), traduzindo-se numa diminuição da carga negativa com a adsorção dos CBDs. Esta variação foi também observada com partículas de celulose pura, nos casos em que se usou uma elevada carga proteica. Como esperado, a variação foi mais significativa quando foram utilizados os CBDs conjugados com lisozima. Esta maior variação também foi observada nos ângulos de contacto, onde a presença dos conjugados tornou o filme de celulose hidrofóbico, devido à diminuição do carácter polar negativo das fibras.

Table of Contents

LIST OF ABBREVIATIONS	X
LIST OF FIGURES.....	XI
LIST OF GENERAL NOMENCLATURE.....	XVI
LIST OF TABLES	XVII
INTRODUCTION.....	1
1. CELLULOSE	1
2. CELLULOLYTIC ENZYMES	2
3. CELLULOSE BINDING DOMAINS.....	9
RESULTS OVERVIEW AND CONCLUSIONS.....	16
<i>Production of CBD by proteolysis</i>	<i>16</i>
<i>Studies using conjugates CBD-FITC</i>	<i>17</i>
<i>Studies of CBDs on fibre modification.....</i>	<i>18</i>
<i>Conclusions.....</i>	<i>20</i>
MANUSCRIPTS	31
M1. LARGE SCALE PRODUCTION OF CELLULOSE-BINDING DOMAINS. ADSORPTION STUDIES USING CBD-FITC CONJUGATES	32
<i>Abstract</i>	<i>32</i>
<i>Introduction.....</i>	<i>33</i>
<i>Materials and Methods.....</i>	<i>34</i>
<i>Results and Discussion.....</i>	<i>37</i>
<i>Conclusions</i>	<i>42</i>
<i>Acknowledgements</i>	<i>42</i>
<i>Bibliography.....</i>	<i>43</i>
<i>Figures</i>	<i>47</i>
M2. DEVELOPMENT OF A METHOD USING IMAGE ANALYSIS AND CBD-FITC CONJUGATES FOR THE MEASUREMENT OF CBDs ADSORBED ONTO CELLULOSE FIBERS	54
<i>Abstract</i>	<i>54</i>
<i>Introduction.....</i>	<i>55</i>
<i>Materials and Methods.....</i>	<i>56</i>

<i>Results and Discussion</i>	60
<i>Conclusion</i>	63
<i>Acknowledgments</i>	63
<i>References</i>	63
<i>Figures</i>	66
<i>Tables</i>	73
M3. QUANTIFICATION OF THE CBD-FITC CONJUGATES SURFACE COATING ON CELLULOSE FIBERS 74	
<i>Abstract</i>	75
<i>Background</i>	75
<i>Results and Discussion</i>	76
<i>Conclusions</i>	78
<i>Methods</i>	78
<i>Authors' contributions</i>	81
<i>Acknowledgements</i>	82
<i>References</i>	82
<i>Figures</i>	85
M4. EFFECT OF CELLULOSE-BINDING DOMAINS ON PULP PAPER PROPERTIES.....	90
<i>Abstract</i>	90
<i>Introduction</i>	91
<i>Materials and Methods</i>	92
<i>Results and Discussion</i>	94
<i>Conclusion</i>	98
<i>Acknowledgments</i>	98
<i>Bibliography</i>	98
<i>Figures</i>	101
<i>Tables</i>	104

List of Abbreviations

AFM	Atomic force microscopy
BET	Brunauer-Emmett-Teller equation
BSA	Bovine serum albumin
CBD	Cellulose-binding domain
CBH	Cellobiohydrolase
CBHI	Cellobiohydrolase I
CBHII	Cellobiohydrolase II
CBM	Cellulose-binding module
CD	Catalytic domain
DMSO	Dimethyl sulfoxide
DNS	Dinitro-salicylic acid
EG	Endoglucanase
FITC	Fluorescein isothiocyanate
FPU	Filter paper units
GC	Gas chromatography
HEPES	4-(2-hydroxyethyl)-1-piperazineethanesulfonic acid
HSAB	N-hydroxysuccinimidyl 4-azidobenzoate
IEC	Ion exchange column
MALDI-TOF	Matrix-assisted laser desorption/ionisation-time of flight
PBS	Phosphate Buffered Saline
pI	Isoelectric point
TC	Terminal complexes
TEM	Transmission Electron Microscopy
TFMS	Trifluoromethanesulfonic acid
UV	Ultraviolet radiation

List of Figures

Figure 1. Detail of a cellulose chain, highlighting the repetitive unit cellobiose (<i>n</i>).	1
Figure 2. Structure of the rosette terminal complexes, and microfibre formation (adapted from Doblin <i>et al.</i> , 2002).	2
Figure 3. Cell wall structure, where microfibrils and hemicellulose chains may be observed mixed with lignin (adapted from Bidlack <i>et al.</i> , 1992).	3
Figure 4. Scheme showing the two mechanisms of enzymatic hydrolysis (Schulein, 2000; Sinnott, 1990).	5
Figure 5. Simplified scheme of the <i>Clostridium thermocellum</i> cellulosome, interacting with the cell surface. <i>CBM</i> – Cellulose Binding Module (adapted from Shoham <i>et al.</i> , 1999).	6
Figure 6. Schematic representation of the cellulose fibre organization, with crystalline and amorphous areas. The enzyme CBHI (Cel7A) act on the fibre from the reducing end (symbolized as full circles in the figure, ‘R’), while CBHII (Cel6A) acts from the non-reducing ends (open circles, ‘NR’). Endoglucanases (EG) act on the middle of the cellulose chains, leading to an increase of the chain ends, wherefrom the CBHs may act (Teeri, 1997).	7
Figure 7. Active sites found in cellulases: a – cleft (endoglucanase from <i>Trichoderma fusca</i>); b – tunnel (cellobiohydrolase from <i>Trichoderma reesei</i>). The catalytic residues are shown in orange (adapted from Davies and Henrissat, 1995).	8
Figure 8. Structural models of CBDs from cellobiohydrolase I (left) and endoglucanase I (right), from <i>Trichoderma reesei</i> . Cel7A has three β -sheets shown by the arrows. The tyrosine (a) and tryptophan (b) residues define an almost plane surface on the CBDs (adapted from Carrard and Linder, 1999, and Mattinen <i>et al.</i> , 1998).	12
Figure 9. Perspective of the structures representative of the CBDs from EGI (left) and CBHI (right). The aromatic residues aligned at the inferior face are highlighted (adapted from Mattinen <i>et al.</i> , 1998).	14

Figure 10. Model of the interaction between the CBDs from cellobiohydrolase I (Cel7A) and endoglucanase I (Cel7B) and the glucose residues present in cellulosic fibres (adapted from Mattinen <i>et al.</i> , 1997).....	15
Figure M1.1. Electropherogram of Celluclast (Cell.), hydrolyzed Celluclast (Hyd. Cell.) and Cellulose-Binding Domains (CBD). Both time and signal are normalized.....	47
Figure M1.2. Electropherogram of Celluclast hydrolyzed with different amounts of papain by protein weight (the dilution factor of the commercial enzyme is shown). Time is normalized.	48
Figure M1.3. MALDI-TOF analysis of the purified CBD peptides.....	48
Figure M1.4. Fluorescence Spectrums of CBD after ultra filtration and the subsequent Ion Exchange purification. Signals are normalized to the highest value obtained on each measurement.....	49
Figure M1.5. Chromatogram of the first amino acid detected on the N-terminal peptide sequencing of the purified CBD. This chromatogram reveals that the isolated CBD is rather pure.....	49
Figure M1.6. MALDI-TOF analysis of the deglycosylated CBD peptides. The heterogeneous peak observed in Figure 3 (8.43kDa) is replaced by a main peak at 5.84 kDa. The complete removal of the glycosidic fraction with TFMS leads to some proteolysis, several peaks not observed prior to TFMS treatment (nor when the treatment is performed under milder conditions) being detected (1700-4000Da).	50
Figure M1.7. Adsorption isotherm of CBDs purified by ion exchange chromatography.....	51
Figure M1.8. Fluorescence microscopy of Whatman CF11 (upper row) and Avicel (lower row) cellulose fibers treated with labeled CBDs, with different initial concentrations (0, 50, 100 and 300 µg/mL). In the control fibers (left column), as expected, no fluorescence was detected. The micrographs were obtained using the same exposure time.	51
Figure M1.9. Images of a mixture of treated and untreated CF11 cellulose fibers with labeled CBD, under fluorescent (first and third column) and bright field (second and	

fourth column) microscopy, with 400 milliseconds of exposure time, put in contact for 0, 24, 48, 98 and 192 hours.....	52
Figure M1.10. Comparison of the crystalline (top row) and phosphoric acid swollen (amorphous – bottom row) Whatman CF11 fibers, both treated with FITC-labeled CBD, at bright field (left) and fluorescent (right) microscopy. The probably amorphous sites of the microfibril (left side of the upper images) have attracted more FITC-labeled CBD.....	53
Figure M2.1. Values of fluorescence intensity (I_A) versus exposure time, obtained using a CBD-FITC concentration of $10.14 \times 10^{-13} \mu\text{mol}\cdot\text{mm}^{-2}$ (or $85.5 \mu\text{g}\cdot\text{mL}^{-1}$), and the corresponding non-linear regression fitting. Inset: photobleaching curve of a mono-exponential correlation, the model used in the calculation of I_A	66
Figure M2.2. Values of fluorescence intensity as a function of the CBD-FITC concentration.....	67
Figure M2.3. Intensity and sensitivity factors variation with CBD concentration for the studied capture times, obtained by averaging a 10×10 pixel area at the centre of each original images (continuous lines connect the values used for the calibration model). Legend: \diamond – Red channel; \blacksquare – Green channel; \blacktriangle – Blue channel.....	68
Figure M2.4. Calibration images obtained at capture time of 300 ms; each surface represents a different CBD-FITC concentration. The inset shows, as an example, the CBD concentration versus pixel intensity, obtained approximately at the center of the images.	69
Figure M2.5. Estimated CBD-FITC per unit area, for three different protein solutions volumes. The labeling classes (TL – top left; TR – top right; C – centre; BL – bottom left; BR – bottom right) refer to average values obtained at different selected regions in the image. The black line corresponds to the expected value. Duplicate values are shown for each volume used.....	70
Figure M2.6. Cellulose film images obtained, for 400 ms of exposure time, at 0 (a) and 20 seconds (b) of exposure to the fluorescence light. The black squares indicate the positions where the measurements were carried out.	70

- Figure M2.7. Images of cellulose films with adsorbed CBD-FITC: (a) and (c) correspond to grey scale images of the films, produced by the fluorescent light emitted by the CBD linked FITC; (b) and (d) correspond to the program treated images, where black color corresponds to $0 \mu\text{mol}\cdot\text{mm}^{-2}$ and white color to the maximum concentration used in the corresponding calibration procedure. 71
- Figure M2.8. Adsorption isotherm of CBD on Whatman CF11 fibers, for 2 hours contact. The line was obtained by nonlinear regression of the Langmuir isotherm, resulting in the constants: $CBD_{Max} = 2.42 \mu\text{mol}\cdot\text{g}^{-1}$ and $k_a = 0.209 \mu\text{M}^{-1}$. The grey circle corresponds to the equilibrium position of samples put in contact with an initial CBD concentration of $400 \mu\text{g}\cdot\text{mL}^{-1}$ 72
- Figure M2.9. AFM surface image of cellulose film, obtained in the air. The upper image corresponds to the *xx* side view. 72
- Figure M3.1. Portucel and Whatman CF11 fibres treated with CBD-FITC. The fibres treated with a concentration of $60 \mu\text{g}/\text{mL}$ (or $2 \text{ mg}_{\text{CBD}}/\text{g}_{\text{fibres}}$). The images were acquired with an exposure time of 600 ms. The white squares identify the areas selected for analysis. The more fluorescent parts (black regions on the analyzed images) are out of range (calibration shown elsewhere), and were therefore excluded from the analysis. 85
- Figure M3.2. Whatman CF11 images. The characteristic curled structure of the fibres (circle). 85
- Figure M3.3. Estimated surface concentration of adsorbed CBD. The estimated fraction of surface coverage is indicated in the figure bars. The values shown are based on the assumption that the protein is adsorbed on the external surface of the fibres only. The values are shown with 95% confidence intervals error bars. 86
- Figure M3.4. Images obtained by fluorescence microscopy of Whatman CF11, amorphous and Sigmacell 20 fibres. The images were obtained before – 1st and 3rd column – and after – 2nd and 4th column – the image analysis of fibres treated with a CBD-FITC concentration of $400 \mu\text{g}/\text{mL}$. The black areas on the treated images correspond to the fluorescence emission, which is higher than the one used in the calibration.

Fluorescence images acquired for 100 ms (CF11) and 80 ms (Amorphous and Sigmacell).....	87
Figure M3.5. Images from confocal microscopy. Three plans of a CF11 fibre are presented, as schematized in the right insertion of figure <i>c</i> . The insertions <i>d</i> , <i>e</i> and <i>f</i> correspond to the pixels intensity (256 grey levels) obtained at the position indicated by the line (white circle), at different depths. The adsorption conditions were 20 mg _{CBD} /g _{Fibre} , for 30 minutes of contact. Each image corresponds to an acquisition thickness of 1 µm.....	88
Figure M3.6. Electron microscopy image of immunolabeling of CBD-treated Whatman CF11 fibers.	89
Figure M4.1. Schopper-Riegler index obtained for the several paper fibers studied.....	101
Figure M4.2. Physical properties variation between the CBD treated and untreated (control), at three different beating revolutions (0, 1000 and 3000), of virgin (primary) fibers, with the respective confidence interval at 95%. The stars (*) indicates a statistic meaningful variation ($p < 0.05$).	101
Figure M4.3. Physical properties variation between the CBD treated and untreated (control), at three different beating revolutions (0, 1000 and 3000), of recycled (secondary) fibers, with the respective confidence interval at 95%. The stars (*) indicates a statistic meaningful variation ($p < 0.05$).	102
Figure M4.4. Size exclusion chromatography of the CBD-lysozyme conjugate and of a mixture of the two proteins.....	102
Figure M4.5. Adsorption, on Whatman CF11, of CBD in mixture or conjugated with lysozyme, using the same CBD to lysozyme molar ratio.....	103

List of Nomenclature

CBD_{Bound}	CBDs adsorbed to cellulose	($\mu\text{mol/g}$)
CBD_{Free}	Unbound CBDs	($\mu\text{mol/mL}$)
CBD_{Initial}	Initial CBDs concentration	($\mu\text{mol/mL}$)
CBD_{Max}	Maximum molar amount adsorbed	($\mu\text{mol/g}$)
CBD_{Unbound}	Unbound CBDs	($\mu\text{mol/mL}$)
f_R, f_G, f_B	Sensitivity factors for each RGB channel	(dimensionless)
I	Fluorescence intensity	(dimensionless)
I_0	Initial fluorescence intensity	(dimensionless)
I_A	Acquired fluorescence intensity	(dimensionless)
I_R, I_G, I_B	Intensity of each RGB channel	(dimensionless)
k_a	Adsorption equilibrium constant	(μM^{-1})
K_d	Photobleaching constant	(s^{-1})
m_{CF11}	Whatman CF11 quantity	(g)
$^{\circ}\text{SR}$	Schopper-Riegler degree	($^{\circ}\text{SR}$)
Q_{CBD}	Quantity of CBDs per unit area	(mol/mm^2)
t	Time	(s)
V_R	Total adsorption volume	(mL)
WRV	Water retention value	(g/g)

Greek Symbols

θ	Contact angle	($^{\circ}$)
$\Delta G_{\text{cvc}}^{\text{T}}$	Variation of the total free energy	(mJ/m^2)
γ^+, γ^-	Positive and negative surface tension components	(mJ/m^2)
γ^{LW}	Surface tension apolar component (Lifshitz-van der Waals interaction)	(mJ/m^2)

List of Tables

Table 1. Structural classification of cellulolytic enzymes (Bayer <i>et al.</i> , 1998; Coutinho and Henrissat, 1999; Henrissat and Davies, 1997; Rabinovich <i>et al.</i> , 2002).	4
Table M2.1. Sensitivity factor values for each channel, as a function of the capture time.....	73
Table M2.2. Values of the fluorescence intensity at 0 (I_0) and 20 seconds (I) of continuous exposure to fluorescence light and for the calculated photobleaching constant rate.....	73
Table M4.1. Water retention value (WRV) obtained for the fibers used (\pm confidence interval at 95%).....	104
Table M4.2. Permeability of papersheets obtained for the cellulose types used (\pm confidence interval at 95%).....	104
Table M4.3. Physical properties of the Portucel fibers without treatment (Blank) and CBD or conjugate treated (\pm confidence interval at 95%).....	105
Table M4.4. ZETA-potential measurements (mV), by streaming potential, of <i>Portucel</i> and Eucalyptus (two different refinement conditions) fibers, without treatment (Blank) and CBD or conjugate treated, and of Sigmacell fibers made by electrophoretic mobility (\pm confidence interval at 95%).	105
Table M4.5. Surface tension components (γ^{LW} , γ^+ and γ^- , mJ/m ²) and degree of hydrophobicity (ΔG_{cwc} , mJ/m ²) for cellulose fibers without treatment (Blank) and CBD or conjugate treated, obtained by contact angle. Examples of contact images of water drops are also shown. The protein concentration used are as referred in Table M4.4.....	106

INTRODUCTION

1. Cellulose

Cellulose is the most abundant polymer in nature: it is the main constituent of plants, where it plays a structural role, but is also present in bacteria, algae and even in animals (Kimura and Itoh, 2004; Tamai *et al.*, 2004). Cellulose is a material with properties convenient for quite different applications and industries (Belgacem *et al.*, 1995): excellent mechanical properties, availability in huge amounts, both from vegetable and microbial sources, varied morphology, geometry and surface properties, recycling possibility, low cost.

The fibres are constituted by linear chains of anhydrous glucose, linked by covalent β -1,4 bonds (Srisodsuk, 1994). The glucose residues are twisted by 180° in the polymeric chain (Figure 1), taking different conformations. The repetitive unit is the dimer cellobiose, and not glucose as in starch.

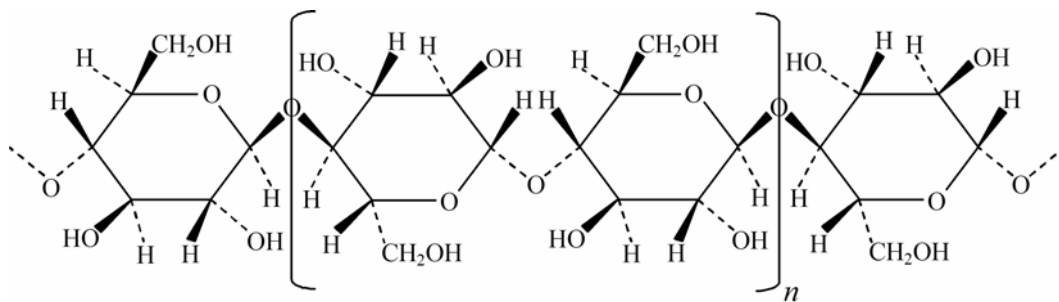


Figure 1. Detail of a cellulose chain, highlighting the repetitive unit cellobiose (n).

The cellulose chains are formed at the plasmatic membrane, through the addition of UDP-Glucose units by enzymatic structures called Terminal Complexes, TC (Kimura *et al.*, 1999). These complexes are constituted by linear aggregates, in the case of bacteria and algae, or rosettes, in the case of vascular plants (Brown *et al.*, 1996; Kimura *et al.*, 1999). The rosettes (complexes *CelS*) are formed by aggregates of the polypeptide *CesA* (Figure 2), each producing a polymer with about 2000 to 25000 glucose units (Doblin *et al.*, 2002). Upon its formation, the chains gather to form a cellulose microfibril, stabilized by intermolecular hydrogen bonds.

Cellulose chains type I are then formed, with parallel glucose chains. This kind of structure is meta-stable, that is, it is not the most favourable thermodynamically. Cellulose type II – the more stable one – displays cellulose chains with anti-parallel orientation. Type I is much more frequent than type II, and is sub-divided in two kinds of crystalline structures, I_α e I_β , distinguished by the pattern of intermolecular hydrogen bonds (O'Sullivan, 1997). These two kinds of cellulose are found, in nature, in different ratios, with I_α predominant in the more primate plants and I_β more commo in superior plants. The rare animal cellulose belongs also to the second kind. There are another 3 kinds of cellulose structure (III, IV e V) but these are produced only by chemical processes, and are not found in nature.

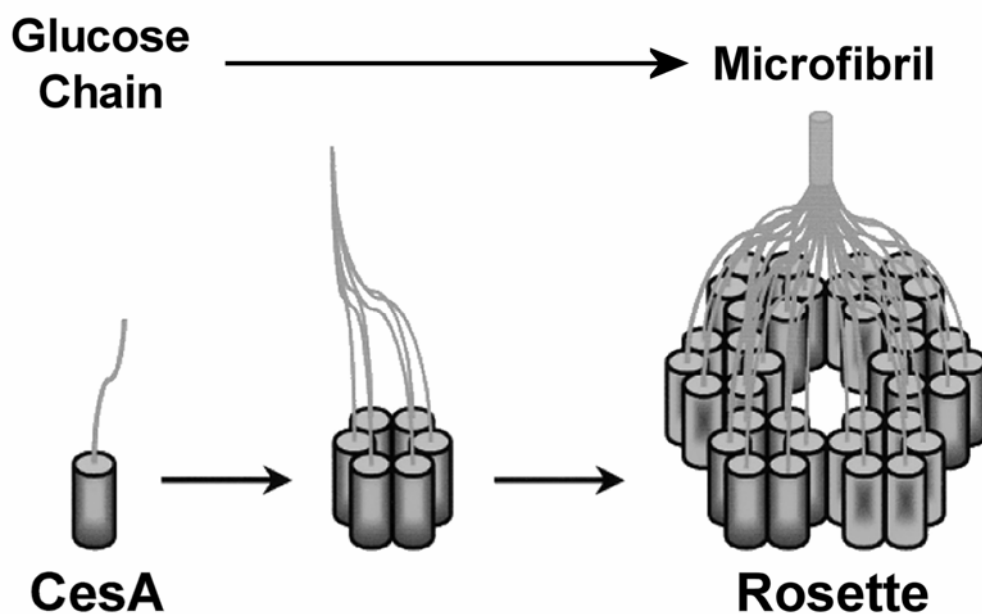


Figure 2. Structure of the rosette terminal complexes, and microfibre formation (adapted from Doblin *et al.*, 2002).

The cellulose microfibrils interact and associate, giving rise either to highly crystalline regions as well as to more amorphous ones. Associated to lignin and hemicellulose (Figure 3), complex super-structures such as fibres, cell walls and pellicles are formed (Bayer *et al.*, 1998).

2. Cellulolytic enzymes

Due to the cellulose structural complexity, microorganisms developed different strategies for its breakdown and utilization as a carbon source. Various enzymes are produced exhibiting different kinds of activity, all necessary due the heterogeneous physical properties of cellulose,

as well as to its mixture with other polymers in the cell wall. These enzymes are, namely, cellobiohydrolases (CBH), endoglucanases (EG), xylanases, cellodextrinases, β -glucosidases, (Warren, 1996).

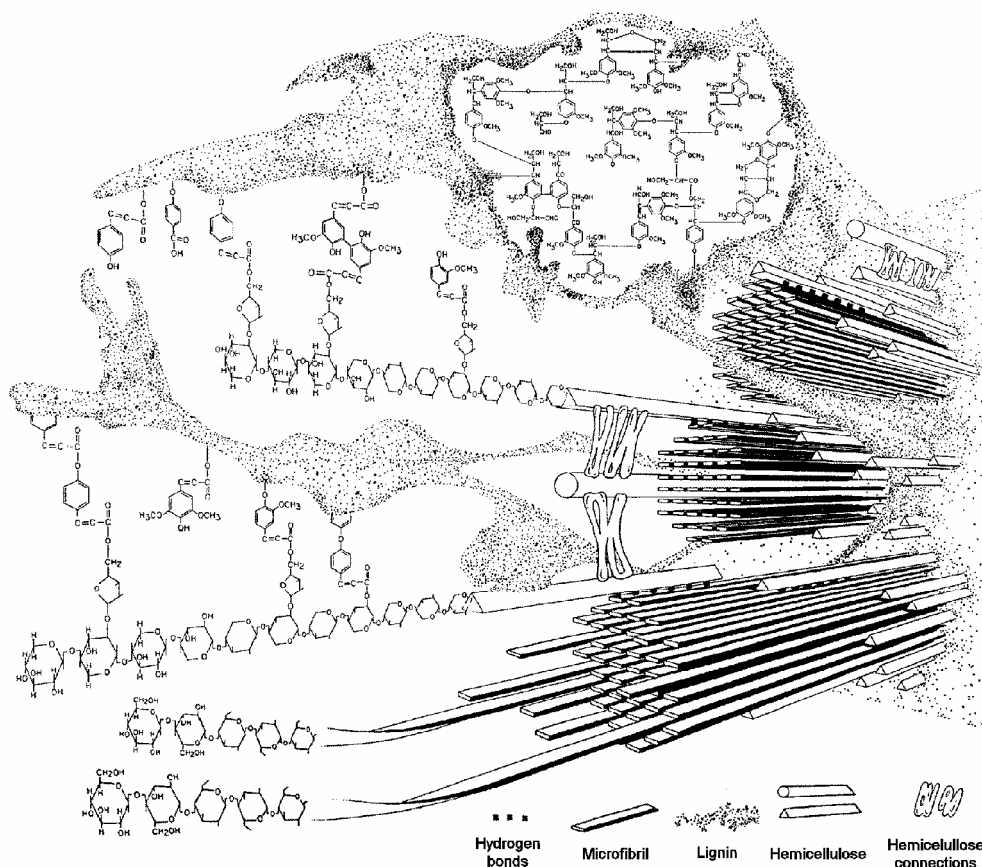


Figure 3. Cell wall structure, where microfibrils and hemicellulose chains may be observed mixed with lignin (adapted from Bidlack *et al.*, 1992).

Cellulases are classified in 14 families (see Table 1), among more than 100 families of glycosyl-hydrolases (Henrissat and Davies, 1997; <http://www.cazy.org/CAZY/>). This classification is proposed according to the homology of aminoacids found in the catalytic domains, following the principle that the sequence homology reflects the conservation of the structure and of the catalytic mechanism. Some of these families are gathered in clusters, based upon the conservation of the three-dimensional structure and upon the conservation of the relative spatial position of the catalytic residues.

Table 1. Structural classification of cellulolytic enzymes (Bayer *et al.*, 1998; Coutinho and Henrissat, 1999; Henrissat and Davies, 1997; Rabinovich *et al.*, 2002).

Family	Cluster	Structure	Enzyme(s)	Taxonomic distribution	Mechanism
5	GHA	$(\beta/\alpha)_8$	Mostly endoglucanases	Bacteria and fungae	Retention
6	–	<i>Distorted (β/α) barrel</i>	Endoglucanases and cellobiohydrolases	Bacteria and fungae	Inversion
7	GHB	β -jelly	Endoglucanases and cellobiohydrolases	Fungae	Retention
8	GHM	$(\alpha/\alpha)_6$	Mostly endoglucanases	Bacteria	Inversion
9	–	$(\alpha/\alpha)_6$	Mostly endoglucanases	Bacteria and fungae	Inversion
10	GHA	$(\beta/\alpha)_8$	Mostly xylanases	Bacteria and fungae	Retention
12	GHC	β -jelly	Endoglucanases	Bacteria and fungae	Retention
26	GHA	$(\beta/\alpha)_8$	Mostly endo-1,4- β -mannosidases	Bacteria	Retention
44	–	–	Endoglucanases	Bacteria	Inversion
45	–	β barrel	Endoglucanases	Bacteria and fungae	Inversion
48	–	$(\alpha/\alpha)_6$	Endoglucanases and cellobiohidrolases	Bacteria	Inversion
51	GHA	$(\beta/\alpha)_8$	Endoglucanases and arabinofuranosidases	Bacteria and fungae	Retention
61	–	–	Endoglucanases	Fungae	–
74	–	<i>7-fold β-propeller</i>	Endoglucanases	Bacteria and fungae	Inversion

The cellulolytic mechanism of hydrolysis implies the retention or the inversion of the anomeric configuration (see Figure 4). In the first case, two carboxylic groups, one charged (the

nucleophile) and the other protonated (acid-base catalyst), with the formation of a covalent intermediary, catalyse the hydrolysis with the retention of the anomeric centre. The inverting enzymes have also two carboxylic groups, one alkaline and the other acid, promoting the direct hydrolysis.

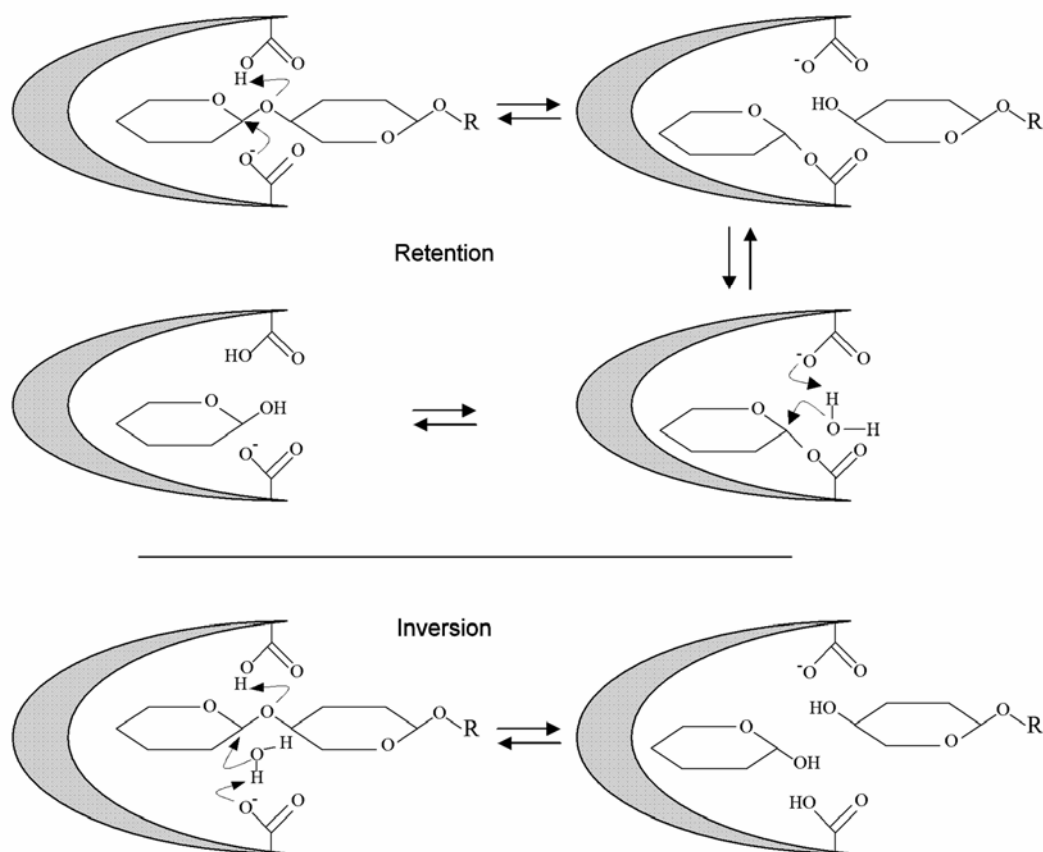


Figure 4. Scheme showing the two mechanisms of enzymatic hydrolysis (Schulein, 2000; Sinnott, 1990).

Microorganisms adopt fundamentally two strategies to breakdown cellulose: the aerobic ones secrete monomeric enzymes and the anaerobic produce enzymatic complexes called cellulossomes (Bayer *et al.*, 2004; Shoham *et al.*, 1999). These structures include, generally, a structure-skeleton (*scaffoldin* or cellulossome integrating protein, *CipA*), which incorporates, at least, one cellulose binding domain (CBD), various domains with enzyme affinity (*cohesin*) and various *dockerin* domains (Belaich *et al.*, 1997; Kruus *et al.*, 1995; Shimon *et al.*, 2000; Shoham *et al.*, 1999). The *dockerin* domain interact with a *cohesin* present in the surface of the cell, as to position the cellulossome next to the cell membrane (Bayer *et al.*, 1985). The enzymes incorporate into the *scaffoldin* through *cohesin-dockerin* interactions (Figure 5). Although the

cellulosomes are, generically, intimately connected with the cell-walls, cases are where the microorganism segregate the complexes into the culture medium (Ponpium *et al.*, 2000).

The fact that cellulosomes are typically expressed by anaerobic microorganisms may be metabolically advantageous. Being positioned close to the cell surface, there is a higher absorption efficacy of the degradation products (Shoham *et al.*, 1999). Another advantage may be that, this way, cells adsorb all of the degradation products, that otherwise would also be used by other cells. On the other hand, the close proximity of enzymes and cells allow for a better control of the enzymatic activity (by inhibition), such that the substrate flow would be proportional to the cell metabolic needs, and therefore allowing a better degradation efficacy (Boisset *et al.*, 1999).

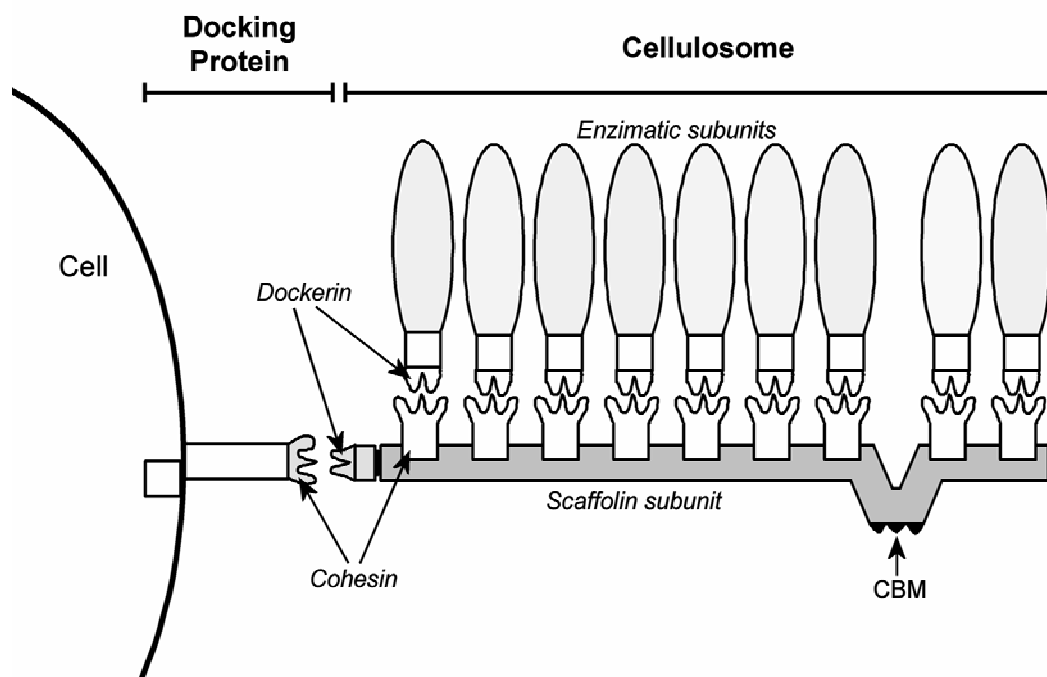


Figure 5. Simplified scheme of the *Clostridium thermocellum* cellulosome, interacting with the cell surface. *CBM* – Cellulose Binding Module (adapted from Shoham *et al.*, 1999).

Cellulases are sub-divided in two groups, endo- and exo-, according to the type of reaction (Teeri, 1997). Endoglucanases (EG) are enzymes that hydrolyse the glycosidic bond indiscriminately along the cellulose chain. In turn, exoglucanases act from the chain end (Figure 6). In the specific case of crystalline cellulose, to make possible an effective cellulose degradation, it is mandatory the presence of a mixture of both kinds of enzyme. The cellulose fibres are long chains and endoglucanases, by creating new chain ends, promote the action of

exoglucanases. Various authors (Irwin *et al.*, 1993; Walker *et al.*, 1992) showed that enzyme mixtures exhibit a hydrolysis potential higher than the sum of the individual enzyme activities, meaning that they act synergistically. In the case of amorphous cellulose, the presence of endoglucanases is not essential for the complete hydrolysis to be carried out.

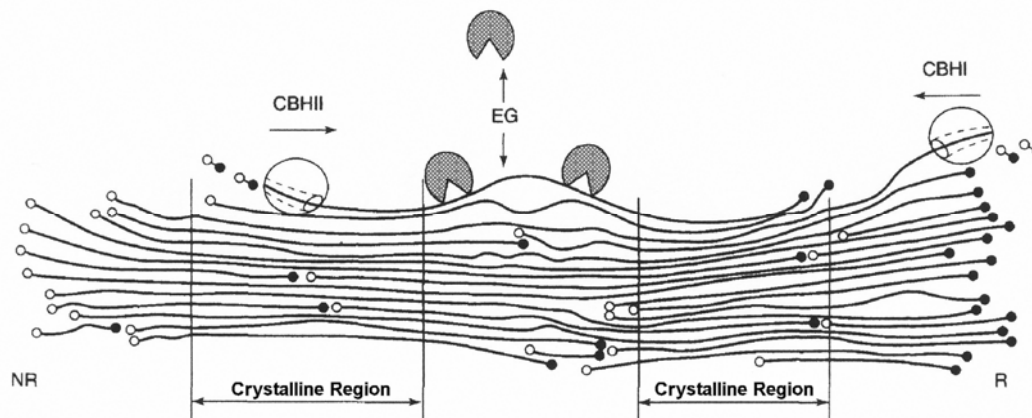


Figure 6. Schematic representation of the cellulose fibre organization, with crystalline and amorphous areas. The enzyme CBHI (Cel7A) act on the fibre from the reducing end (symbolized as full circles in the figure, ‘R’), while CBHII (Cel6A) acts from the non-reducing ends (open circles, ‘NR’). Endoglucanases (EG) act on the middle of the cellulose chains, leading to an increase of the chain ends, wherefrom the CBHs may act (Teeri, 1997).

It was formerly thought that cellobiohydrolases would act only from the non-reducing end of the cellulose chain, but there is now evidence that it is not so (Teeri, 1997). For example, the fungus *Trichoderma reesei* produces only two exoglucanases, cellobiohydrolases I and II (CBHI and CBHII or Cel7A and Cel6A), acting from the reducing and non-reducing end, respectively (see Figure 6).

Another characteristic distinguishing the enzymes action is the active centre structure (Figure 7). Endoglucanases exhibit an active centre with the shape of a sulk, allowing the attachment of the cellulose chain. In turn, exoglucanases bear an active centre with the shape of a tunnel (Divne *et al.*, 1994; Koivula *et al.*, 1998). An individual cellulose chain is allowed to enter the tunnel, where it interacts with the protein, at specific sites present at the entry and inside the protein active site. The hydrolysis leads to the release of a cellobiose molecule, that leaves the tunnel (Divne *et al.*, 1998). The cellulose chain remains linked to the enzyme, allowing its progress along the chain, as it has been observed by AFM (Lee *et al.*, 2000). It should be mentioned that the CBHII tunnel is smaller than the one present in CBHI, thereby facilitating its release from the chain. This subtle difference explains why this enzyme leads to the formation of

smoother fibre-ends, without loosen cellulose fibrils (Teeri, 1997). When, by protein engineering, the tunnel *loops* present in a cellobiohydrolase are removed, the endoglucanolytic activity rises (Meinke *et al.*, 1995), demonstrating that the tunnel present in cellobiohydrolases is essential for the exoglucanolytic activity.

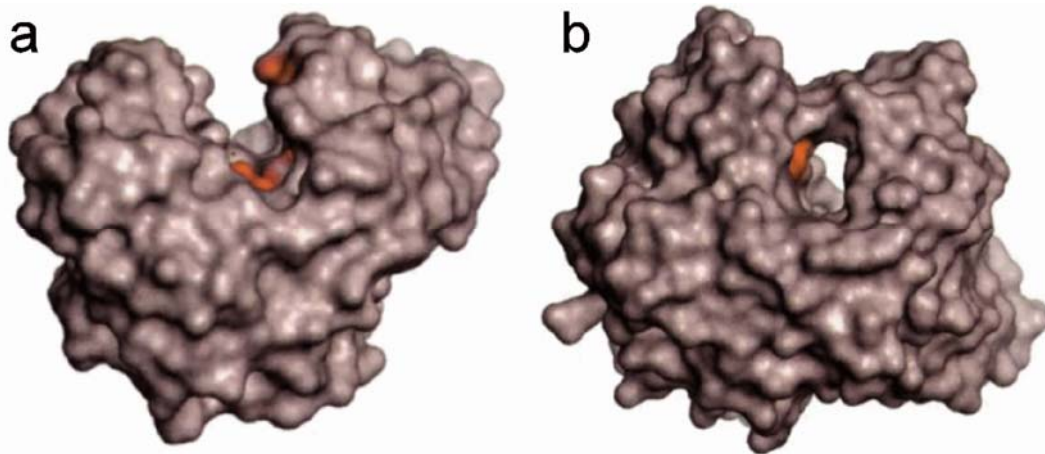


Figure 7. Active sites found in cellulases: a – cleft (endoglucanase from *Trichoderma fusca*); b – tunnel (cellobiohydrolase from *Trichoderma reesei*). The catalytic residues are shown in orange (adapted from Davies and Henrissat, 1995).

Cellulases are used in several biotechnological industries, as a biobleaching pretreatment of paper pulps (Viikari *et al.*, 1990). This process allows for the reduction, or even elimination, of the hypochloride used, in the bleaching process, for the lignin oxidation. Cellulases are also used in the treatment of agricultural fibres, most of the times a waste, for the production of paper (Giovannozzi-Sermanni *et al.*, 2000; Howard *et al.*, 2003), and of *Kenaf* fibres (Kutacova, 1998), which, due to the high yield obtained, are considered as an alternative to pinus and eucalyptus fibres.

The refining of pulps, carried out to defibrillate the fibres and improve the paper mechanical resistance, is highly demanding in terms of energy. The enzymatic pre-treatment requires less energy. This is due to the appearance of a higher amount of microfibrils (Michalopoulos *et al.*, 2005), which allows for a better interfibre interaction. As a result, refining is faster and the process, altogether, becomes less energy consuming (Garcia *et al.*, 2002; Pastor *et al.*, 2001; Seo *et al.*, 2000; Wong *et al.*, 2004).

Recycled fibres are being increasingly used in the paper industry, both for environmental and economical reasons, but also due to the lack of primary fibres worldwide. The incorporation

of recycled fibres in papermaking leads to worse mechanical properties, which may be partially overcome by refining the fibres. In turn, a more intensive refining results in worse drainability during the paper sheet formation, and hence to a lower productivity. Several authors have shown that cellulases – selected ones, operating under controlled conditions - do effectively improve the fibres drainability, without affecting significantly the paper strength (Dienes *et al.*, 2004; Jackson *et al.*, 1993). This effect has been explained as a result of the degradation of amorphous fibres, present in the surface of the fibres (Stork *et al.*, 1995), and of the fines formed during refining (Oksanen *et al.*, 2000).

Another drawback associated to secondary fibres is the presence of contaminants such as pigments, inks and glues. Enzymes may be useful also in solving this problem (Geng and Li, 2003; Viesturs *et al.*, 1999). Enzymes not only remove pigments but they also improve bleaching (Sykes *et al.*, 1996), reduce the level of refining needed (Pelach *et al.*, 2003) and improve the pulps drainability (Jeffries *et al.*, 1996). The use of cellulases for glues removal has proved to be effective and superior to the conventional use of alkaline chemicals (Sykes and Klungness, 1997).

Cellulases are used both in the treatment of paper and of cotton fibres. Cellulases revolutionized the stone washing process, by substituting the stones used in the washing process that was used to produce the fashionable used-like aspect of the garments. (Miettinen-Oinonen, 2004). They are also used for the removal of small fibres – pills – present in the surface of cotton fabrics, such that they prevent pilling formation (Heikinheimo, 2002). Another industrial application relates to food oil extraction. By acting upon the seed cell walls, cellulases elicit higher oil extraction yields (Concha *et al.*, 2004; Soto *et al.*, 2004).

3. Cellulose Binding Domains

The enzymes (not only cellulases, but most enzymes that act on polysaccharides) that are segregated to the culture medium (as opposed to cellulases in cellulosomes) have a simplified modular structure (Srisodsuk, 1994): a catalytic domain – *CD* – linked to a carbohydrate binding module (with affinity for cellulose, starch, chitin,...) – *CBM* – through a peptide chain highly glycosylated – *linker*. Some enzymes have more than one binding module, for instance the endoglucanase E4 from *Thermomonospora fusca* (Irwin *et al.*, 1998), which have an internal CBD and an external one linked through a fibronectin like domain, and the enzyme Xyn10A

from *Rhodothermus marinus*, with two N-terminal CBMs (Abou Hachem *et al.*, 2000), or endoglucanase C from *Cellulomonas fimi*, which have also two N-terminal CBMs (Kormos *et al.*, 2000).

CBMs may be either C- or N-terminal. As mentioned previously, the catalytic and the binding modules are linked through a highly glycosylated peptide sequence (rich in serine, threonine, proline and glycine). In fungi, the linker is 31 to 44 aminoacids long. When this chain is truncated, or eliminated, the fibre affinity/activity of the enzymes is modified. When the *linker* was partially eliminated in the enzyme cellobiohydrolase I (Srisodsuk *et al.*, 1993), from *Trichoderma reesei*, the enzymatic activity was not significantly reduced, although the cellulose affinity was slightly reduced. The complete elimination of the linker, in turn, resulted in the significant reduction of the activity on crystalline substrate (Black *et al.*, 1997; Shen *et al.*, 1991; Srisodsuk *et al.*, 1993). This effect is explained as arising from the lack of mobility of the catalytic domain, which consequently cannot position conveniently on the substrate.

The carbohydrate binding modules are organized in 45 families (CAZY server, <http://afmb.cnrs-mrs.fr/CAZY/>), according to the sequence homology of the aminoacids in the three-dimensional structure. This classification was formerly used only for the cellulose binding domains, but has been extended to other carbohydrates binding proteins. The following list describes shortly the thirteen families which have a least one cellulose binding domain, CBD (Tomme *et al.*, 1998):

Family 1 – With between 33 and 36 aminoacids (aa); its a family with more than 200 members, all – exception made to a CBD from the algae *Colletotrichum gloeosporioides f. sp. Malvae* – belonging to fungae. The structure of the CBDs from the enzymes Cel6A e Cel7A (*Trichoderma reesei*), and of Cel7D (*Phanerochaete chrysosporium*) have been solved.

Family 2 – With more than 100 aa; more than 190 members belong to this family, some with affinity for chitin and xylan; the structure of two CBD, from *Cellulomonas fimi* xylanases and of one chitosanase from *Pyrococcus furiosus* have been solved.

Family 3 – With between 130 and 170 aa; currently have 97 members, one with chitin binding ability; the structure of four of these CBDs is known.

- Family 4 – With between 125 and 170 aa; currently have 29 members, none binding crystalline cellulose. These CBDs preferably bind to amorphous cellulose, xylan, glucan; the structure of three of these CBDs is known.
- Family 5 – With about 60 aa; more than 200 members have been recognized; the structure of one endoglucanase and of two chitinases have been solved.
- Family 6 – With about 120 aa; more than 100 members have been recognized, with low affinity for crystalline cellulose; the structure of five of these CBDs is known.
- Family 7 – No entries.
- Family 8 – With about 152 aa; currently only four members are registered in this family, none with known structure.
- Family 9 – With about 170 aa; 40 members have been recognized, mostly xylanases; cellulose binding ability was demonstrated in one case.
- Family 10 – With about 50 aa; 25 members have been recognized, one binding to cellulose. The structure of CBMs from a xylanase (*Cellvibrio japonicus*) has been determined.
- Family 11 – With between 180 and 200 aa; five members belong to this family, one a cellulose binding domain.
- Family 12 – With between 40 and 50 aa; has 66 members, most are chitinases; the structure of a CBD from *Bacillus circulans* has been solved.
- Family 13 – With about 150 aa; this family possesses 341 members, CBMs present in triplets, exception made to xylanase II from *Actinomadura sp. FC7*; The structure of 15 CBMs has been solved.

The presence of CBDs is essential for the enzyme activity on insoluble substrates. Indeed, when the catalytic domains alone are used – as demonstrated for instance with Ces and Cena, from *Cellulomonas fimi*, or Cel7A and Cel7B, from *Trichoderma reesei* – the adsorption to crystalline cellulose is drastically reduced, which parallels with the lower hydrolytic activity (Gilkes *et al.*, 1988; Gilkes *et al.*, 1992; Srisodsuk *et al.*, 1997; Tomme *et al.*, 1995). However, the activity on soluble substrates does not vary significantly in those cases (Black *et al.*, 1997; Hamada *et al.*, 2001). The reverse was also demonstrated: when a CBD is fused to an enzyme that does not have one naturally, its activity upon insoluble substrates is improved (Limon *et al.*,

2001). It becomes clear that CBDs act by increasing the enzyme concentration on the surface of the insoluble substrate, thereby improving the catalytic efficiency. Another kind of activity, the disruption of fibres, has been reported by several authors, although the details of this activity remain unclear. It was demonstrated that the CBD from CenA, an enzyme from the bacteria *Cellulomonas fimi*, disrupts the fibres in a non-catalytic process (Din *et al.*, 1991).

The 3D structure of several CBDs was solved (Ikegami *et al.*, 2000; Sorimachi *et al.*, 1996), namely of endoglucanase I – Cel7B – and cellobiohydrolase I – Cel7A –, both from *Trichoderma reesei* (Kraulis *et al.*, 1989; Mattinen *et al.*, 1998). Both proteins exhibit aromatic rings in one of the protein faces (Figure 8).

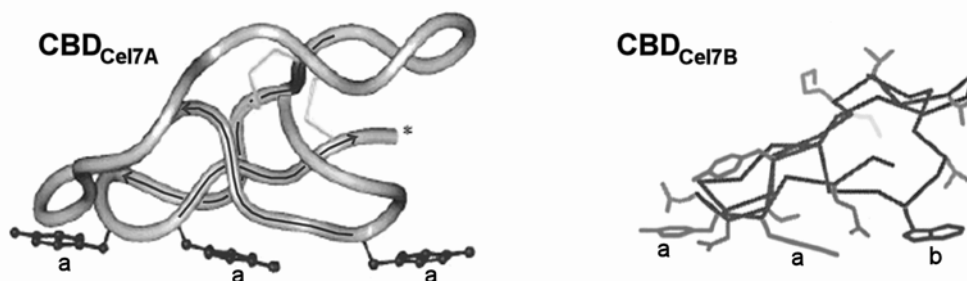


Figure 8. Structural models of CBDs from cellobiohydrolase I (left) and endoglucanase I (right), from *Trichoderma reesei*. Cel7A has three β -sheets shown by the arrows. The tyrosine (a) and tryptophan (b) residues define an almost plane surface on the CBDs (adapted from Carrard and Linder, 1999, and Mattinen *et al.*, 1998).

The presence and relative position of the aromatic residues in the binding domains has been observed also in CBMs with different specificity. Mutagenesis studies, replacing these aminoacids by non-aromatic ones (Nagy *et al.*, 1998; Ponyi *et al.*, 2000; Simpson and Barras, 1999), showed clearly that these residues are directly involved in the interaction with the cellulose/chitin/xylan chains of crystalline substrates. In some cases, the substitution of aminoacids lead to a modification of the substrate recognition specificity. In the case of CBM from family 2b (xylan binding), the replacement of the arginine, at position 262, by an glycine – R262G – (Simpson *et al.*, 2000), induces a reorientation of tryptophan (aa 259) by 90°, thus creating a surface along with the protein surface, similar to the one of the binding domain of CBM family 2a. As a result, the CBM has no longer affinity for xylan, and rather adheres to cellulose. In the case of the CBDs from cellobiohydrolase I (Linder *et al.*, 1999), from *Trichoderma reesei*, the substitution of tyrosine with histidine modifies the adsorption profile

with pH. This observation leads to the design of binding domains where the adsorption may be switched by pH control.

In the 3D structure shown in Figure 8, it is possible to identify the existence of three aromatic rings defining a smooth surface (inferior plane in the image). These aromatic rings (Figure 9) may be almost superposed to the glucose residues rings in a cellulose crystallite. The interaction of cellobiose with CBDs, studied by NMR spectroscopy (Mattinen *et al.*, 1997), allowed the authors to suggest a model of the CBD-cellulose interaction, as shown in Figure 10. As it may be observed in the figure, the aromatic rings are almost aligned with the glucose units. This misalignment may allow an *imperfect* adsorption, in other words, it may prevent the CBD from maintaining a fixed position over the microfibril glucose chain, which would undoubtedly diminish the hydrolysis efficiency of the catalytic domain. Some CBDs seem to adsorb cellulose irreversibly (Carrard and Linder, 1999), which is the case of the CBD from cellobiohydrolase II, as opposed to the reversible adsorption of the CBD from cellobiohydrolase I. The main structural difference between the two CBDs is the presence of a tryptophan residue, in the former, instead of a tyrosine, in the latter (see Figure 9). This irreversibility does not mean that the CBDs are immobilized in the surface of the fibres. As a matter of fact, CBDs from CenA and Cex, both from the *Cellulomonas fimi*, although irreversibly bound, surface diffuse, as do the intact enzymes (Jervis *et al.*, 1997).

Besides mediating the adsorption of the catalytic domains on the substrate, the structure of some CBDs define a sulk, in the region where they interact with the substrate, which appears to be directly related with the recognition specificity (Johnson *et al.*, 1999). These CBDs recognize amorphous cellulose, but not the crystalline one, probably because in the first case the cellulose chains have enough mobility to enter the CBDs sulk.

The binding domains may have binding ability for more than one substrate. For example, CelK, from the anaerobic bacteria *Clostridium thermocellum*, have affinity for *BMCC* (bacterial microcrystalline cellulose), liquenan, glucomannan and barley β -glucan (Kataeva *et al.*, 2001). In the case of *Phanerochaete chrysosporium*, the expression of CBDs from two exocellobiohydrolases is apparently mediated by the presence of the substrate (Birch *et al.*, 1995); an intron inserted in the gene, that codifies for the CBD, may or may not be transcribed depending on the substrate present in the culture medium, leading to different CBDs to be expressed with differential affinity to each of those substrates. On the other hand, different CBDs

even adsorbing to the same substrate, may adsorb to different spots in the fibres surface. This was demonstrated by fusing different CBDs to the same catalytic domain (CD) of the *Clostridium thermocellum* endoglucanase CelD. It was demonstrated that, when the recombinant enzymes with different CBDs were added to a reaction mixture, where BMCC was hydrolysed, the sequential addition of the distinct engineered enzymes was more productive than the successive addition of the same complex CBD-CD (Carrard *et al.*, 2000).

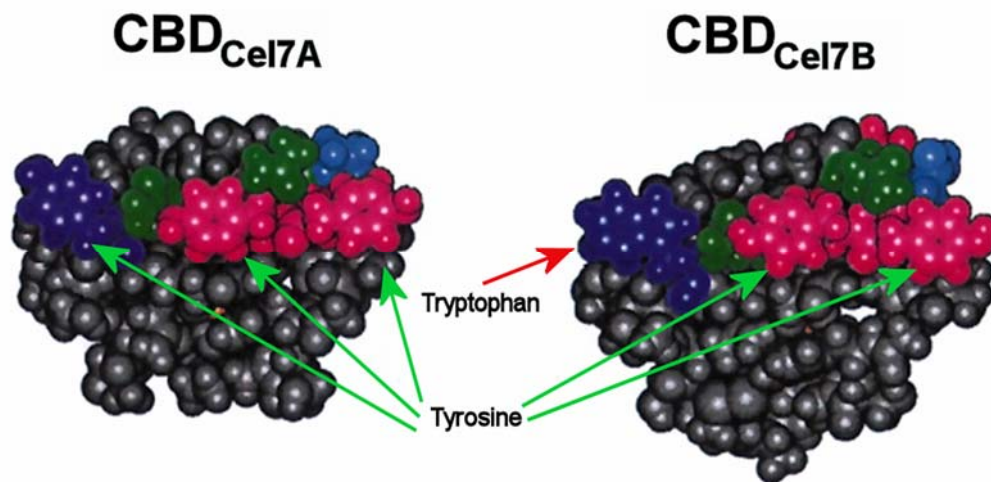


Figure 9. Perspective of the structures representative of the CBDs from EGI (left) and CBHI (right). The aromatic residues aligned at the inferior face are highlighted (adapted from Mattinen *et al.*, 1998).

The binding domains, due to the ability to adsorb to cellulose without degrading it, have great biotechnological potential. The direct adsorption to cotton was shown to improve the dye affinity (Cavaco-Paulo *et al.*, 1999). They can be used also on the purification of recombinant proteins (Jiang and Radford, 2000; Reinikainen *et al.*, 1997). A recombinant protein, fused to a CBD, is easily purified using an inexpensive cellulose column. A purification yield of about 90% of the target protein has been reported (Greenwood *et al.*, 1989; Kaseda *et al.*, 2001), in only one purification stage. Another strategy consists in fusing the CBD with a protein from *Staphylococcus* (Shpigel *et al.*, 2000): adsorbed to a cellulose matrix, this support may be used in the purification of IgGs.

Another application consists in the expression of CBDs at the surface of cells, such that they may be thereafter immobilised in cellulosic materials. This strategy allowed the immobilisation of different kinds of cells: *Staphylococcus* (Lehtio *et al.*, 2003), *Saccharomyces cerevisiae* (Nam *et al.*, 2002) and *Escherichia coli* (Wang *et al.*, 2001). The expression of both

CBDs and an organophosphorous hydrolase, in the surface of *Escherichia coli* (Wang *et al.*, 2002), allowed the cells immobilisation on a cellulose material. The cells performed the fast and steady degradation of paraoxon, at near 100%, for 45 days. In this way, the immobilisation of cells in inexpensive materials is easily carried out.

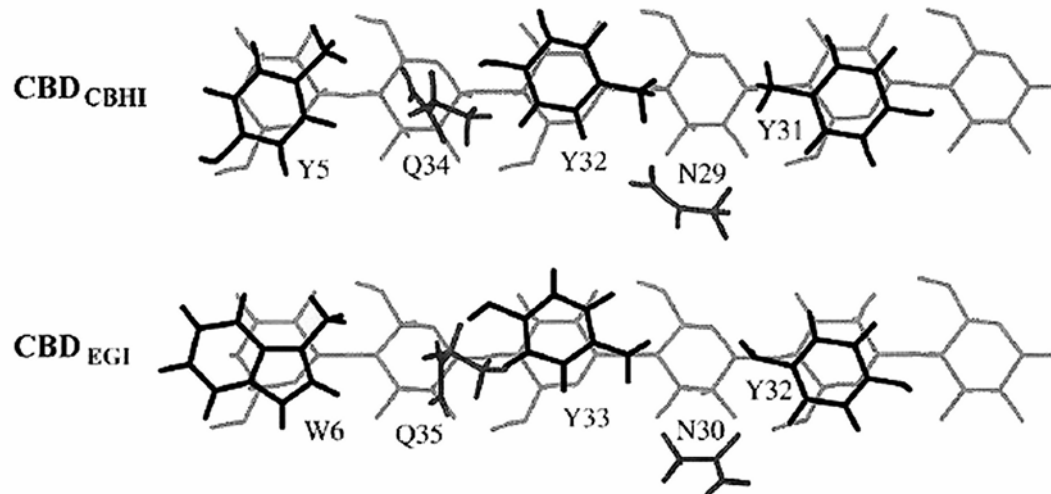


Figure 10. Model of the interaction between the CBDs from cellobiohydrolase I (Cel7A) and endoglucanase I (Cel7B) and the glucose residues present in cellulosic fibres (adapted from Mattinen *et al.*, 1997).

The simple presence of CBDs, in solution during pollen germination, lead to elongation of the pollen tubes and also to the length increase of *Arabidopsis* roots (Shpigel *et al.*, 1998). Another surprising finding was that the CBDs induced an increase, of up to 5 times, of the cellulose production in *Acetobacter xylinum*. This effect was explained as arising from the interference of the CBDs in the crystallization step, during the microfibril assembly.

RESULTS OVERVIEW AND CONCLUSIONS

Production of CBD by proteolysis

One of the goals of this thesis was to develop a method to produce a high amount of cellulose-binding domains (CBD), making possible experiments requiring such large quantities. The protein source chosen was the commercial preparation Celluclast[®], due to its availability in large volume. This preparation was obtained from the fermentation of the fungus *Trichoderma reesei*, which produces mainly two exocellulases (cellobiohydrolases I and II) and three endocellulases (endoglucanases I, II and V). Following this previous work, the preparation was firstly filtered using an ultrafiltration membrane (30 kDa cutoff), which retains the exocellulases present in the preparation (~50 kDa), in order to clean it from low molecular weight material (preservatives and other proteins). Afterwards, the protease Papain was added, in order to cleave the linker between the catalytic and the binding domains. To achieve an optimum reaction, a ratio of 1 gram of Papain to 1200 grams of the ultrafiltered cellulase was used. A higher ratio leads to extensive hydrolysis, as assessed by capillary electrophoresis analysis.

The CBD were then isolated by ultrafiltration, with a 10 kDa cutoff membrane. To further purify the CBD, the concentrated protein obtained (by precipitation with ammonium sulphate) was purified in an ion exchange column (IEC). The obtained CBDs (unbound peak) present around 30% (w/w) of carbohydrates, mainly mannose (85%). The correct size was assessed by MALDI-TOF (~8.4 kDa). Glycosylation of the protein is responsible for the appearance of several peaks in the MALDI spectrum, due to heterogeneity of the carbohydrates (the difference between the peaks is 162 Da, corresponding to one sugar residue). The purified CBDs belong to cellobiohydrolase I, as confirmed by N-terminal protein sequencing. Indeed, the sequence (-GNPPG-) is only present between the catalytic domain and the linker sequence of cellobiohydrolase I. The analysis also showed that the obtained CBD is highly pure.

The purified protein has, as expected, high affinity for cellulose, as demonstrated by the adsorption isotherm. The Langmuir adsorption constants CBD_{Max} (maximum molar amount adsorbed per mass unit) and k_a (adsorption equilibrium constant) are 2.42 $\mu\text{mol/g}$ and 0.209 μM^{-1} , respectively.

Studies using conjugates CBD-FITC

To analyse the adsorption of CBDs on the cellulose surface, conjugates of CBD with a fluorescence probe, fluorescein isothiocyanate (FITC), were produced. The observation by light microscopy of the adsorbed CBD-FITC reveals that the adsorption on the fibre surface is not uniform. The fibre ends and surface spots display a much higher fluorescent emission. These regions are less ordered (amorphous regions), and probably more accessible, enabling a higher CBD adsorption. When the CBDs are adsorbed on amorphous fibres (phosphoric acid swollen cellulose), the adsorption is apparently homogenous. These results demonstrate the interest of using CBD-FITC to visualize/identify the amorphous/crystalline (bright/darker) regions on the fibres, as to evaluate its physical conditions (low/high damage).

Another aspect evaluated, with the use of CBD-FITC, was the reversibility of the CBD adsorption to the cellulose fibres. For that purpose, fibres with and without adsorbed CBD-FITC were mixed. The reversibility of the CBD adsorption would expectedly lead to the fibres becoming uniformly fluorescent, due to desorption/re-adsorption of CBD. Indeed, this was observed, but very slowly. After 192 hours, it was still possible to observe less bright fibres in the mixture. This shows that the adsorption of CBDs onto Whatman CF11 fibres is reversible, but also that desorption is a rather slow process.

When increasing concentrations of CBD-FITC are used, it is possible to observe an increase in the fluorescent emission intensity of the fibres. This indicates that it may be possible to measure the quantity of adsorbed protein on the fibres' surface. Having this in mind, a Matlab script was developed, in order to produce a calibration routine, allowing the conversion of the fluorescence emission of the adsorbed FITC-CBD into an estimation of the CBD fibre surface coating.

To carry out the calibration, the fluorescent emission of CBD-FITC was measured, using solutions with different concentrations in an Improved Neubauer chamber. This expeditious approach showed to have a high accuracy. Since the emission of FITC is in the green spectrum (three colour channels), a merging function was developed in order to maximize the sensitivity to small fluorescence variations. This equation is valid for non-saturating levels (close to 255) on any of the three colour channels. Also, due to virtual memory restrictions, the images were downsized to 260x206 pixels. Another aspect that was taken into consideration was the photobleaching of the FITC fluorophore. A mono-exponential equation, that describes the photobleaching, was integrated in function of time, in order to correlate the total fluorescence emission during each exposure time period. From the non-linear regression of these values, the initial fluorescence intensity values for each CBD-FITC concentration are then multiplied by the

exposure time of the images to be quantified, and a linear regression is applied. The regression parameters are then saved in a Matlab native format as to be used in the later quantification. The regression was performed at each pixel position due to the non-uniform background illumination acquired by the image sensor.

From the assays made with adsorbed CBD-FITC on cellulose films, it was shown that the photobleaching effect could be neglected. The excitation of FITC for twenty seconds, a much higher acquisition time than the used in the fibres quantification, implied only 0.42% decrease in the measured fluorescent intensity.

When a solution of CBD-FITC with a concentration of 400 $\mu\text{g/mL}$ (expected to saturate the surface) was left in contact with a cellulose film (obtained from cellulose acetate), the quantified surface concentration of CBD was equivalent to 1.6 to 2 protein layers. This figure is higher than the theoretically expected, that is, one layer at saturation. This may be explained as arising from the penetration of the CBDs into inner layers of the film.

The estimation of CBD surface concentration was also carried out using cellulose fibres. Two different initial CBD-FITC concentrations were used: 2 and 20 mg of protein per gram of fibres. The lower amount was chosen since it is the range of concentration used in paper fibres treatment; the higher amount was used to assess the maximum coverage that could be obtained at saturation. For the lower concentration, a coverage of 77% was found for the secondary fibres (*Portucel*) and of 110% for pure cellulose fibres (Whatman CF11). These values are higher than expected, showing that with a relatively low concentration of protein a high coverage is possible, subsequently implying a change in the fibres' surface properties. For the higher concentration, the number of estimated layers of CBDs was 4, 6 and 5.3 for Whatman CF11, Amorphous CF11 and Sigmacel 20, respectively. The adsorption isotherms do not suggest the existence of several protein layers at saturation. Rather, the apparent high surface coating is probably associated with both surface irregularities and penetration of CBDs in the fibres structure. Indeed, confocal microscopy showed that the surface of a fibre is not perfectly smooth, but rather irregular, which will increase the real surface area (as compared to the assumed flat surface). Also confocal microscopy showed the presence of CBD-FITC in the inner core of the fibres. This evidence was confirmed by TEM-immunolabeling, which revealed black spots (presence of CBDs) in the middle of the Whatman CF11 fibres.

Studies of CBDs on fibre modification

The effect of CBDs on the pulp and paper properties was analysed, using primary (virgin) and secondary (recycled) cellulose fibres. As a general trend, the CBDs both decreased the

Schopper-Riegler index ($^{\circ}$ SR) and increased the water retention value (WRV). Similar results were described by other authors, using cellulases, an effect that was associated to the hydrolytic activity toward the amorphous regions on fibres' surface. In the present work, no activity was detected by DNS analysis (reducing sugar quantification). Then, it is possible to associate these results mainly to the presence of adsorbed CBDs, due to stabilisation of fines or to steric effects due to the oligosaccharides present in the linker peptide.

The air permeability of the papersheets increases with the CBDs adsorption, especially for the secondary fibres without refining and for the Pine fibres at PFI of 3000 revolutions. This may allow a faster production rate and/or lower heat consumption. The strength parameters decreased, with adsorbed CBDs, as the PFI revolutions were increased.

To study the influence of the protein electric charge on the fibres properties, a conjugate of CBD with lysozyme (a protein with a high isoelectric point, 11.3) was produced. The conjugate have a high positive charge, at the adsorption assay conditions. To conjugate the proteins, the chemical N-hydroxysuccinimidyl 4-azidobenzoate (HSAB) was used. HSAB firstly reacts with a free amine in the linker's terminal (the only free amine present on CBDs), and then with lysozyme. This strategy allows the coupling of CBD to lysozyme molecules (one or more, as shown by size exclusion chromatography), excluding the possibility of homoconjugates to be formed. The effect of the conjugates on the papersheets was similar to the obtained with CBDs, except for the permeability, that was enhanced.

In relation to the surface properties, only the ZETA potential of unrefined Eucalyptus fibres presented a significant variation with both CBD and conjugates (CBD with lysozyme) adsorption. This is explained by the lower surface area of the unrefined fibres, thus higher surface coverage by the proteins. With pure cellulose, at high protein content, the electric charge of the fibres turned from negative to positive with CBD, an effect even more evident with the conjugates. This trend was also observed with the other fibres, but not so extensively, because of the lower surface coverage. From the contact angle measurements, no significant variation was observed with adsorbed CBD, only a small increment of hydrophilicity in the primary and pure cellulose fibres. The secondary fibres showed a decrease of the negative polar component after the adsorption of both CBDs and conjugates. The conjugates significantly changed the surface energy of pure cellulose. The fibres had their negative polar component highly reduced, which induced the fibres to become hydrophobic.

Conclusions

Cellulases have been widely used in industrial processes, including paper properties enhancement, garments treatment, etc. However, the hydrolytic activity is responsible for an elevated mass loss of the treated products. Carbohydrates-binding modules (CBM), on the other hand, even though not showing hydrolytic activity, are able to produce equivalent effects as the whole enzymes counterparts, as was demonstrated by the Schopper-Riegler index ($^{\circ}\text{SR}$) and by water retention values (WRV) measurements on handsheets production. These effects are probably due to the CBDs adsorption on the fibres, with a high surface coating, as measured by fluorescence microscopy. The demonstration that CBMs penetrate deep in the fibres suggest that the properties of these fibres may be modified not only through surface properties modification.

CBMs may also be used to target different molecules to the cellulose surface. As shown with lysozyme, it was possible in this work to modify the cellulose surface properties, from hydrophilic to hydrophobic. This demonstrates the feasibility of engineering conjugates that would allow the manufacturing of new cellulose based materials.

The CBMs used in this work are highly glycosylated, and are in this regard different from the recombinant proteins obtained by expression in a bacterial host. However, the use of recombinant CBMs (bearing attached functional proteins) is recommended for future work. A better understanding of the effects of CBMs on the surface and structural properties of cellulosic fibres is required (surface coating and modification, adsorption reversibility, CBMs competition and affinity for different sites in the surface, surface diffusion, penetration of the fibres). The techniques developed in this work may contribute to those studies.

Bibliography

Abou Hachem M., Karlsson E.N., Bartonek-Roxa E., Raghothama S., Simpson P.J., Gilbert H.J., Williamson M.P., Holst O. 2000. Carbohydrate-binding modules from a thermostable *Rhodothermus marinus* xylanase: cloning, expression and binding studies. *Biochemical Journal* **345**: 53-60

Bayer E.A., Belaich J.P., Shoham Y., Lamed R. 2004. The cellulosomes: Multienzyme machines for degradation of plant cell wall polysaccharides. *Annual Review of Microbiology* **58**: 521-554

Bayer E.A., Chanzy H., Lamed R., Shoham Y. 1998. Cellulose, cellulases and cellulosomes. *Current Opinion in Structural Biology* **8**: 548-557

Bayer E.A., Setter E., Lamed R. 1985. Organization and distribution of the cellulosome in *Clostridium thermocellum*. *The Journal of Bacteriology* **163**: 552-559

Belaich J.P., Tardif C., Belaich A., Gaudin C. 1997. The cellulolytic system of *Clostridium cellulolyticum*. *Journal of Biotechnology* **57**: 3-14

Belgacem M.N., Czeremuskin G., Sapiuha S., Gandini A. 1995. Surface characterization of cellulose fibres by XPS and inverse gas chromatography. *Cellulose* **2**: 145-157

Bidlack J., Malone M., Benson R. 1992. Molecular Structure and Component Integration of Secondary Cell Walls in Plants. *Proceedings of the Oklahoma Academy of Science* **72**: 51-56

Birch P.R.J., Sims P.F.G., Broda P. 1995. Substrate-Dependent Differential Splicing of Introns in the Regions Encoding the Cellulose-Binding Domains of two Exocellobiohydrolase-I-Like Genes in *Phanerochaete-Chrysosporium*. *Applied and Environmental Microbiology* **61**: 3741-3744

Black G.W., Rixon J.E., Clarke J.H., Hazlewood G.P., Ferreira L.M.A., Bolam D.N., Gilbert H.J. 1997. Cellulose binding domains and linker sequences potentiate the activity of hemicellulases against complex substrates. *Journal of Biotechnology* **57**: 59-69

Boisset C., Chanzy H., Henrissat B., Lamed R., Shoham Y., Bayer E.A. 1999. Digestion of crystalline cellulose substrates by the *Clostridium thermocellum* cellulosome: structural and morphological aspects. *Biochemical Journal* **340**: 829-835

Brown R.M., Saxena I.M., Kudlicka K. 1996. Cellulose biosynthesis in higher plants. *Trends in Plant Science* **1**: 149-156

Carrard G., Koivula A., Soderlund H., Beguin P. 2000. Cellulose-binding domains promote hydrolysis of different sites on crystalline cellulose. *Proceedings of the National Academy of Sciences of the United States of America* **97**: 10342-10347

Carrard G., Linder M. 1999. Widely different off rates of two closely related cellulose-binding domains from *Trichoderma reesei*. *European Journal of Biochemistry* **262**: 637-643

Cavaco-Paulo A., Morgado J., Andreus J., Kilburn D. 1999. Interactions of cotton with CBD peptides. *Enzyme and Microbial Technology* **25**: 639-643

Concha J., Soto C., Chamy R., Zuniga M.E. 2004. Enzymatic pretreatment on rose-hip oil extraction: Hydrolysis and, pressing conditions. *Journal of the American Oil Chemists Society* **81**: 549-552

Coutinho P.M., Henrissat B. 1999. Carbohydrate-active enzymes: an integrated database approach. *In: Recent Advances in Carbohydrate Bioengineering* (Ed. Gilbert H.J., Davies G., Henrissat B., and Svensson B.). The Royal Society of Chemistry, Cambridge

Davies G., Henrissat B. 1995. Structures and Mechanisms of Glycosyl Hydrolases. *Structure* **3**: 853-859

Dienes D., Egyhazi A., Reczey K. 2004. Treatment of recycled fiber with *Trichoderma* cellulases. *Industrial Crops and Products* **20**: 11-21

Din N., Gilkes N.R., Tekant B., Miller R.C., Warren A.J., Kilburn D.G. 1991. Non-Hydrolytic Disruption of Cellulose Fibers by the Binding Domain of A Bacterial Cellulase. *Bio-Technology* **9**: 1096-1099

Divne C., Stahlberg J., Reinikainen T., Ruohonen L., Pettersson G., Knowles J.K.C., Teeri T.T., Jones T.A. 1994. The 3-Dimensional Crystal-Structure of the Catalytic Core of Cellobiohydrolase-I from *Trichoderma-Reesei*. *Science* **265**: 524-528

Divne C., Stahlberg J., Teeri T.T., Jones T.A. 1998. High-resolution crystal structures reveal how a cellulose chain is bound in the 50 angstrom long tunnel of cellobiohydrolase I from *Trichoderma reesei*. *Journal of Molecular Biology* **275**: 309-325

Doblin M.S., Kurek I., Jacob-Wilk D., Delmer D.P. 2002. Cellulose biosynthesis in plants: from genes to rosettes. *Plant and Cell Physiology* **43**: 1407-1420

Garcia O., Torres A.L., Colom J.F., Pastor F.I.J., Diaz P., Vidal T. 2002. Effect of cellulase-assisted refining on the properties of dried and never-dried eucalyptus pulp. *Cellulose* **9**: 115-125

Geng X.L., Li K.C. 2003. Deinking of recycled mixed office paper using two endo-glucanases, CelB and CelE, from the anaerobic fungus *orpinomyces* PC-2. *Tappi Journal* **2**: 29-32

Gilkes N.R., Jervis E., Henrissat B., Tekant B., Miller R.C., Warren R.A.J., Kilburn D.G. 1992. The Adsorption of A Bacterial Cellulase and Its two Isolated Domains to Crystalline Cellulose. *Journal of Biological Chemistry* **267**: 6743-6749

Gilkes N.R., Warren R.A.J., Miller R.C., Kilburn D.G. 1988. Precise Excision of the Cellulose Binding Domains from two *Cellulomonas fimi* Cellulases by A Homologous Protease and the Effect on Catalysis. *Journal of Biological Chemistry* **263**: 10401-10407

Giovanozzi-Sermanni G., Cappelletto P., Mongardini F., Brizzi M., D'Annibale A. 2000. Paper pulp by enzymatic treatment of agricultural residues and waste paper.

Greenwood J.M., Gilkes N.R., Kilburn D.G., Miller R.C., Warren R.A.J. 1989. Fusion to An Endoglucanase Allows Alkaline-Phosphatase to Bind to Cellulose. *Febs Letters* **244**: 127-131

Hamada N., Kodaira R., Nogawa M., Shinji K., Ito R., Amano Y., Shimosaka M., Kanda T., Okazaki M. 2001. Role of cellulose-binding domain of exocellulase I from white rot basidiomycete *Irpex lacteus*. *Journal of Bioscience and Bioengineering* **91**: 359-362

Heikinheimo L. *Trichoderma reesei* cellulases in processing of cotton. 2002. Tampere University of Technology. 82p.

Henrissat B., Davies G. 1997. Structural and sequence-based classification of glycoside hydrolases. *Current Opinion in Structural Biology* **7**: 637-644

Howard R.L., Abotsi E., Jansen van Rensburg E.L., Howard S. 2003. Lignocellulose biotechnology: issues of bioconversion and enzyme production. *African Journal of Biotechnology* **2**: 602-619

Ikegami T., Okada T., Hashimoto M., Seino S., Watanabe T., Shirakawa M. 2000. Solution structure of the chitin-binding domain of *Bacillus circulans* WL-12 chitinase A1. *Journal of Biological Chemistry* **275**: 13654-13661

Irwin D., Shin D.H., Zhang S., Barr B.K., Sakon J., Karplus P.A., Wilson D.B. 1998. Roles of the catalytic domain and two cellulose binding domains of *Thermomonospora fusca* E4 in cellulose hydrolysis. *Journal of Bacteriology* **180**: 1709-1714

Irwin D.C., Spezio M., Walker L.P., Wilson D.B. 1993. Activity Studies of 8 Purified Cellulases - Specificity, Synergism, and Binding Domain Effects. *Biotechnology and Bioengineering* **42**: 1002-1013

Jackson L.S., Heitmann J.A., Joyce T.W. 1993. Enzymatic Modifications of Secondary Fiber. *Tappi Journal* **76**: 147-154

Jeffries T.W., Sykes MS., Rutledge-Cropsey K., Klungness J.H., Abubakr S. 1996. Enhanced removal of toners from office waste papers by microbial cellulases. 141-144

Jervis E.J., Haynes C.A., Kilburn D.G. 1997. Surface diffusion of cellulases and their isolated binding domains on cellulose. *Journal of Biological Chemistry* **272**: 24016-24023

Jiang M., Radford A. 2000. Exploitation of a cellulose-binding domain from *Neurospora crassa*. *Enzyme and Microbial Technology* **27**: 434-442

Johnson P.E., Brun E., MacKenzie L.F., Withers S.G., McIntosh L.P. 1999. The cellulose-binding domains from *Cellulomonas fimi* beta-1,4-glucanase CenC bind nitroxide spin-labeled celooligosaccharides in multiple orientations. *Journal of Molecular Biology* **287**: 609-625

Kaseda K., Kodama T., Fukui K., Hirose K. 2001. A novel approach for purification of recombinant proteins using the dextran-binding domain. *Febs Letters* **500**: 141-144

Kataeva I.A., Seidel R.D., Li X.L., Ljungdahl L.G. 2001. Properties and mutation analysis of the CelK cellulose-binding domain from the *Clostridium thermocellum* cellulosome. *Journal of Bacteriology* **183**: 1552-1559

Kimura S., Itoh T. 2004. Cellulose synthesizing terminal complexes in the ascidians. *Cellulose* **11**: 377-383

Kimura S., Laosinchai W., Itoh T., Cui X., Linder C.R., Brown R.M. 1999. Immunogold Labeling of Rosette Terminal Cellulose-Synthesizing Complexes in the Vascular Plant *Vigna angularis*. *THE PLANT CELL* **11**: 2075-2086

Koivula A., Kinnari T., Harjunpaa V., Ruohonen L., Teleman A., Drakenberg T., Rouvinen J., Jones T.A., Teeri T.T. 1998. Tryptophan 272: an essential determinant of crystalline cellulose degradation by *Trichoderma reesei* cellobiohydrolase Cel6A. *Febs Letters* **429**: 341-346

Kormos J., Johnson P.E., Brun E., Tomme P., McIntosh L.P., Haynes C.A., Kilburn D.G. 2000. Binding site analysis of cellulose binding domain CBDN1 from endoglucanase C of *Cellulomonas fimi* by site-directed mutagenesis. *Biochemistry* **39**: 8844-8852

Kraulis P.J., Clore G.M., Nilges M., Jones T.A., Pettersson G., Knowles J., Gronenborn A.M. 1989. Determination of the 3-Dimensional Solution Structure of the C-Terminal Domain of Cellobiohydrolase-I from *Trichoderma-Reesei* - A Study Using Nuclear Magnetic-Resonance and Hybrid Distance Geometry Dynamical Simulated Annealing. *Biochemistry* **28**: 7241-7257

Kruus K., Lua A.C., Demain A.L., Wu J.H.D. 1995. The Anchorage Function of Cipa (Cell), A Scaffolding Protein of the *Clostridium-Thermocellum* Cellulosome. *Proceedings of the National Academy of Sciences of the United States of America* **92**: 9254-9258

Kutacova P. Enzymatic Modification Of Kenaf Pulp. 1998. University of Toronto. 138p.

Lee I., Evans B.R., Woodward J. 2000. The mechanism of cellulase action on cotton fibers: evidence from atomic force microscopy. *Ultramicroscopy* **82**: 213-221

Lehtio J., Sugiyama J., Gustavsson M., Fransson L., Linder M., Teeri T.T. 2003. The binding specificity and affinity determinants of family 1 and family 3 cellulose binding modules. *Proceedings of the National Academy of Sciences of the United States of America* **100**: 484-489

Limon M.C., Margolles-Clark E., Benitez T., Penttila M. 2001. Addition of substrate-binding domains increases substrate-binding capacity and specific activity of a chitinase from *Trichoderma harzianum*. *Fems Microbiology Letters* **198**: 57-63

Linder M., Nevanen T., Teeri T.T. 1999. Design of a pH-dependent cellulose-binding domain. *Febs Letters* **447**: 13-16

Mattinen M.L., Linder M., Drakenberg T., Annala A. 1998. Solution structure of the cellulose-binding domain of endoglucanase I from *Trichoderma reesei* and its interaction with cello-oligosaccharides. *European Journal of Biochemistry* **256**: 279-286

Mattinen M.L., Linder M., Teleman A., Annala A. 1997. Interaction between celohexaose and cellulose binding domains from *Trichoderma reesei* cellulases. *Febs Letters* **407**: 291-296

Meinke A., Damude H.G., Tomme P., Kwan E., Kilburn D.G., Miller R.C., Warren R.A.J., Gilkes N.R. 1995. Enhancement of the Endo-Beta-1,4-Glucanase Activity of An Exocellobiohydrolase by Deletion of A Surface Loop. *Journal of Biological Chemistry* **270**: 4383-4386

Michalopoulos D.L., Ghosh D., Murdoch B. 2005. Enhancement of Wood Pulps by Cellulase Treatment.

Miettinen-Oinonen A. *Trichoderma reesei* strains for production of cellulases for the textile industry. 2004. University of Helsinki. 100p.

Nagy T., Simpson P., Williamson M.P., Hazlewood G.P., Gilbert H.J., Orosz L. 1998. All three surface tryptophans in Type IIa cellulose binding domains play a pivotal role in binding both soluble and insoluble ligands. *Febs Letters* **429**: 312-316

Nam J.M., Fujita Y., Arai T., Kondo A., Morikawa Y., Okada H., Ueda M., Tanaka A. 2002. Construction of engineered yeast with the ability of binding to cellulose. *Journal of Molecular Catalysis B-Enzymatic* **17**: 197-202

O'Sullivan A.C. 1997. Cellulose: the structure slowly unravels. *Cellulose* **4**: 173-207

Oksanen T., Pere J., Paavilainen L., Buchert J., Viikari L. 2000. Treatment of recycled kraft pulps with *Trichoderma reesei* hemicellulases and cellulases. *Journal of Biotechnology* **78**: 39-48

Pastor F.I.J., Pujol X., Blanco A., Vidal T., Torres A.L., Diaz P. 2001. Molecular cloning and characterization of a multidomain endoglucanase from *Paenibacillus* sp BP-23: evaluation of its performance in pulp refining. *Applied Microbiology and Biotechnology* **55**: 61-68

Pelach M.A., Pastor F.J., Puig J., Vilaseca F., Mutje P. 2003. Enzymic deinking of old newspapers with cellulase. *Process Biochemistry* **38**: 1063-1067

Ponpium P., Ratanakhanokchai K., Kyu K.L. 2000. Isolation and properties of a cellulosome-type multienzyme complex of the thermophilic *Bacteroides* sp strain P-1. *Enzyme and Microbial Technology* **26**: 459-465

Ponyi T., Szabo L., Nagy T., Orosz L., Simpson P.J., Williamson M.P., Gilbert H.J. 2000. Trp22, Trp24, and Tyr8 play a pivotal role in the binding of the family 10 cellulose-binding module from *Pseudomonas xylanase A* to insoluble ligands. *Biochemistry* **39**: 985-991

Rabinovich M.L., Melnick M.S., Bolobova A.V. 2002. The structure and mechanism of action of cellulolytic enzymes. *Biochemistry-Moscow* **67**: 850-871

Reinikainen T., Takkinen K., Teeri T.T. 1997. Comparison of the adsorption properties of a single-chain antibody fragment fused to a fungal or bacterial cellulose-binding domain. *Enzyme and Microbial Technology* **20**: 143-149

Schulein M. 2000. Protein engineering of cellulases. *Biochimica et Biophysica Acta-Protein Structure and Molecular Enzymology* **1543**: 239-252

Seo Y.B., Shin Y.C., Jeon Y. 2000. Enzymatic and mechanical treatment of chemical pulp. *Tappi Journal* **83**: 64-64

Shen H., Schmuck M., Pilz I., Gilkes N.R., Kilburn D.G., Miller R.C., Warren R.A.J. 1991. Deletion of the Linker Connecting the Catalytic and Cellulose-Binding Domains of Endoglucanase-A (Cena) of *Cellulomonas-Fimi* Alters Its Conformation and Catalytic Activity. *Journal of Biological Chemistry* **266**: 11335-11340

Shimon L.J.W., Pages S., Belaich A., Belaich J.P., Bayer E.A., Lamed R., Shoham Y., Frolow F. 2000. Structure of a family IIIa scaffoldin CBD from the cellulosome of *Clostridium cellulolyticum* at 2.2 angstrom resolution. *Acta Crystallographica Section D-Biological Crystallography* **56**: 1560-1568

Shoham Y., Lamed R., Bayer E.A. 1999. The cellulosome concept as an efficient microbial strategy for the degradation of insoluble polysaccharides. *Trends in Microbiology* **7**: 275-281

Shpigel E., Goldlust A., Eshel A., Ber I.K., Efroni G., Singer Y., Levy I., Dekel M., Shoseyov O. 2000. Expression, purification and applications of staphylococcal Protein A fused to cellulose-binding domain. *Biotechnology and Applied Biochemistry* **31**: 197-203

Shpigel E., Roiz L., Goren R., Shoseyov O. 1998. Bacterial cellulose-binding domain modulates in vitro elongation of different plant cells. *Plant Physiology* **117**: 1185-1194

Simpson H.D., Barras F. 1999. Functional analysis of the carbohydrate-binding domains of *Erwinia chrysanthemi* Cel5 (endoglucanase Z) and an *Escherichia coli* putative chitinase. *Journal of Bacteriology* **181**: 4611-4616

Simpson P.J., Xie H.F., Bolam D.N., Gilbert H.J., Williamson M.P. 2000. The structural basis for the ligand specificity of family 2 carbohydrate-binding modules. *Journal of Biological Chemistry* **275**: 41137-41142

Sinnott M.L. 1990. Catalytic Mechanisms of Enzymatic Glycosyl Transfer. *Chemical Reviews* **90**: 1171-1202

Sorimachi K., Jacks A.J., LeGalCoeffet M.F., Williamson G., Archer D.B., Williamson M.P. 1996. Solution structure of the granular starch binding domain of glucoamylase from *Aspergillus niger* by nuclear magnetic resonance spectroscopy. *Journal of Molecular Biology* **259**: 970-987

Soto C.G., Chamy R., Zuniga M.E. 2004. Effect of enzymatic application on borage (*Borago officinalis*) oil extraction by cold pressing. *Journal of Chemical Engineering of Japan* **37**: 326-331

Srisodsuk M. Mode of action of *Trichoderma reesei* cellobiohydrolase I on crystalline cellulose. 1994. VTT Publications 188. 107p.

Srisodsuk M., Lehtio J., Linder M., MargollesClark E., Reinikainen T., Teeri T.T. 1997. *Trichoderma reesei* cellobiohydrolase I with an endoglucanase cellulose-binding domain: action on bacterial microcrystalline cellulose. *Journal of Biotechnology* **57**: 49-57

Srisodsuk M., Reinikainen T., Penttila M., Teeri T.T. 1993. Role of the Interdomain Linker Peptide of *Trichoderma-Reesei* Cellobiohydrolase-I in Its Interaction with Crystalline Cellulose. *Journal of Biological Chemistry* **268**: 20756-20761

Stork G., Pereira H., Wood T.M., Dusterhoft E.M., Toft A., Puls J. 1995. Upgrading Recycled Pulps Using Enzymatic Treatment. *Tappi Journal* **78**: 79-88

Sykes M., Klungness J.H., Abubakr S., Tan F. 1996. Upgrading Recovered Paper With Enzyme Pretreatment and Pressurized Peroxide Bleaching. *Progress in Paper Recycling* **6**: 39-46

Sykes MS., Klungness J.H. 1997. Enzymatic Removal of Stickie Contaminants. 687-691

Tamai N., Tatsumi D., Matsumoto T. 2004. Rheological properties and molecular structure of tunicate cellulose in LiCl/1,3-dimethyl-2-imidazolidinone. *Biomacromolecules* **5**: 422-432

Teeri T.T. 1997. Crystalline cellulose degradation: New insight into the function of cellobiohydrolases. *Trends in Biotechnology* **15**: 160-167

Tomme P., Boraston A., McLean B., Kormos J., Creagh A.L., Sturch K., Gilkes N.R., Haynes C.A., Warren R.A.J., Kilburn D.G. 1998. Characterization and affinity applications of cellulose-binding domains. *Journal of Chromatography B* **715**: 283-296

Tomme P., Driver D.P., Amandoron E.A., Miller R.C., Antony R., Warren J., Kilburn D.G. 1995. Comparison of A Fungal (Family-I) and Bacterial (Family-Ii) Cellulose-Binding Domain. *Journal of Bacteriology* **177**: 4356-4363

Viesturs U., Leite M., Eisimonte M., Eremeeva T., Treimanis A. 1999. Biological deinking technology for the recycling of office waste papers. *Bioresource Technology* **67**: 255-265

Viikari L., Kantelinen A., Poutanen K., Ranua M. 1990. Characterization of pulps treated with hemicellulolytic enzymes prior to bleaching. *In: Biotechnology in pulp and paper manufacture* (Ed. Kirk T.K. and Chang H.). Butterworth-Heinemann, Boston

Walker L.P., Wilson D.B., Irwin D.C., Mcquire C., Price M. 1992. Fragmentation of Cellulose by the Major Thermomonospora-Fusca Cellulases, Trichoderma-Reesei Cbhi, and Their Mixtures. *Biotechnology and Bioengineering* **40**: 1019-1026

Wang A.A., Mulchandani A., Chen W. 2001. Whole-cell immobilization using cell surface-exposed cellulose-binding domain. *Biotechnology Progress* **17**: 407-411

Wang A.J.A., Mulchandani A., Chen W. 2002. Specific adhesion to cellulose and hydrolysis of organophosphate nerve agents by a genetically engineered Escherichia coli strain with a surface-expressed cellulose-binding domain and organophosphorus hydrolase. *Applied and Environmental Microbiology* **68**: 1684-1689

Warren R.A.J. 1996. Microbial hydrolysis of polysaccharides. *Annual Review of Microbiology* **50**: 183-212

Wong K.K.Y., Hamilton N.T., Signal F.A., Campion S.H. 2004. High-humidity performance of paperboard after treatment with xylanase, endoglucanase, and their combination. *Biotechnology and Bioengineering* **85**: 516-523

MANUSCRIPTS

M1. Large Scale Production of Cellulose-Binding Domains. Adsorption Studies Using CBD-FITC Conjugates

(Published in *Cellulose* **13**, 557-569)

Ricardo Pinto, Joana Carvalho, Manuel Mota and Miguel Gama*

Centro de Engenharia Biológica, Universidade do Minho, Campus de Gualtar, 4710-057 Braga, Portugal

* Author for Correspondence (e-mail: fmgama@deb.uminho.pt; phone: +351 253604400; fax: +351 253678986)

Abstract

A method for the gram-scale production of Cellulose-Binding Domains (CBD) by proteolytic digestion of a commercial enzymatic preparation (Celluclast[®]), was developed. The CBD obtained, isolated from *Trichoderma reesei* cellobiohydrolase I, is highly pure and heavily glycosylated. The purified peptide has a molecular weight of 8.43 kDa, comprising the binding module, a part of the linker, and about 30% of glycosidic moiety. Its properties may thus be different from recombinant ones, expressed in bacteria. CBD-fluorescein isothiocyanate conjugates were used to study the CBD-cellulose interaction. The observation of the fluorescent peptides adsorbed on crystalline and amorphous cellulose fibers suggest that amorphous regions have a higher concentration of binding sites. It is also shown that the adsorption is reversible, but also that desorption is a very slowly process.

Key Words: Cellulose-Binding Domains, Proteolysis, Adsorption, FITC

Abbreviations: CBHI, cellobiohydrolase I; CBHII, cellobiohydrolase II; CBD, cellulose-binding domain; CBD_{CBHI}, cellulose-binding domain of cellobiohydrolase I; FITC, fluorescein isothiocyanate

Introduction

Cellulose is a polymer formed by chains of thousands of glucose molecules linked by β -1,4-glycosidic bonds. These chains pack together through hydrogen bonds, forming microfibrils, which in turn gather to form fibers with a predominantly crystalline character. Microorganisms use a consortium of enzymes to degrade this insoluble material efficiently.

One of these microorganisms is *Trichoderma reesei*, a fungus that produces mainly (80-90%) two exoglucanases (cellobiohidrolase I and II), and several endoglucanases (I, II and V) (Srisodsuk 1994). These two types of enzyme either act from the loose ends of the microfibrils (exoglucanases) or randomly in the macromolecular chain (endoglucanases). One common feature in many of these enzymes is their modular assembly, formed by a catalytic domain, a cellulose-binding domain (CBD) and a highly glycosylated linker (Hui et al. 2001).

CBDs greatly contribute to the enzymes function, by endowing the proteins with cellulose affinity (Srisodsuk et al. 1993). CBDs have highly conserved sequences, namely a three aromatic residue strip that appears to be implicated in the binding process (Mattinen et al. 1997). Two features differentiates CBDs from cellobiohydrolases I and II: one of the CBH II residues in the hydrophobic strip is a tryptophan instead of tyrosine; and the number of disulfide bridges is different (three in CBH II, only two in CBH I). These differences appear to have a major impact in the adsorption behavior: $CBD_{CBH II}$ irreversibly binds BMCC, whereas $CBD_{CBH I}$ adsorption is reversible (Carrard and Linder 1999; Linder et al. 1999).

Xiao et al. (2001) showed that CBD from endoglucanase III has the ability to disrupt the crystalline structure of cellulose fibers. A similar result was observed with a CBD from *Penicillium janthinellum*, in the treatment of cotton fibers (Gao et al. 2001). Another interesting work (Carrard et al. 2000) showed that different CBDs adsorb to different sites in the surface of crystalline cellulose. These results strongly suggest that CBDs may be functionally more sophisticated than just a tool for the enzyme adsorption.

Limited proteolysis of cellulases as been used by other authors to isolate the catalytic domain (Tilbeurgh et al. 1986; Harrison et al. 2002; Lemos et al. 2000), but not the large scale production of binding modules, as described in this work. In order to study the interaction with cellulose, the CBDs obtained were used to analyze the FITC-labeled CBD adsorption and distribution on different cellulose materials.

Materials and Methods

Chemicals

FITC was obtained from Sigma. The cellulose samples used were obtained from Fluka (Avicel PH-101) and Sigma-Aldrich (Whatman CF11). All chemicals were of the highest purity available.

CBD Production

The commercial enzymatic preparation Celluclast 1.5L (Novozymes A/S, Denmark), produced by the fungus *Trichoderma reesei*, was firstly diluted 1:4 with acetate buffer (pH 5.0, 25 mM) and dia-filtered through a 30 kDa ultra filtration membrane, using a Pellicon 2 TFF System (Millipore, USA). The papain activation was carried out mixing a diluted solution (1:1000 v/v) of β -Mercaptoethanol with papain (1:10) for 15 minutes. After 4 hours of proteolysis at room temperature, the solution was filtered through a 10 kDa membrane and the permeate recovered. Ammonium sulphate was then added (700 g/L) to the permeate solution in order to precipitate the peptides, which were recovered by centrifugation at 12225 RCF (relative centrifugal acceleration) for 40 minutes (Sigma 4K10, B. Braun). This concentrated solution was finally dialyzed against phosphate buffer (pH 7.5, 20 mM), using a 1 kDa cutoff membrane. Deglycosylated CBD were prepared as described elsewhere (Edge et al. 1981). Treatment with trifluoromethanesulfonic acid (TFMS) was carried out for 30 minutes. Longer periods lead to fragmentation of the protein, while shorter periods were insufficient for the complete sugar removal (as monitored by sugar and protein quantification of the dialysed material).

Ion Exchange Chromatography

The peptides were further purified using a column packed with DEAE Sepharose Fast-Flow gel (Amersham Pharmacia Biotech AB, Sweden), using phosphate buffer (pH 7.5, 20 mM) as eluent and a flow rate of 3 mL/min. The first peak (non adsorbed protein) was recovered and lyophilized.

N-terminal Peptide Sequencing

Purified CBDs were sequenced on an Applied Biosystems Procise 491 HT, according to manufacturer's specifications.

Capillary Electrophoresis

A BioFocus 2000 Capillary Electrophoresis System (Bio-Rad) was used. All the solutions used were purchased from Bio-Rad (CE-SDS Protein Kit). An uncoated fused-silica (Bio-Rad) capillary, with an internal diameter of 50 μm and a length of 24 cm, was used. The electrophoresis run conditions were as follows: capillary temperature of 20 $^{\circ}\text{C}$, CE-SDS Protein Run Buffer, 15 kV constant run voltage, on-line detection at 220 nm and electrophoretic injection by application of 15 kV for 10 seconds. Calibration was performed with three proteins (Sigma-Aldrich) of known molecular sizes: BSA (66 kDa), Pepsin (35 kDa) and Lysozyme (14.5 kDa).

Sugar analysis

The monosaccharides in the CBD glycosidic fraction were released by Saeman hydrolysis (Selvendran et al. 1979) and analyzed as their alditol acetates by gas chromatography (Blakeney et al. 1983; Harris et al. 1988), using a Chrompack CP9001 equipped with a Flame Ionization Detector and a Varian CP-Sil 88 column. Total sugars were also measured using the phenol-sulfuric method (Dubois et al. 1956), with mannose as standard.

MALDI-TOF

The measurements were made on a Voyager-DETM STR (Applied Biosystems). The sample was diluted on the matrix reagent, sinapinic acid. Calibration was performed using the Pepmix 3 (LaserBio Labs, France) peptide mix.

CBD Affinity and Binding Reversibility

Suspensions of Whatman CF11 fibers, with a concentration of 10 mg per mL in Sodium Acetate buffer (50 mM, pH 5.0) were incubated for 16 hours at 5 $^{\circ}\text{C}$, with magnetic agitation, in the presence of different CBD concentrations ($CBD_{Initial}$). Afterwards, the fibers were centrifuged at 4000 rpm for 10 minutes, and the CBD concentration in the supernatant ($CBD_{Unbound}$) was measured in a Jasco FP6200 spectrofluorimeter, operated at an emission and excitation wavelengths of 341 and 275 nm, respectively. The apparatus was calibrated using CBD solutions with determined concentration using BCA Protein Assay, from Pierce. The bound CBD was calculated using the following equation:

$$CBD_{Bound} = \frac{[CBD_{Initial}] - [CBD_{Unbound}]}{m_{CF11}} \cdot V_R \quad (\mu\text{mol}_{CBD}/\text{g}_{CF11})$$

where V_R corresponds to the volume of buffer used, $[CBD_x]$ to the molar concentration of CBD and m_{CF11} to the fibers mass.

Fluorescence Spectroscopy

A FP-6200 Spectrofluorimeter apparatus (Jasco Corporation, Japan) was used. The band width of excitation and emission was 5 nm and the scan speed was 1000 nm/min. A constant excitation at 275 nm was used.

Amorphous Cellulose Preparation

Amorphous cellulose was prepared treating Whatman CF11 fibers with phosphoric acid. Briefly, 0.17 g of Whatman CF11 were slowly mixed with 10 mL of cold (4 °C) phosphoric acid (85%) and left in contact for 5 minutes. Then, 600 mL of cold water were added and the suspension was filtered through a test sieve (mesh width 71 μm according to DIN 4188). Finally, the fibers were extensively washed, firstly in tap water and afterwards with distilled water. The obtained material was lyophilized and stored.

CBD-FITC Conjugation and Adsorption

Fluorescein isothiocyanate (FITC) is a fluorescent probe widely used to attach a fluorescent label to proteins, by reacting with amine groups. CBD were labeled by standard procedures. Briefly, 20 μg of FITC was added per mg of CBD (in a concentration of 2 mg protein/mL in 0.1 M HEPES buffer, pH 9.0). This solution was incubated overnight in the dark, at room temperature, with magnetic stirring. To separate unbound FITC from FITC-CBD, the mixture was filtered through a BIO-GEL P-4 (BIO-RAD) column, previously equilibrated with 50 mM sodium acetate buffer (pH 5.0). Fractions containing significant amounts of FITC-CBD were pooled. The fluorescence at an excitation/emission of 275/310 nm and 495/525 nm was measured, to determine CBD concentration and FITC fluorescence, respectively.

Adsorption assays were carried out at 4 °C. FITC-labeled CBD solutions with different concentrations were mixed in the dark with cellulose fibers (20 g/L), in 50 mM sodium acetate buffer, to a final volume of 4 mL. The suspension was continuously stirred. After 2 hours reaction, cellulose fibers with bound CBD were removed by centrifugation at 3219 RCF for 10 minutes (Heraeus Megafuge 1.0R). The difference between the initial amount of CBD and that of the supernatant allowed the calculation of the bound CBD, gained from the fluorescence emission at 310 nm with an excitation of 275 nm.

Fluorescence microscopy observations were performed in a Zeiss AxiosKop microscope. The images were acquired with a Zeiss AxioCam HRc camera and analyzed with the AxioVision 3.1 software.

Results and Discussion

Large scale production of CBDs

The main enzymes produced by *Trichoderma reesei* have an average size of approximately 50 kDa, as obtained from Swiss-Prot database (Gasteiger et al. 2003). The capillary electrophoresis analysis (Figure M1.1) of the Celluclast proteins provides an estimation of the apparent molecular weight, of approximately 90 kDa, according to the calibration performed with protein standards. This overestimation may be due to the glycosidic moiety of the enzymes, which may affect the migration time by changing the overall protein charge (Leach et al. 1980; Legaz et al. 1998). These authors showed that the glycosidic moiety may increase the negative charge of an anionic protein, since the hydroxyl groups in the sugar structure behave as weak acids. Consequently, migration of glycosylated proteins in CE is affected by the glycosidic moiety, therefore this technique herein used to monitor, qualitatively, the relative size of the peptides obtained by papain proteolysis.

The proteolysis of Celluclast using several dilutions of the activated papain was performed. As can be seen in the electropherogram shown in Figure M1.2, heavier loads of papain results in a more dramatic reduction of the main peak corresponding to higher molecular weight proteins, with the concomitant increase of the peaks corresponding to lower molecular weight material. Based on these studies, the relative amounts of papain/cellulase were selected for the production of CBDs (1 g of activated papain for each 1200 g of protein in the 30 kDa ultrafiltered Celluclast). With higher papain concentration, hydrolysis is too extensive. The production of a mixture of fragments with low molecular weight was avoided, using the selected concentration of papain, as it is shown ahead. Finally, the electropherogram obtained with the purified CBDs (Figure M1.1) reveals a low molecular weight peptide, with no apparent contamination from higher molecular weight material. Again, the migration time of this peptide was higher than the expected for a CBD, corresponding to a mass of about 20-30 kDa. This high apparent molecular weight may be explained by the glycosidic moiety present on the linker (rich in threonin and serine residues), since CBD has no potential sites for glycosylation (Harrison et al. 1998; Hui et al. 2001). Indeed, the obtained peptide have 30% (w/w) of carbohydrates, as

determined by total sugars analysis, with a monosaccharide composition of 85% mannose, 12% galactose and minor amounts of other sugars, as determined by GC.

The MALDI-TOF analysis of the purified CBD is shown in Figure M1.3. The sample is highly micro-heterogeneous in size, a main peak being detected at 8.43 kDa. The several satellite peaks have an almost constant difference from one another of $162(\pm 1)$ mass units (8106, 8267, 8430, 8591, 8755, 8917, 9080 Da) that presumably arises from differential glycosilation (Letourneur et al. 2001; Hui et al. 2001). A lower molecular weight group of peaks, at 4.21 kDa, corresponds to the same peptide, with a charge of +2. Indeed, a series of peaks with half the mass of the ones listed above are detected (4053, 4134, 4215, 4296, 4379, 4459, 4539, 4622 Da), with a difference between peaks of $81(\pm 1)$ mass units. This pattern, in our view, can be attributed only to a protein with heterogeneous glycosilation. The concentration of fragments with a very narrow size distribution (from 8 to 9 kDa) means that proteolysis was quite mild, otherwise a scattered size distribution of low molecular weight peptides would be observed, in spite of the fact that papain is a proteolytic enzyme with a broad specificity (Price and Johnson 1990). The MALDI spectra furthermore suggests (as demonstrated ahead by sequential analysis) that the peptide is highly pure, since no high molecular weight peaks were detected.

Proteolysis of Celluclast allowed the production of over 2 g of CBD, starting from 50 g of protein. This material was further purified by ion exchange chromatography. The obtained chromatogram revealed a main peak of non-adsorbed material (uncharged, corresponding to CBDs) and a second peak, eluted with a NaCl gradient, corresponding to charged material (cellulases and catalic domains with acidic pI). To further characterize this purified peptides, the fluorescence spectra of the CBD samples were analyzed, before and after ion exchange chromatography. Tyrosine and tryptophan residues have a maximum emission at, respectively, 305 and 340 nm. According to spectra in Figure M1.4, the chromatography step removed a substantial part of the tryptophan residues present in the solution. The CBD from cellobiohidrolase I (CBHI) is, among the enzymes produced by *Trichoderma reesei*, the only one missing tryptophan (Kraulis et al. 1989; Gasteiger et al. 2003). Consequently, it appears that the CBDs obtained are mostly from CBHI, as expected, since this is the most abundant enzyme secreted from *T. reesei*. N-terminal sequence analysis confirms this hypothesis. Indeed, the sequence obtained, GNPPG, is present only in CBHI, between the catalytic domain and the linker (Gasteiger et al. 2003). Since the isolated peptides are produced by papain cleavage, the presence of N-terminal blocked peptides in the mixture is rather unlikely. Thus, the result in Figure M1.5 demonstrates that the CBD purified by Ion Exchange chromatography is rather pure, since only one amino acid is released in each step of the N-terminal sequence analysis.

Taken together with evidence from MALDI analysis, it is possible to conclude that highly pure CBD have been obtained, and that papain (in the conditions of the assay), cleaves CBHI in a single position of the peptide sequence, a somewhat surprising result. This suggests a protection of the linker against proteolysis, due to glycosylation, and that there is only one site exposed to the protease. The theoretical molecular weight of the protein exhibiting the N-terminal GNPPG is 6.22 kDa (Gasteiger et al. 2003). This is coherent with a protein with 8.43 kDa (determined by MALDI) and about 30% of sugars. Several authors (Hui et al. 2001; Harrison et al. 1998) reported strains of *Trichoderma reesei* with different peptide sequence than the one reported in the Swiss-Prot database (<http://www.expasy.ch/cgi-bin/niceprot.pl?P62694>), where the arginine in position 442 is substituted by two prolines (⁴³¹NPSGGNPPGG NPPGTTTTRR⁴⁵⁰). In this case, a protein with 5.84 kDa, exhibiting the N-terminal sequence GNPPG, would be obtained by proteolysis. MALDI-TOF analysis of the deglycosylated CBD (Figure M1.6) reveals a protein (the main one in the mixture) that exactly matches this value, 5.84 kDa.

The removal of the tryptophan containing peptides, by Ionic Exchange Chromatography, has led also to an increase in the cellulose affinity of the remaining material, as revealed by the analysis of the Langmuir adsorption isotherm (Kim et al. 2001):

$$CBD_{Bound} = \frac{CBD_{Max} \cdot K_a \cdot [CBD]_{Free}}{1 + K_a \cdot [CBD]_{Free}}$$

where CBD_{Bound} is the molar amount of protein adsorbed, per unit weight of cellulose, $[CBD]_{Free}$ is the molar protein concentration in the liquid phase at the adsorption equilibrium, CBD_{Max} and K_a are the maximum molar amount of protein adsorbed, per unit weight of cellulose, and the adsorption equilibrium constant, respectively. Non-linear regression analysis was used to calculate the parameters of the adsorption isotherm (Figure M1.7): CBD_{Max} and K_a are equal to 4.62 $\mu\text{mol/g}$ and 0.192 L/ μmol as compared to 3.13 $\mu\text{mol/g}$ and 0.133 L/ μmol , respectively, for CBDs before and after ionic chromatography (Pinto et al. 2004). Values for the partition coefficient (initial slope of the adsorption isotherm) increased from 0.35 L/g (previous data) to 0.89 L/g. It appears that the chromatographic step mainly remove peptides with low cellulose affinity.

Cellulose-binding modules may be obtained, with high purity, using DNA technology (Bothwell et al. 1997; Creagh et al. 1996; Linder et al. 1999). Purification of CBD by proteolysis of cellulases, as described in this work, provides large amounts of peptides in a rather fast way. This method may be useful for a number of applied and analytical studies. The CBD obtained include a part of the linker, and is heavily glycosylated, as expressed by fungi. In this regard, these peptides are different from those available by recombinant DNA technology, and

furthermore, in our view, its properties should be analyzed and compared to nonglycosylated CBDs. This material may as well be used for structural studies of oligosaccharides from the CBHI linker.

Studies on the adsorption of CBD-FITC conjugates

Cellulose is the main component in many commercial products, from textile to paper and filtration membranes. CBD can mediate the targeting of functional molecules to cellulose-containing materials (Levy 2002), bringing new properties and functionalities to those materials. On the other hand, as it has been suggested by some authors (Gao et al. 2001; Xiao et al. 2001), CBD are capable of non-hydrolytic disruption activity and surface modification of cellulose fibers. Previous studies demonstrated that CBD may have a beneficial effect on pulp properties (Suurnakki et al. 2000) and can be useful in paper recycling (Pala et al. 2001). CBD technology is consequently a valuable tool in the development of modified materials with improved properties.

Having this in mind, we attempted in this work to evaluate CBD distribution in cellulose surfaces. This was achieved by attaching a fluorescent probe (FITC) to CBD; the fibers treated with labeled CBDs are then observed microscopically, using a filter to select fluorescence emission. A control assay was carried out using free FITC (not linked to CBDs), in order to detect non-specific adsorption to cellulose. The presence of free FITC molecules mixed with CBD-FITC is unlikely, because it was removed by exclusion chromatography, as described in the methods section. As reported by other authors (Hildén *et al.*, 2003), we verified that the presence of the free fluorescent probe in the surface of cellulose fibers is not detected, in the conditions of the experiment. A range of concentrations, from 0 to 300 µg/mL of labeled CBDs, was used in the treatment of different cellulose fibers: Avicel and Whatman CF11. As may be seen in Figure M1.8 (left column), no fluorescent emission was detected in the control (non-treated) fibers. As the FITC labeled CBD concentration raises (50, 100 and 300 µg/mL) and, consequently, the amount of adsorbed labeled peptides (a minimum of 79% adsorption was recorded), the fluorescence emission increases as well. It appears that this approach allows, at least, a qualitative characterization of the relative concentration of adsorbed CBDs. Indeed, it has been possible to quantitatively estimate the amount of adsorbed protein (to be shown elsewhere). It should be noticed that CBD distribution on the fibers is not uniform, they rather concentrate around the fiber extremities.

In another experiment, we aimed at checking whether the CBD adsorption is a reversible process. Cellulose fibers, previously treated with labeled CBDs, were mixed in fresh buffer with

untreated fibers. This mixture of fibers was kept in suspension with orbital stirring, and samples were collected for microscopic observation, from time to time. The goal of this experiment was to evaluate whether CBD would transfer among fibers. In Figure M1.9, we may see that initially (0 hours – top row) both fluorescent and non-fluorescent fibers are detected, by comparing the images obtained with bright field or fluorescent microscopy. Only the fibers pretreated with CBD-FITC are visible using both fluorescent and bright field, while the untreated fibers are visible only using bright field. As the time of contact in aqueous suspension, of untreated and CBD-FITC treated fibers, increases, it appears that gradually (2-192 h), all of the fibers become fluorescent. However, a uniform distribution of CBDs is not observed even after a long time of contact (~192 h), as expected if the CBD were perfectly reversibly adsorbed. In an earlier work (Pinto et al. 2004), it was shown that the dilution of fibers with adsorbed CBDs (in equilibrium with soluble peptides) did not lead to an increase of the unbound CBD concentration. This has led to the conclusion that CBD were irreversibly adsorbed. The results now obtained demonstrate that, in fact, CBD are not totally irreversibly adsorbed. This experiment also shows that desorption may be a rather slow process. For instance, after 24 h of incubation some fibers, observed with bright field, are still not detected when a filter for select fluorescent emission is used. Several experiments were conducted and the images shown in Figure M1.9 represent the general trend observed: labeled CBDs transfer, very slowly, from fiber to fiber. It should be remarked that the results shown in Figure M1.9 represent a consistent general trend, by microscopic observation of the fibers. An alternative approach to study the transfer of CBDs among fibers was considered, based on the analysis of the fluorescence exhibited by one specific fiber, and its variation along with the incubation time, checking the release (desorption) of adsorbed CBDs. However, this is not a feasible approach, since the specific fluorescence of the fibers is modified upon repeated observation.

Whatman CF11 is essentially a crystalline cellulose (Pinto et al. 2004), but a few amorphous spots, e.g. fiber's terminations and middle twisted regions are also present in celluloses purified from wood (Teeri 1997). Disordered microfibrils packing characterize these regions (non-uniformity), resulting in a higher surface area available for CBD adsorption. This would explain why the extremities and some middle regions of the crystalline fibers present a brighter fluorescence (Figure M1.10 – top pictures). This may be due either to a higher peptide affinity, or to a higher concentration of adsorbing sites at the fibers surface (Hildén et al. 2003). As a matter of fact, it has been shown by other authors (Linder et al. 1996; Bothwell et al. 1997) that CBDs have differential affinity for celluloses with different crystallinity and/or surface areas. It is therefore likely that the non-uniform surface distribution of CBDs may reveal this

differential affinity (which may depend on different degrees of cellulose organization, hydrophilicity, irregularity, etc). The mode of action of the CBH I enzyme can also explain this behavior, since it acts from the loose ends of microfibrils (Teeri 1997). Therefore, it seems likely that CBD_{CBHI} would adsorb preferentially at the microfibril's loose ends (mainly in amorphous regions). It appears that the labeled CBD may be used to identify, and possibly quantify, the amorphous regions/fibers of cellulose products.

Conclusions

With the CBD production method presented herein, it is possible to obtain grams of protein in a relatively fast way. The CBDs obtained are almost pure and identified as belonging to *Trichoderma reesei*'s cellobiohydrolase I, according to the N-terminal sequencing, MALDI analysis and the fluorescence spectrum. The purified protein comprises the CBD with the attached glycosylated linker. In forthcoming work, the effect of oligosaccharides on the CBD properties will be analyzed. The microscopic observation of fibers treated with FITC labeled CBDs reveals that these have higher affinity towards amorphous cellulose. It was also shown that CBDs adsorption is partially reversible, although desorption occurs at a very low rate. FITC-labeled CBD may be used to implement a quick method to visually detect the crystallinity degree of celluloses from different sources.

Acknowledgements

Ricardo Pinto was supported by Fundação para a Ciência e a Tecnologia (FCT) grant SFRH/BD/6934/2001. The authors thank funding from EU and FCT, respectively, through the projects GLK3/CT/2000/273 and POCTI AGR/38253/2009.

We wish to acknowledge Ana Varela Coelho for providing the MALDI-TOF data and Maria Manuela Regalla for the N-terminal sequencing analysis, both at the Instituto de Tecnologia Química e Biológica, Universidade Nova de Lisboa, Oeiras, Portugal.

Bibliography

Blakeney A.B., Harris P.J., Henry R.J. and Stone B.A. 1983. A simple and rapid preparation of alditol acetates for monosaccharide analysis. *Carbohydr Res* 113: 291–299.

Bothwell M. K., Daughhetee S. D., Chau G. Y., Wilson D. B. and Walker L. P. 1997. Binding capacities for *Thermomonospora fusca* E3, E4 and E5, the E3 binding domain, and *Trichoderma reesei* CBHI on avicel and bacterial microcrystalline cellulose. *Bioresource Tech* 60: 169–178.

Carrard G. and Linder M. 1999. Widely different off rates of two closely related cellulose-binding domains from *Trichoderma reesei*. *Eur J Biochem* 262: 637–643.

Carrard G., Koivula A., Söderlund H. and Béguin P. 2000. Cellulose-binding domains promote hydrolysis of different sites on crystalline cellulose. *PNAS* 97: 10342–10347.

Creagh A., Ong E., Jervis E., Kilburn D. Haynes C. 1996. Binding of the cellulose-binding domain of exoglucanase Cex from *Cellulomonas fimi* to insoluble microcrystalline cellulose is entropically driven. *Proc Natl Acad Sci USA* 93: 12229–12234.

Dubois M., Gilles K. A., Hamilton J. K., Rebers P. A., Smith F. 1956. Colorimetric method for determination of sugars and related substances. *Analyt Chem* 28: 350–356.

Edge A.S.B., Connie R.F., Hof L., Reichert L.E. and Weber P. 1981. Deglycosylation of glycoproteins by trifluoromethanesulfonic acid. *Anal Biochem* 118: 131–137.

Gao P.-J., Chen G.-J., Wang T.-H., Zhang Y.-S. and Liu J. 2001. Non-hydrolytic disruption of crystalline structure of cellulose by cellulose binding domain and linker sequence of cellobiohydrolase I from *Penicillium janthinellum*. *Acta Biochimica et Biophysica Sinica* 33: 13–18.

Gasteiger E., Gattiker A., Hoogland C., Ivanyi I., Appel R.D. and Bairoch A. 2003. ExPASy: the proteomics server for in-depth protein knowledge and analysis. *Nucleic Acids Res* 31: 3784–3788.

Harris P.J., Blakeney A.B., Henry R.J. and Stone B.A. 1988. Gas chromatographic determination of the monosaccharide composition of plant cell wall preparations. *J Assoc Off Anal Chem* 71: 272–275.

Harrison M.J., Nouwens A.S., Jardine D.R., Zachara N.E., Gooley A.A., Nevalainen H. and Packer N.H. 1998. Modified glycosylation of cellobiohydrolase I from a high cellulase-producing mutant strain of *Trichoderma reesei*. *Eur. J. Biochem.* 256: 119–127.

Harrison M.J., Wathugala I.M., Tenkanen M., Packer N.H. and Nevalainen K.M.H. 2002. Glycosylation of acetylxyylan esterase from *Trichoderma reesei*. *Glycobiol* 12: 291–298.

Hildén L., Daniel G. and Johansson G. 2003. Use of a fluorescence labelled, carbohydrate-binding module from *Phanerochaete chrysosporium* Cel7D for studying wood cell wall ultrastructure. *Biotech Lett* 25: 553–558.

Hui J.P.M., Lanthier P., White T.C., McHugh S.G., Yaguchi M., Roy R. and Thibault P, 2001. Characterization of cellobiohydrolase I (Cel7A) glycoforms from extracts of *Trichoderma reesei* using capillary isoelectric focusing and electrospray mass spectrometry. *J Chromatogr B* 752: 349–368.

Kim D. W., Jang Y. H., Kim C. S. and Lee N.-S. 2001. Effect of metal ions on the degradation and adsorption of two cellobiohydrolases on microcrystalline cellulose. *Bull Korean Chem Soc* 22: 716–720.

Kraulis P.J., Clare G.M., Nilges M., Jones T.A., Pettersson G., Knowles J. and Gronenborn A.M. 1989. Determination of the three-dimensional solution structure of the C-terminal domain of cellobiohydrolase I from *Trichoderma reesei*. A study using nuclear magnetic resonance and hybrid distance geometry-dynamical simulated annealing. *Biochemistry* 28: 7241–7257.

Leach B. S., Collawn J. F. and Fish W. W. 1980. Behavior of glycopeptides with empirical molecular weight estimation methods. *Biochemistry* 19: 5734–5741.

Legaz M.E., Pedrosa M.M., Armas R., Rodríguez C.W., Rios V. and Vicente C. 1998. Separation of soluble glycoproteins from sugarcane juice by capillary electrophoresis. *Anal Chim Acta* 372: 201–208.

Lemos M.A., Teixeira J.A., Mota M. and Gama F.M. 2000. A simple method to separate cellulose-binding domains of fungal cellulases after digestion by a protease. *Biotech Lett* 22: 703–707.

Letourneur O., Gervasi G., Gaia S., Pages J., Watelet B. and Jolivet M. 2001. Characterization of *Toxoplasma gondii* surface antigen 1 (SAG1) secreted from *Pichia pastoris*: evidence of hyper O-glycosylation. *Biotechnol Appl Biochem* 33: 35–45.

Levy I., Shani Z. and Shoseyov O. 2002. Modification of polysaccharides and plant cell wall by endo-1,4- β -glucanase and cellulose-binding domains. *Biomol Eng* 19: 17–30.

Linder M., Salovuori I., Ruohonen L. and Teeri T.T. 1996. Characterization of a Double Cellulose-binding Domain. Synergistic High Affinity Binding To Crystalline Cellulose. *J Biol Chem* 271: 21268–21272.

Linder I., Nevanen T. and Teeri T.T. 1999. Design of a pH-dependent cellulose-binding domain. *FEBS Lett* 447: 13–16.

Mattinen M.-L., Linder M., Teleman A. and Annala A. 1997. Interaction between cellobiohexanase and cellulose binding domains from *Trichoderma reesei* cellulases. *FEBS Lett* 407: 291–296.

Pala H., Lemos M.A., Mota M. and Gama F.M. 2001. Enzymatic upgrade of old paperboard containers. *Enzyme Microb Technol* 29: 274–279.

Pinto R., Moreira S., Mota M. and Gama M. 2004. Studies on the cellulose-binding domains adsorption to cellulose. *Langmuir* 20: 1409–1413.

Price N.C., Johnson C.M. 1990. Proteinases as probes of conformation of soluble proteins. In R.J. Beynon and Bond J.S (eds.) *Proteolytic enzymes: A practical approach*. IRL Press, Oxford, pp. 163–180.

Selvendran R.R., March J.F. and Ring S.G. 1979. Determination of aldoses and uronic acid content of vegetable fiber. *Anal Biochem* 96:282–292.

Srisodsuk M., Reinikainen T., Pentillä M. and Teeri T.T. 1993. Role of the interdomain linker peptide of *Trichoderma reesei* Cellobiohydrolase I in its interaction with crystalline Cellulose. *J Biol Chem* 266: 20756–20761.

Srisodsuk M. 1994. Mode of action of *Trichoderma reesei* cellobiohydrolase I on crystalline cellulose. Ph.D. Thesis, Technical Research Centre of Finland (VTT), Helsinki, Finland.

Suurnakki A., Tenkanen M., Siika-aho M., Niku-Paavola M.-L., Viikari L. and Buchert J. 2000. *Trichoderma reesei* cellulases and their core domains in the hydrolysis and modification of chemical pulp. *Cellulose* 7: 189–209.

Tilbeurgh H.V., Tomme P., Claeysens M., Bhikhabhai R. and Pettersson G. 1986. Limited proteolysis of the cellobiohydrolase I from *Trichoderma reesei*. Separation of functional domains. *FEBS Letters* 204: 223–227.

Teeri T.T. 1997. Crystalline cellulose degradation: new insight into the function of cellobiohydrolases. *Trends in Biotech* 15: 160–167.

Xiao Z., Gao P., Qu Y. and Wang T. 2001. Cellulose-binding domain of endoglucanase III from *Trichoderma reesei* disrupting the structure of cellulose. *Biotechnol Letters* 23: 711–715

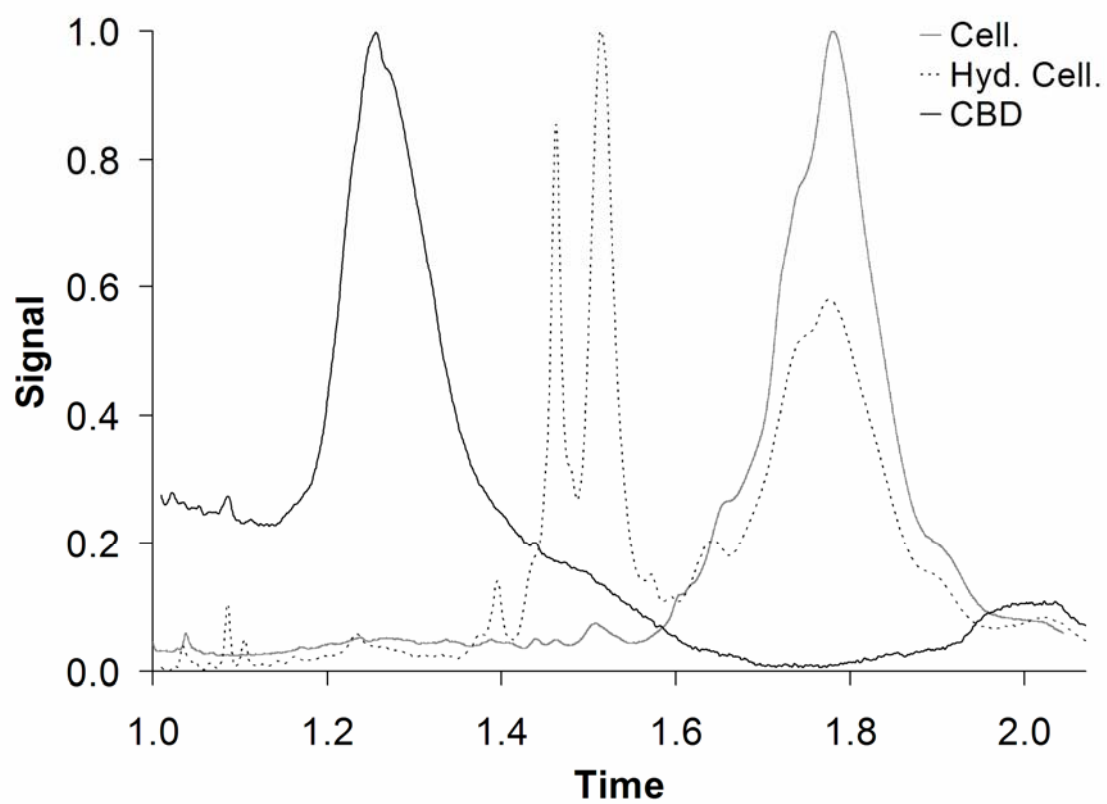
Figures

Figure M1.1. Electropherogram of Celluclast (Cell.), hydrolyzed Celluclast (Hyd. Cell.) and Cellulose-Binding Domains (CBD). Both time and signal are normalized.

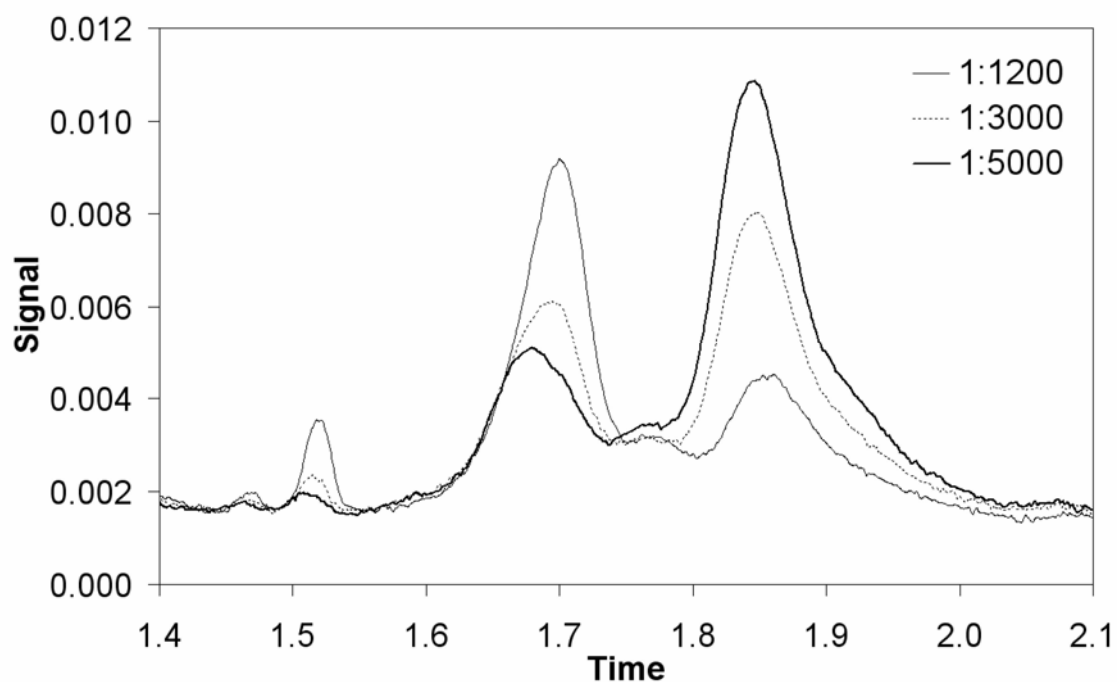


Figure M1.2. Electropherogram of Celluclast hydrolyzed with different amounts of papain by protein weight (the dilution factor of the commercial enzyme is shown). Time is normalized.

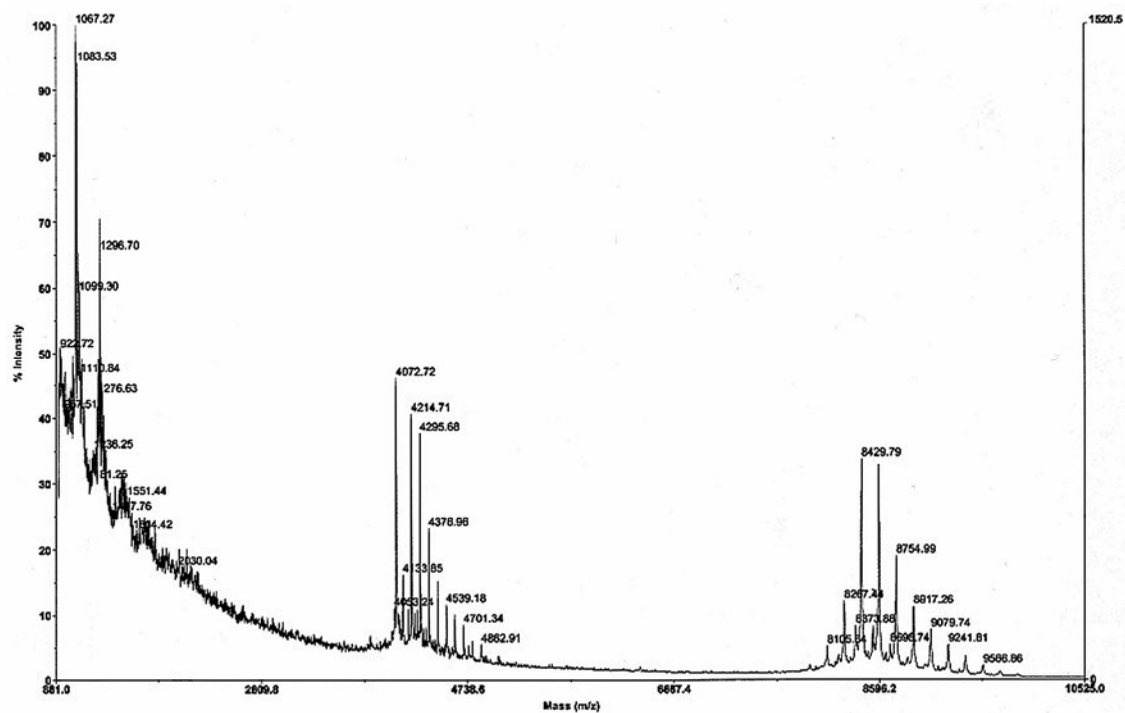


Figure M1.3. MALDI-TOF analysis of the purified CBD peptides.

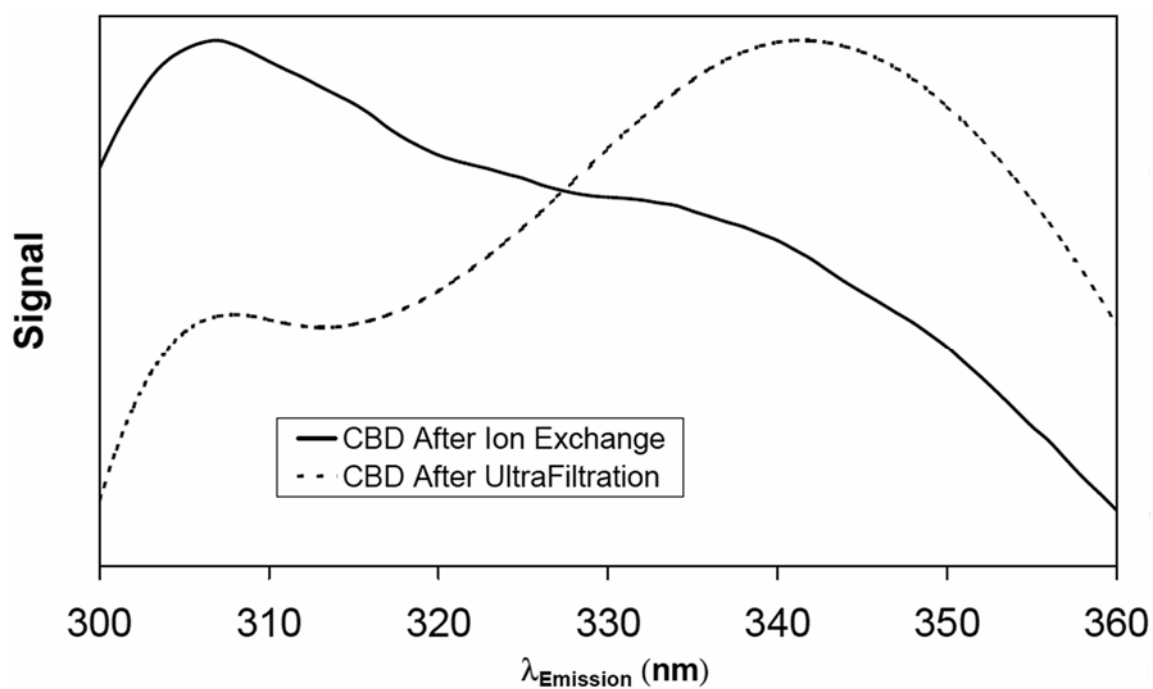


Figure M1.4. Fluorescence Spectrums of CBD after ultra filtration and the subsequent Ion Exchange purification. Signals are normalized to the highest value obtained on each measurement.

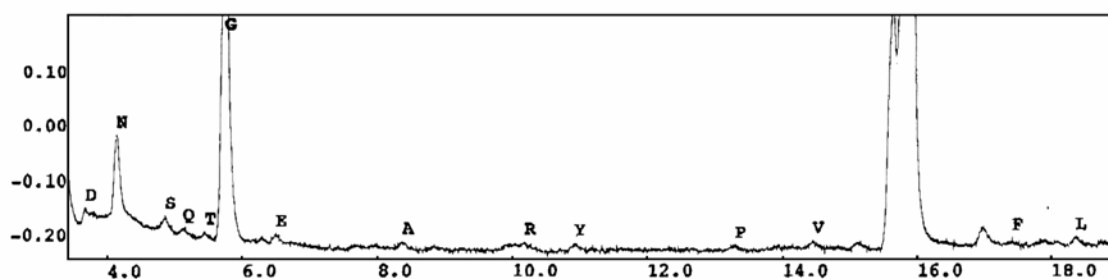


Figure M1.5. Chromatogram of the first amino acid detected on the N-terminal peptide sequencing of the purified CBD. This chromatogram reveals that the isolated CBD is rather pure.

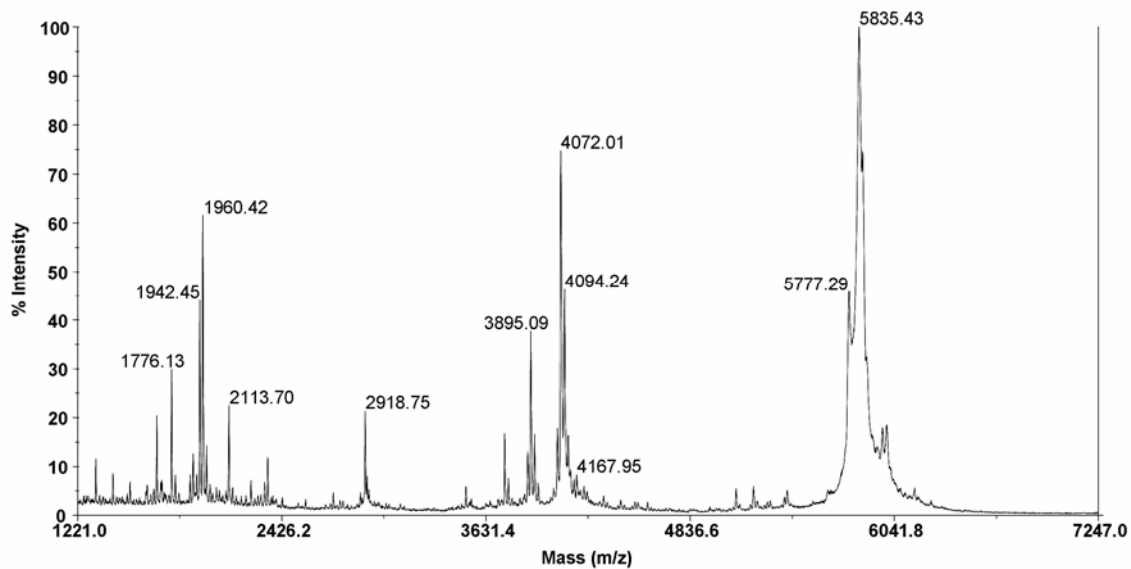


Figure M1.6. MALDI-TOF analysis of the deglycosylated CBD peptides. The heterogeneous peak observed in Figure 3 (8.43kDa) is replaced by a main peak at 5.84 kDa. The complete removal of the glycosidic fraction with TFMS leads to some proteolysis, several peaks not observed prior to TFMS treatment (nor when the treatment is performed under milder conditions) being detected (1700-4000Da).

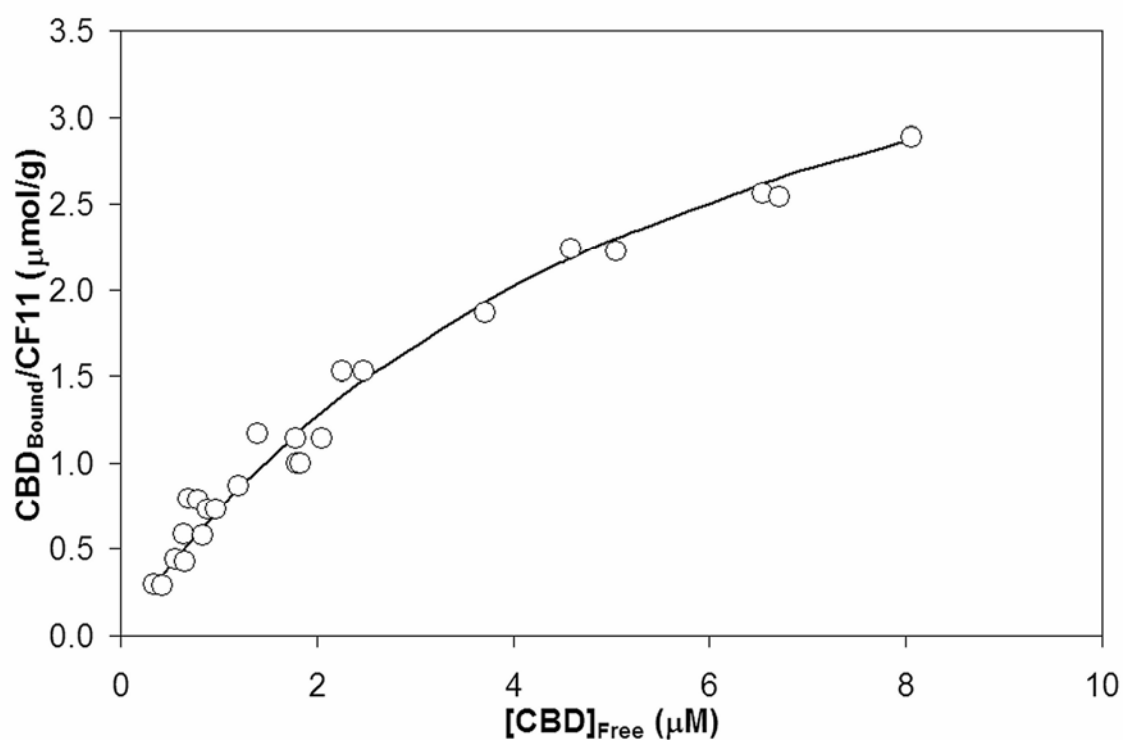


Figure M1.7. Adsorption isotherm of CBDs purified by ion exchange chromatography.

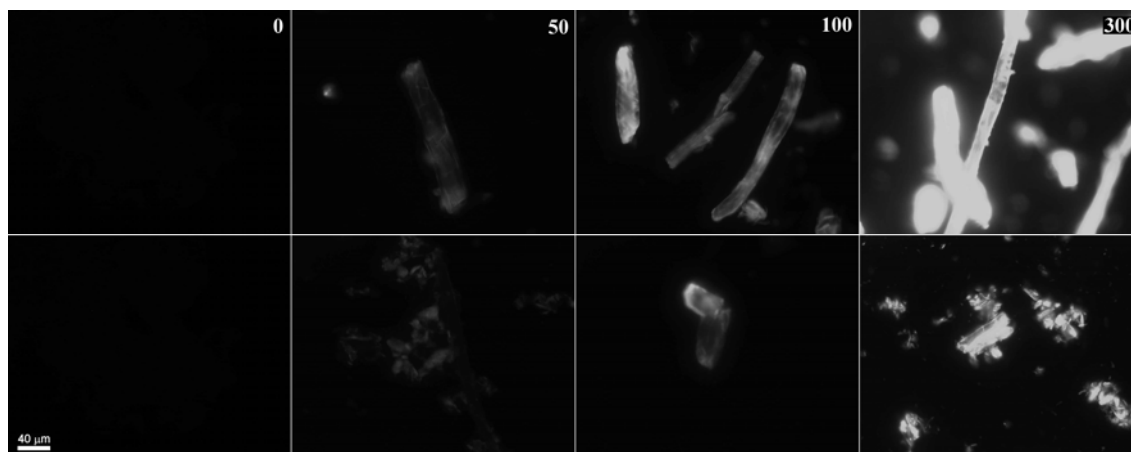


Figure M1.8. Fluorescence microscopy of Whatman CF11 (upper row) and Avicel (lower row) cellulose fibers treated with labeled CBDs, with different initial concentrations (0, 50, 100 and 300 μg/mL). In the control fibers (left column), as expected, no fluorescence was detected. The micrographs were obtained using the same exposure time.

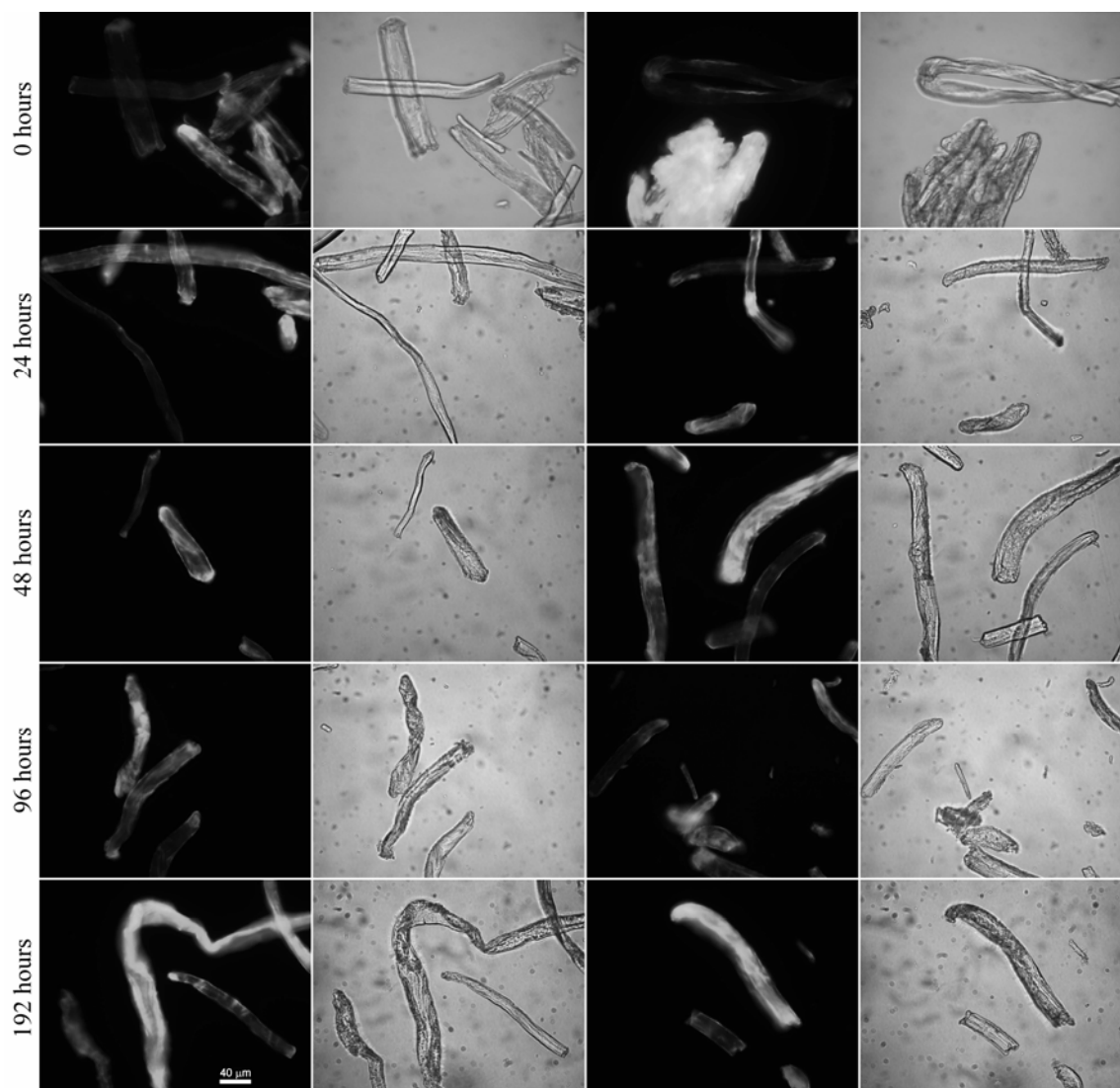


Figure M1.9. Images of a mixture of treated and untreated CF11 cellulose fibers with labeled CBD, under fluorescent (first and third column) and bright field (second and fourth column) microscopy, with 400 milliseconds of exposure time, put in contact for 0, 24, 48, 98 and 192 hours.

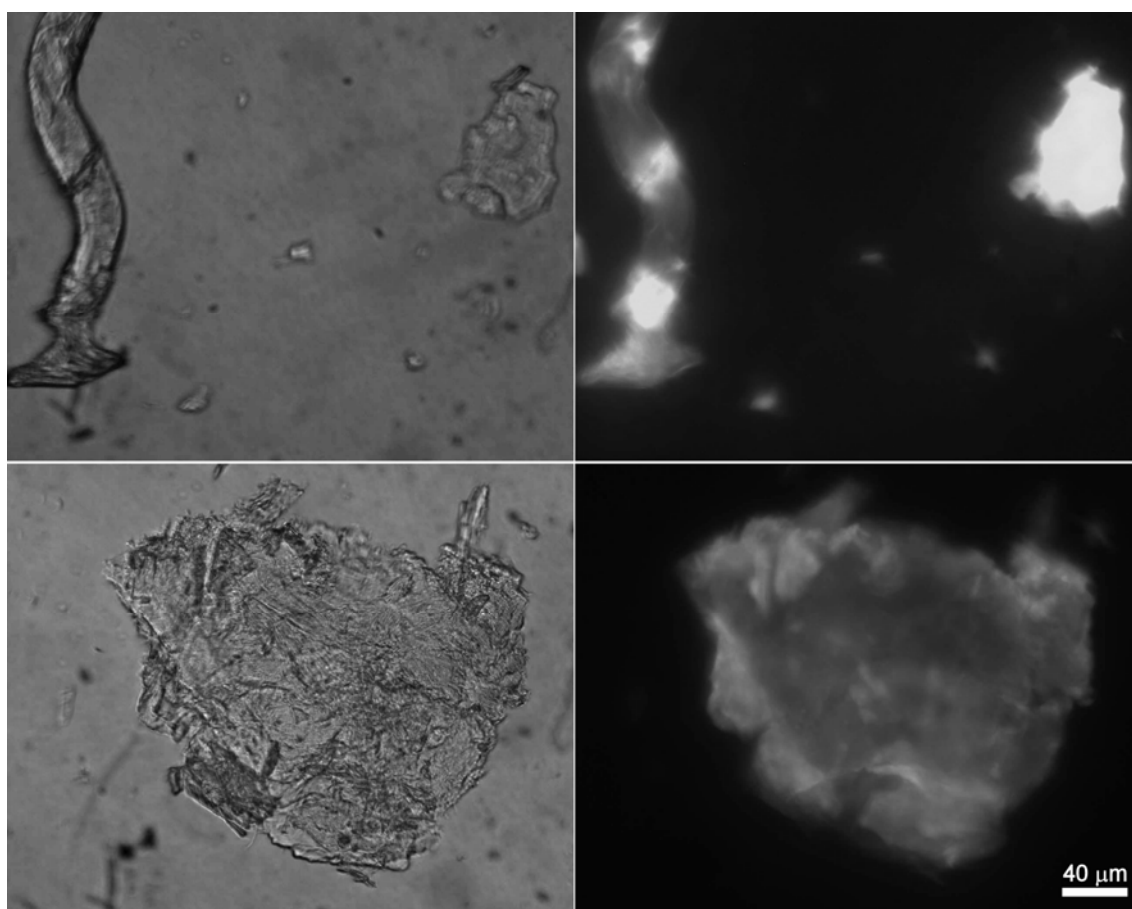


Figure M1.10. Comparison of the crystalline (top row) and phosphoric acid swollen (amorphous – bottom row) Whatman CF11 fibers, both treated with FITC-labeled CBD, at bright field (left) and fluorescent (right) microscopy. The probably amorphous sites of the microfibril (left side of the upper images) have attracted more FITC-labeled CBD.

M2. Development of a method using image analysis and CBD-FITC conjugates for the measurement of CBDs adsorbed onto cellulose fibers

(Submitted to *Journal of Biotechnology*)

Ricardo Pinto¹, António Luís Amaral^{1,2}, Joana Carvalho¹, Eugénio Campos Ferreira¹, Manuel Mota¹, Miguel Gama^{1,*}

¹Centro de Engenharia Biológica, Universidade do Minho
4710-057 Braga, Portugal.

²Departamento de Tecnologia Química, ESTIG, IPB
Apartado 1038, 5301-854 Bragança, Portugal.

*e-mail: fmgama@deb.uminho.pt; phone: +351253604400; fax: +351253678986.

Abstract

The surface concentration of CBD-FITC conjugates, adsorbed on cellulose fibers, was determined by image analysis. The program consists of two scripts, the first dedicated to the elaboration of the calibration curve. The emission of fluorescent light, detected by image analysis, is correlated with the concentration of CBD solutions. This calibration is then used (second script) to determine the concentration of CBDs adsorbed on cellulosic fibers. This method allows the direct estimation of the surface concentration of adsorbed CBDs, which usually is not accurately calculated from depletion studies, since the surface area is hardly known. By observing different spots in the surface of the fibers, site specific information is obtained. It was verified that the physically heterogeneous fibers exhibit different amounts of adsorbed CBDs.

Keywords: Cellulose-binding domain, fluorescein, adsorption, cellulose, fiber

Abbreviations: AFM, atomic force microscopy; BSA, bovine serum albumin; CBD, cellulose-binding domain; CBHI, cellobiohydrolases I; f , sensitivity factor; FITC, fluorescein isothiocyanate; HEPES, 4-(2-hydroxyethyl)-1-piperazineethanesulfonic acid; I , fluorescence intensity; I_A , acquired fluorescence intensity; I_0 , initial fluorescence intensity; K_d , photobleaching constant; t , time

Introduction

The majority of cellulases has a modular assembly, formed by a catalytic domain, a Cellulose-Binding Domain (CBD) and a highly glycosylated linker (Srisodsuk et al., 1993). CBDs have the ability of enhancing the enzyme catalytic activity, by increasing its concentration on the insoluble cellulose surface (Black et al., 1997; Limón et al., 2001; Srisodsuk M., 1994). The CBD from Cellobiohydrolase I (*Trichoderma reesei*) has an amino acid sequence that includes three aromatic residues (tyrosine) which seem to be implicated in the adsorption to cellulose (Mattinen et al., 1997). Carrard et al. (2000) showed that different CBDs adsorb to different sites on the surface of crystalline cellulose. The direct measurement of CBDs adsorbed on fibers with different properties, such as crystallinity or surface area, would therefore be very useful in the characterization of biochemical properties of CBDs.

Pala et al. (2001) showed that the presence of CBD, during paper production, modified the technological properties of the pulp and paper. In the present work, having in mind its biotechnological relevance, we aim at quantifying the CBD adsorbed on cellulosic surfaces, with the help of the fluorescent complex CBD-FITC. The use of image analysis methodologies was then validated as a means to quantify the adsorbed CBD-FITC.

Image processing and analysis techniques have been shown to be an extremely useful tool in a vast number of applications, since they allow the elimination of human analysis subjectivity and also the extraction of quantitative data that would be very difficult or even impossible to acquire by other means. As a matter of fact, there is a stepwise increment in the use of image analysis methodologies in processes that involve identification or even fluorescence quantification, both in microorganisms and fluorescent probes (Wiersba et al., 1995; Levy, 2001).

Materials and Methods

Chemicals

Fluorescein isothiocyanate (FITC) was obtained from Sigma, cellulosic fibers CF11 from Whatman (pure cellulose). All chemicals were of the highest purity available.

CBD Production

The CBDs were prepared according to the following methodology: the Celluclast[®] commercial enzymatic preparation (Novozymes A/S, Denmark) was digested with Papain (1:1200, on a protein basis). The resulting CBDs were separated by ultrafiltration through a 10 kDa membrane (Pellicon 2 TFF System from Millipore, USA) and concentrated by precipitation with ammonium sulphate (Merck, Darmstadt, Germany). After dialysis, CBDs were further purified on a Sepharose Fast-Flow gel (Amersham Pharmacia Biotech AB, Sweden); the non-adsorbed protein (CBD) was collected and lyophilized. Although produced by proteolysis, the obtained CBD is rather pure (Pinto et al., 2006). It is the CBD from *Trichoderma reesei* CBHI, with a heavily glycosylated linker attached. The purity of this protein has been demonstrated by N-terminal sequencing and MALDI-TOF.

CBD-FITC production

The conjugation of CBD with the labeling probe was carried out by mixing 20 µg of FITC per mg of CBD (in a concentration of 2 mg protein/mL in 0.1 M HEPES buffer, pH 9.0). This solution was incubated overnight in the dark, at room temperature, with magnetic stirring. To eliminate the unbound FITC, the labeled CBD mixture was filtered through a column packed with BIO-GEL P-4 (BIO-RAD, Hercules, USA), previously equilibrated with 50 mM sodium acetate buffer (Panreac, Barcelona, Spain).

CBD Adsorption Isotherm

Suspensions of Whatman CF11 fibers, with a concentration of 10 mg per mL in Sodium Acetate buffer (50 mM, pH 5.0), were incubated for 2 hours at 5°C, with magnetic stirring, in the presence of different CBD concentrations ($CBD_{Initial}$, $\mu\text{mol}\cdot\text{mL}^{-1}$). The fibers were then centrifuged at 4000 rpm for 10 minutes. The CBD concentration in the supernatant (CBD_{Free} , $\mu\text{mol}\cdot\text{mL}^{-1}$) was measured in a Jasco FP6200 spectrofluorimeter, operated at an emission and excitation wavelengths of 341 and 275 nm, respectively. The apparatus was calibrated using

CBD solutions with known concentrations (BCA Protein Assay – Pierce – using BSA as protein standard). The bound CBD ($\mu\text{mol}\cdot\text{g}^{-1}$) was calculated using the following equation:

$$CBD_{Bound} = \frac{[CBD_{Initial}] - [CBD_{Free}]}{m_{CF11}} \cdot V_R \quad (1)$$

where V_R (L) correspond to the volume of buffer used and m_{CF11} (g) the fibers mass.

The values of the adsorbed versus free CBDs where correlated, by non-linear regression analysis, with the Langmuir adsorption isotherm (Kim et al., 2001):

$$CBD_{Bound} = \frac{CBD_{Max} \cdot k_a \cdot CBD_{Free}}{1 + k_a \cdot CBD_{Free}} \quad (2)$$

where CBD_{Max} is the maximum molar amount of adsorbed protein ($\mu\text{mol}\cdot\text{g}^{-1}$) and k_a the adsorption equilibrium constant (μM^{-1}).

Production of cellulose films and CBD Adsorption

Cellulose films were obtained by evaporation, on a glass surface, of a solution of cellulose acetate in acetone. Then, the films were saponified in 0.1 M ethanolic solution of sodium hydroxide, at 40 °C, for 2 hours. After saponification, the films were rinsed in ultrapure water.

AFM topography images (512×512 pixels) of a cellulose film were obtained in tapping mode using a MultiMode™ SPM (Digital Instruments) apparatus.

Adsorption assays of FITC-labeled CBD were carried out at 4 °C. The conjugates ($400 \mu\text{g}\cdot\text{mL}^{-1}$) were allowed to adsorb on the cellulose film (circles with \varnothing 2 mm), in 50 mM sodium acetate buffer (final volume of 4 mL), with continuous magnetic stirring, in the dark, for 2 hours. The cellulose films with bound CBD were then washed with sodium acetate buffer, to remove the non-adsorbed CBD-FITC.

Adsorption on a single side of the cellulose films was achieved by placing a drop of the CBD-FITC solution on the surface of the film. After 30 minutes, the film was washed with sodium acetate buffer and fluorescent images were taken from both sides, using an Axioskop microscope (Zeiss, Oberkochen, Germany), with an AxioCam HRc attached camera (Zeiss, Oberkochen, Germany). This experiment was carried out to compare the fluorescent intensity observed, depending on whether the radiation has to cross (or not) the cellulose film (according to the side of the film, with and without CBDs, exposed to the camera).

Image Analysis – Calibration

Fluorescence microscopy observations were performed in an Axioskop microscope, with an AxioCam HRc attached camera. All images were acquired at 1300x1030 pixels and 24 bits color depths (8 bits per channel) by the AxioVision 3.1 software (Zeiss, Oberkochen, Germany). Solutions with different CBD-FITC concentrations, determined using the BCA Protein Assay Kit (Pierce), were used to perform calibrations in an Improved Neubauer chamber. Images obtained with these solutions were related to the quantity of CBD (Q_{CBD} , mol·mm⁻²) by the following equation:

$$Q_{CBD} = \frac{[CBD] \cdot 0.10}{8.43 \times 10^9} \quad (3)$$

where $[CBD]$ is the concentration of CBD-FITC (mg·mL⁻¹), 0.10 is the depth of the liquid in the Neubauer chamber (mm) and 8.43×10^9 is the molecular weight of the CBD used ($\mu\text{g} \cdot \text{mol}^{-1}$), as determined by MALDI (Pinto et al., 2006).

To estimate the quantity of CBD-FITC adsorbed to cellulose fibers, an image processing and analysis program was developed in Matlab (The Mathworks, Inc, Natick). This program consists of two scripts, the first focused on the calibration curve, the second on the quantification of the adsorbed CBD-FITC.

To perform the calibration, 5 to 10 different concentrations of CBD and different acquisition times (in the range of 200 to 3000 milliseconds) were used, in order to determine the adsorbed CBDs in a range of concentration as large as possible. The first step of calibration consisted in the determination of the RGB channels merging function that maximizes the sensitivity to small fluorescence variations. This merging function ($I = f_R I_R + f_G I_G + f_B I_B$) allows the fusion of the three channels images (I_R , I_G and I_B) in one single image of intensity I , taking in account the sensitivity factors for each channel (f_R , f_G and f_B), calculated as defined ahead. The average intensity was determined for each RGB channel, for each different CBD-FITC concentration and capture time. The channel's sensitivity factor was calculated as the ratio $f_R = I_R / (I_R + I_G + I_B)$, $f_G = I_G / (I_R + I_G + I_B)$ and $f_B = I_B / (I_R + I_G + I_B)$, for each image capture time and CBD-FITC concentration. Finally, the general sensitivity factors were determined, for each channel, by averaging the asymptotic values for all of the capture times and for each concentration. By applying these factors to each channel of the acquired images, a unique single-channel (gray scale) image of maximum sensitivity was obtained.

The ultimate objective of the first Matlab script consisted in the elaboration of a calibration curve for each data acquisition time, correlating the CBD-FITC concentration to the intensity value and spatial localization in the image (due to the non-uniform illumination of the field). Therefore, for each acquired image, corresponding to a specific CBD-FITC concentration

and data acquisition time, the three color channels are merged into one single image, by the afore-mentioned merging function. Due to execution time and virtual memory limitations, it was necessary to resize each image to 1/5 of its original size (from 1300×1030 pixels to 260×206 pixels). Since the original images are relatively soft at the transition level between neighbor pixels, the image reduction does not imply significant errors.

The FITC fluorophore is known to photobleach due to several factors, such as concentration, exposure time or light intensity, among others (Markham and Conchello, 2001). This bleaching effect can be described using the mono-exponential equation:

$$I = I_0 \cdot e^{-k_d \cdot t} \quad (4)$$

Where I_0 and I are the fluorescence intensities before and after t seconds of exposure and k_d is the photobleaching constant rate, s^{-1} (Ghauharali and Brakenhoff, 2000; Song et al., 1997).

The images obtained with the AxioCam sensor corresponds to the total fluorescence detected during the exposure time (t) or, graphically, to the grey shaded area in the inset of Figure M2.1. Thus, integrating Eq. (4):

$$I_A = \frac{I_0}{k_d} \cdot (1 - e^{-k_d \cdot t}) \quad (5)$$

The values of I_0 and k_d parameters are determined from a non-linear regression of Eq. (5) (Figure M2.1), where I_A is the fluorescence emission of the calibration images. This regression is made at each pixel position, for the various CBD-FITC concentrations. The values of I_0 are then multiplied by the exposure time of the images to be quantified, in order to obtain the total unbleached fluorescence (area) for that exposure, and a linear regression is performed for $I_0 \cdot t$ versus the concentration of CBD-FITC (Figure M2.2). The coefficient values, for each pixel, are then saved in a Matlab native format, to be used in the second script.

Image analysis – CBD quantification

The second Matlab script was devoted to the determination of the CBD-FITC concentration in cellulose films/fibers. Images were obtained, exhibiting the appropriate level of signal intensity. A convenient capture time was selected, based on the criteria of obtaining the maximum (at non-saturation) signal intensity, thus maximizing the fibers image sensitivity. For each of the acquired images, the three color channels were merged into one single image, which was then resized to 1/5 of its original size (from 1300×1030 pixels to 260×206 pixels). Finally, the pixel intensity values of the fibers image was converted to their corresponding concentration values, by the use of the appropriate calibration model. Then, the fiber-target zone(s) were selected for the determination of the adsorbed CBD-FITC average concentration. Since the fiber-

target zone(s) have uniform intensities, the size reduction does not introduce significant errors. The average concentrations of the fiber-target zone(s) are then saved in a text file, together with their cardinal positions.

Results and Discussion

The calibration of the fluorescence obtained in microscopic images has been done by other authors, using polyvinylalcohol films with embedded fluorescein (Zwier et al., 2004). This approach presents some inconvenients: a shift in the fluorescent emission may occur, due to the different medium surrounding the fluorescent probe (a polymer film in the calibration, water in the case of the studies with CBD-FITC); secondly, this is a more laborious approach. Indeed, the calibration procedure developed in this work, based on the use of solutions with the fluorescent probe, in an Improved Neubauer chamber, allowed both a higher accuracy and a simpler methodology.

The three channel images (I_R , I_G and I_B) were merged into a single image of intensity I , using sensitivity factors experimentally determined for each channel (f_R , f_G and f_B), for each CBD-FITC concentration and image capture time. Saturated images (exhibiting intensity points close to 255 in any channel), were excluded from the sensitivity factors determination. For instance, at 300 ms capture time, and for concentrations above $100 \times 10^{-13} \text{ mol} \cdot \text{mm}^{-2}$, the green channel becomes saturated (Figure M2.3).

As described before, the sensitivity factors were calculated from the ratio between each channel intensity and the sum of all channels' intensities. It was verified that, for values below the image saturation threshold (255), the sensitivity factor is a constant value, independent of the CBD-FITC concentration and capture time (Figure M2.3). The obtained values are presented in Table M2.1. The sensitivity factors calculated are constant and independent of the capture time. Therefore, the merging function could be determined as:

$$I = 0.208 \times I_R + 0.695 \times I_G + 0.096 \times I_B \quad (6)$$

Several analysis were performed, using different capture times and CBD-FITC concentrations. Good correlations were obtained, using the calculated sensitivity factors. As an example, images obtained for different CBD-FITC concentrations (I vs xy pixel), using a capture time of 300 ms, are shown in Figure M2.4. This figure reveals a non-uniform background illumination, resulting in a significant variation of the intensities measured at different pixel locations. Several authors (Benson et al., 1985; Ghauharali et al., 1998; Ghauharali and

Brakenhoff, 2000) used a ‘mask’ image to correct this type of non-uniformity. In this work, this approach was not used, since it gives rise to color artifacts in the image borders. Nevertheless, with the strategy used in the calibration, this spatial variation is overcome. Figure M2.4 also shows the proportional increase of the measured intensity with the CBD-FITC concentration.

To ensure that the color intensity values were not dependent on the quantity of CBD solution used on the Neubauer chamber, an additional experiment was performed. The CBD-FITC quantification was carried out using volumes of 3.34, 6.66 and 10.00 μL . The same CBD-FITC solution was used in each case; although the used volume varies, the theoretical surface concentration of CBDs is the same, $10 \times 10^{-13} \mu\text{mol}\cdot\text{mm}^{-2}$, since the depth of the solution (z-axis in the Neubauer chamber) is the same. The surface concentration calculated for the three different volumes of protein solution is shown in Figure M2.5. This figure shows a small increase in the estimated concentration, towards the expected value of $10 \times 10^{-13} \mu\text{mol}\cdot\text{mm}^{-2}$, raising the volume 3.34 to 10 μL . Therefore, and for subsequent analysis, a 10 μL volume was chosen in the development of the calibration models, because of the higher accuracy.

To validate further the methodology, measurements of CBD-FITC adsorbed to cellulose films were made. The photobleaching of the CBD-FITC adsorbed to a cellulose surface was analyzed. In the case of adsorbed protein, the k_d determination implies special care. Image acquisition, for different exposure times, cannot be carried out on the same surface spot, due to photobleaching accumulation. On the other hand, because the surface is heterogeneous, variations in the fluorescence intensity may occur if different spots of the surface are chosen (for analysis using different exposure times). To overcome these difficulties, the following method was adopted: two images were recorded (acquisition time of 400 ms) 20 seconds apart, during which the film was continuously exposed to fluorescence light, as to photobleach the fluorophore. Considering that the acquisition time was much smaller than the total time, the intensity measured in the first image could be considered equivalent to the initial fluorescence (I_0) and the second image to the fluorescence (I) after 20 seconds (t). Eq. (4) allows, using these values, the calculation of k_d . The images used in this experiment are shown in Figure M2.6. The fluorescence intensities measured, along with the calculated k_d , are presented in Table M2.2. The average value of k_d corresponds to a low photobleaching rate: an exposure time of 1 second implies a decrease of 0.42% fluorescence intensity ($I_0 \times t$). Therefore, in the course of fluorescence intensity measurements, the photobleaching of adsorbed CBD-FITC may be neglected, under the experimental conditions of this work.

Figure M2.7 shows images of cellulose films with adsorbed CBD-FITC, where the black regions that are surrounded by pure white pixels correspond to saturated areas of intensity

superior to the value of the highest CBD-FITC concentration used in the calibration. A CBD concentration expected to lead to saturation was used ($400 \mu\text{g}\cdot\text{mL}^{-1}$, the equivalent to 20 milligrams of CBD per gram of fibers). Figure M2.8 shows the adsorption isotherm for CBDs adsorbed on Whatman CF11. The grey circle represents the equilibrium position for CBD at the initial concentration of $400 \mu\text{g}\cdot\text{mL}^{-1}$. At this concentration, the CF11 fibers are saturated. Considering the much lower surface area of the material used in this work (a cellulose film instead of microparticles), the CBDs are expected to saturate the surface of the film. The cellulose films were produced by evaporation of cellulose acetate, dissolved in acetone, on a glass surface, which is likely to have scratches that may explain the highly fluorescent lines seen in the images (higher concentration of CBD-FITC adsorbed). These regions were therefore ignored in the concentration calculations, as shown in Figure M2.6 and Figure M2.7. The average intensity values obtained for the selected regions in Figure M2.7 correspond to a concentration of CBD, per square millimeter, between 9.9 and $12.6 \times 10^{-13} \mu\text{mol}$.

When observing a cellulose film (or fiber), the fluorescence detected may be produced by fluorescent molecules present on both sides of the film (fiber). For quantitative purposes, it is important to clarify whether the optical path through the fiber affects, or not, the intensity observed. An experiment was carried out (as described in the materials and methods section), to clarify this issue: a cellulose film, with CBD-FITC adsorbed on only one of the sides, was analyzed, exposing the surface with adsorbed CBDs directly to the digital camera in the microscope, or upside down. The intensity difference detected is below 5%. Then, it can be considered that the total fluorescence have a similar contribution from the CBDs adsorbed on both sides of the cellulose film. Considering a CBD with $3.0 \times 1.8 \text{ nm}$ (Kraulis et al., 1989), a monolayer of CBDs is expected to correspond approximately to $3.08 \times 10^{-13} \mu\text{mol}\cdot\text{mm}^{-2}$. It is then possible to calculate 1.6 to 2.0 layers of CBD, in each side of the film. As seen in Figure M2.9, the surface of the cellulose acetate film has very low roughness, and only slightly this would increase the estimated surface concentration. A more plausible explanation, however, is advanced by Lee et al. (2000), according to whom CBDs from *T. reesei* CBHI, are able to penetrate cotton fibers. The film used in this work has low crystallinity (68%), and may allow the penetration of surface diffusing CBDs. This would raise the adsorbed amount of CBD. Indeed, the presence of CBD multilayers in the surface of the film is unlikely. Rather, the CBDs are adsorbed in the external surface, but may also penetrate to other (internal) layers of the material.

Conclusion

A methodology was developed, based on the image analysis of adsorbed CBD-FITC conjugates, which allow the estimation of the protein surface concentration. This method is based on the production of a grey scale image, obtained using the merging function $I = 0.208 \times I_R + 0.695 \times I_G + 0.096 \times I_B$. The calculated value of intensity is correlated with CBD-FITC concentration in a xy plane. This correlation elicits the estimation of CBDs adsorbed in any kind of cellulosic material (particle, fiber, etc). It has been shown that the photobleaching of adsorbed CBD-FITC is not relevant in the assay conditions. Preliminary results suggest that, at saturation, the CBDs adsorbed in a cellulose film accumulate in multiple layers. Other hypothesis to explain the high CBD concentration may be the protein penetration of the cellulose fibers. These issues will be studied in a future investigation.

Acknowledgments

Ricardo Pinto was supported by Fundação para a Ciência e a Tecnologia (FCT) grant SFRH/BD/6934/2001.

References

Benson, D.M., Bryan, J., Plant, A.L., Gotto, A.M., Smith, L.C., 1985. Digital imaging fluorescence microscopy: spatial heterogeneity of photobleaching rate constants in individual cells. *J. Cell Biol.* 100, 1309–1323.

Black, G.W., Rixon, J.E., Clarke, J.H., Hazlewood, G.P., Ferreira, L.M.A., Bolam, D.N., Gilbert, H.J., 1997. Cellulose binding domains and linker sequences potentiate the activity of hemicellulases against complex substrates. *J. Biotechnol.* 57, 59–69.

Ghauharali, R.I., Hofstraat, J.W., Brakenhoff, G.J., 1998. Fluorescence photobleaching-based shading correction for fluorescence microscopy. *J. Microsc.-Oxford* 192, 99–113.

Ghauharali, R.I., Brakenhoff, G.J., 2000. Fluorescence photobleaching-based image standardization for fluorescence microscopy. *J. Microsc.-Oxford* 198, 88–100.

Kraulis, P.J., Clore, G.M., Nilges, M., Jones, T.A., Petterson, G., Knowles, J., Gronenborn, A.M., 1989. Determination of the three-dimensional solution structure of the C-terminal domain of cellobiohydrolase I from *Trichoderma reesei*. A study using nuclear magnetic resonance and hybrid distance geometrydynamical simulated annealing. *Biochemistry* 28, 7241–7257.

Kim, D.W., Jang, Y.H., Kim, C.S., Lee, N.-S., 2001. Effect of metal ions on the degradation and adsorption of two cellobiohydrolases on microcrystalline cellulose. *Bull. Korean Chem. Soc.* 22, 716–720.

Lee, I., Evans, B.R., Woodward, J., 2000. The mechanism of cellulase action on cotton fibres: evidence from atomic force microscopy. *Ultramicroscopy* 82, 213–221.

Levy, I., Shoseyov, O., 2001. Expression, refolding and indirect immobilization of horseradish peroxidase (HRP) to cellulose via a phage-selected peptide and cellulose-binding domain (CBD). *J. Pept. Sci.* 7, 50–57.

Limón, M.C., Margolles-Clark, E., Benítez, T., Penttilä, M., 2001. Addition of substrate-binding domains increases substrate-binding capacity and specific activity of a chitinase from *Trichoderma harzianum*. *FEMS Microbiol. Lett.* 198, 57–63.

Markham, J., Conchello, J.-A., 2001. Artefacts in restored images due to intensity loss in three-dimensional fluorescence microscopy. *J. Microsc.-Oxford* 204, 93–98.

Mattinen, M.-L., Linder, M., Teleman, A., Annala, A., 1997. Interaction between cellobiohexaose and cellulose binding domains from *Trichoderma reesei* cellulases. *FEBS Lett.* 407, 291–296.

Pala, H., Lemos, M.A., Mota, M., Gama, F.M., 2001. Enzymatic upgrade of old paperboard containers. *Enzyme Microb. Tech.* 29, 274–279.

Pinto, R., Carvalho, J., Mota, M., Gama, M., 2006. "Large-scale production of cellulose-binding domains. Adsorption studies using CBD-FITC conjugates," *Cellulose* 13, 557-569.

Song, L., van Gijlswijk, R.P.M., Young, I.T., Tanke, H.J., 1997. Influence of fluorochrome labeling density on the photobleaching kinetics of fluorescein in microscopy. *Cytometry* 27, 213–223.

Srisodsuk, M., Reinikainen, T., Pentillä, M., Teeri, T.T., 1993. Role of the interdomain linker peptide of *Trichoderma reesei* cellobiohydrolase I in its interaction with crystalline Cellulose. *J. Biol. Chem.* 266, 20756–20761.

Srisodsuk, M., 1994. Mode of action of *Trichoderma reesei* cellobiohydrolase I on crystalline cellulose. Ph.D. Thesis, VTT Publications 188, Helsinki, Finland.

Wierzba, A., Reichl, U., Turner, R.F.B., Warren, R.A.J., Kilburn, D.G., 1995. Adhesion of mammalian cells to a recombinant attachment factor, CBD/RGD, analyzed by image analysis. *Biotech. Bioeng.* 46, 185–193.

Zwier, J.M., Van Rooij, G.J., Hofstraat, J.W., Brakenhoff, G.J., 2004. Image calibration in fluorescence microscopy. *J. Microsc.-Oxford* 216, 15–24.

Figures

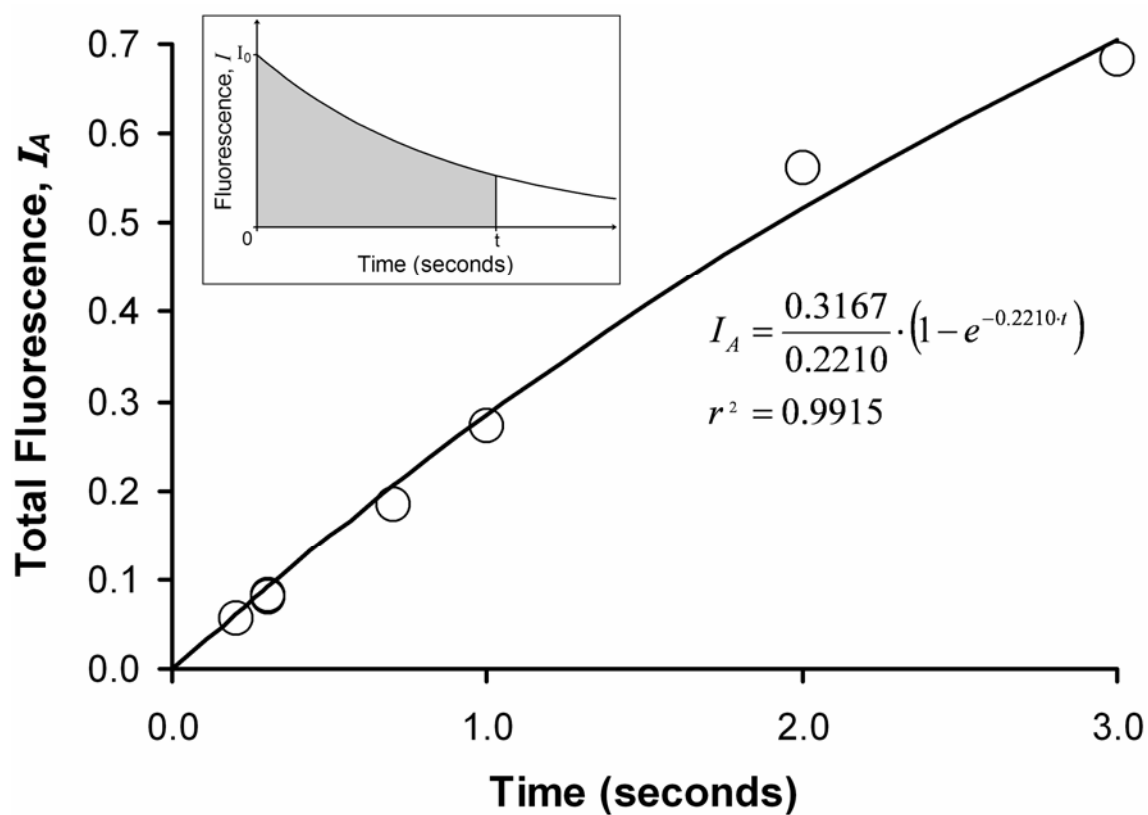


Figure M2.1. Values of fluorescence intensity (I_A) versus exposure time, obtained using a CBD-FITC concentration of $10.14 \times 10^{-13} \mu\text{mol} \cdot \text{mm}^{-2}$ (or $85.5 \mu\text{g} \cdot \text{mL}^{-1}$), and the corresponding non-linear regression fitting. Inset: photobleaching curve of a mono-exponential correlation, the model used in the calculation of I_A .

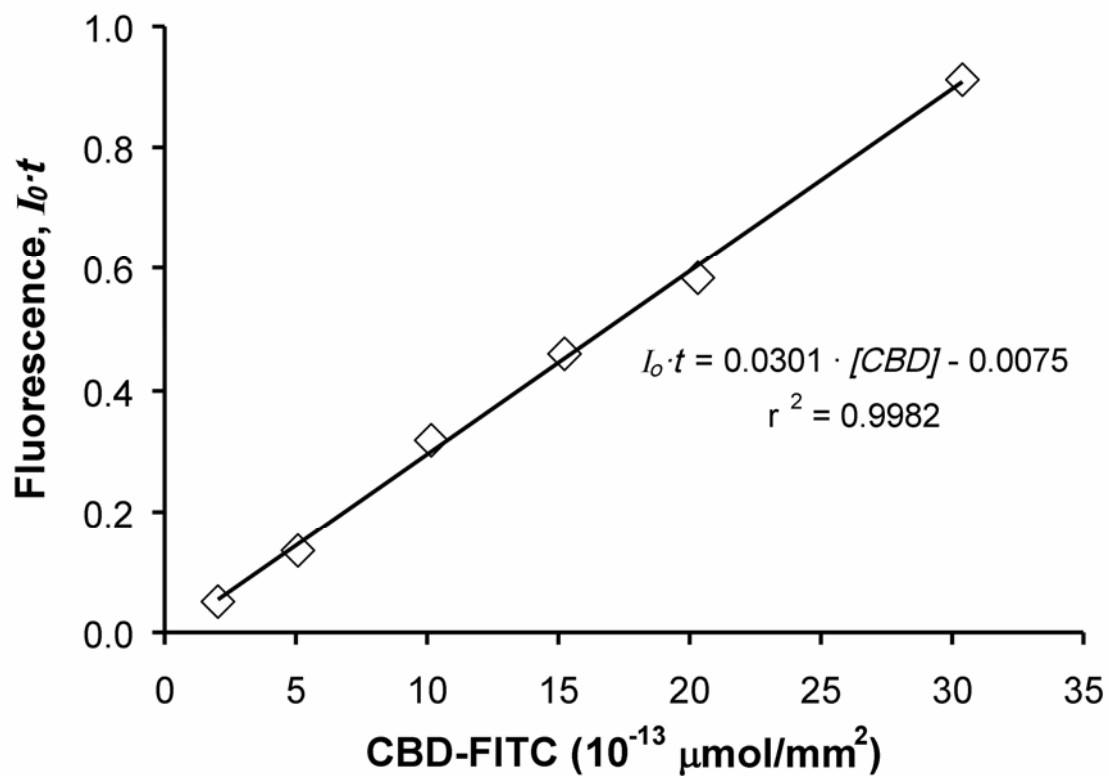


Figure M2.2. Values of fluorescence intensity as a function of the CBD-FITC concentration.

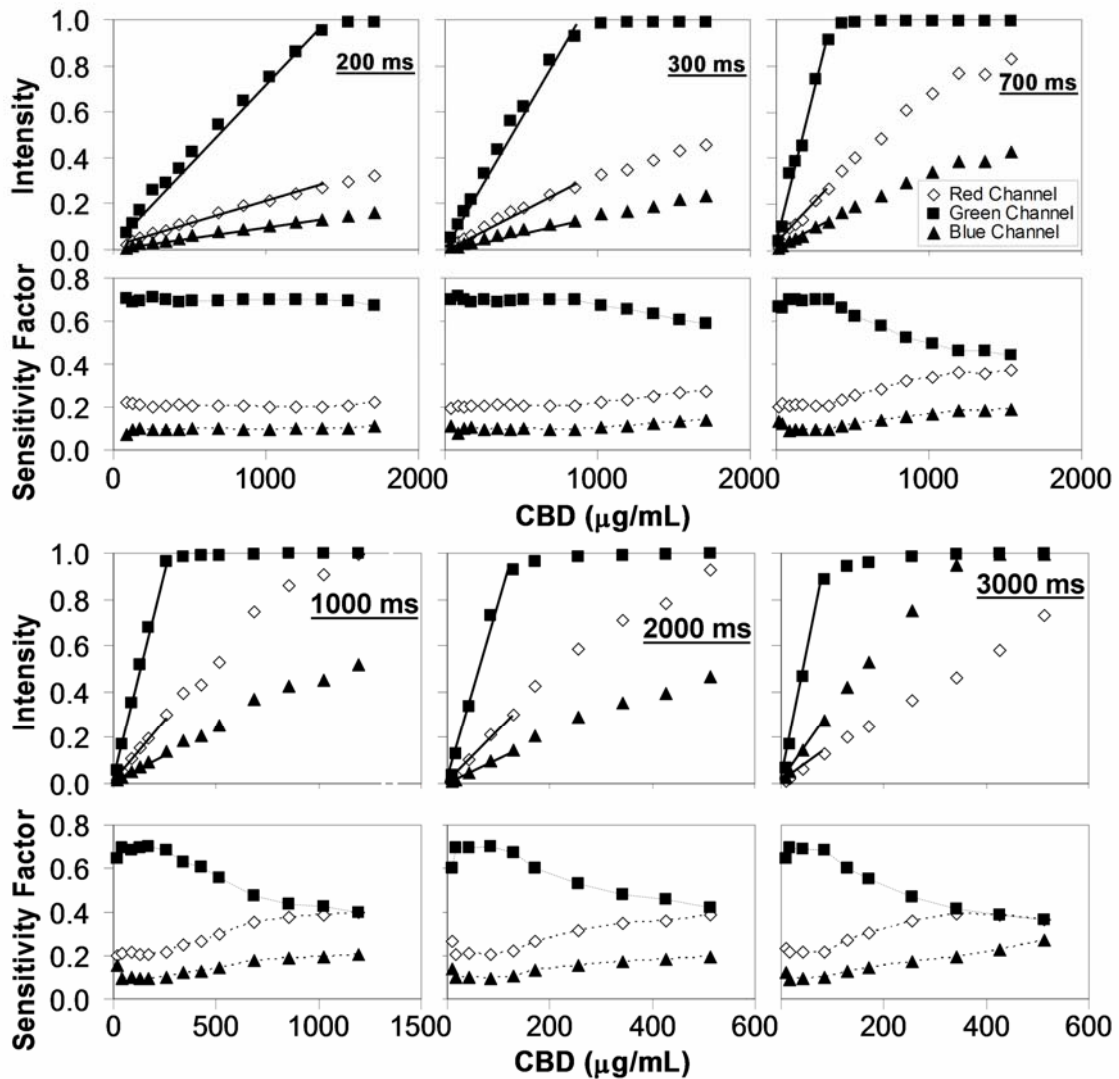


Figure M2.3. Intensity and sensitivity factors variation with CBD concentration for the studied capture times, obtained by averaging a 10×10 pixel area at the centre of each original images (continuous lines connect the values used for the calibration model). Legend: \diamond – Red channel; \blacksquare – Green channel; \blacktriangle – Blue channel.

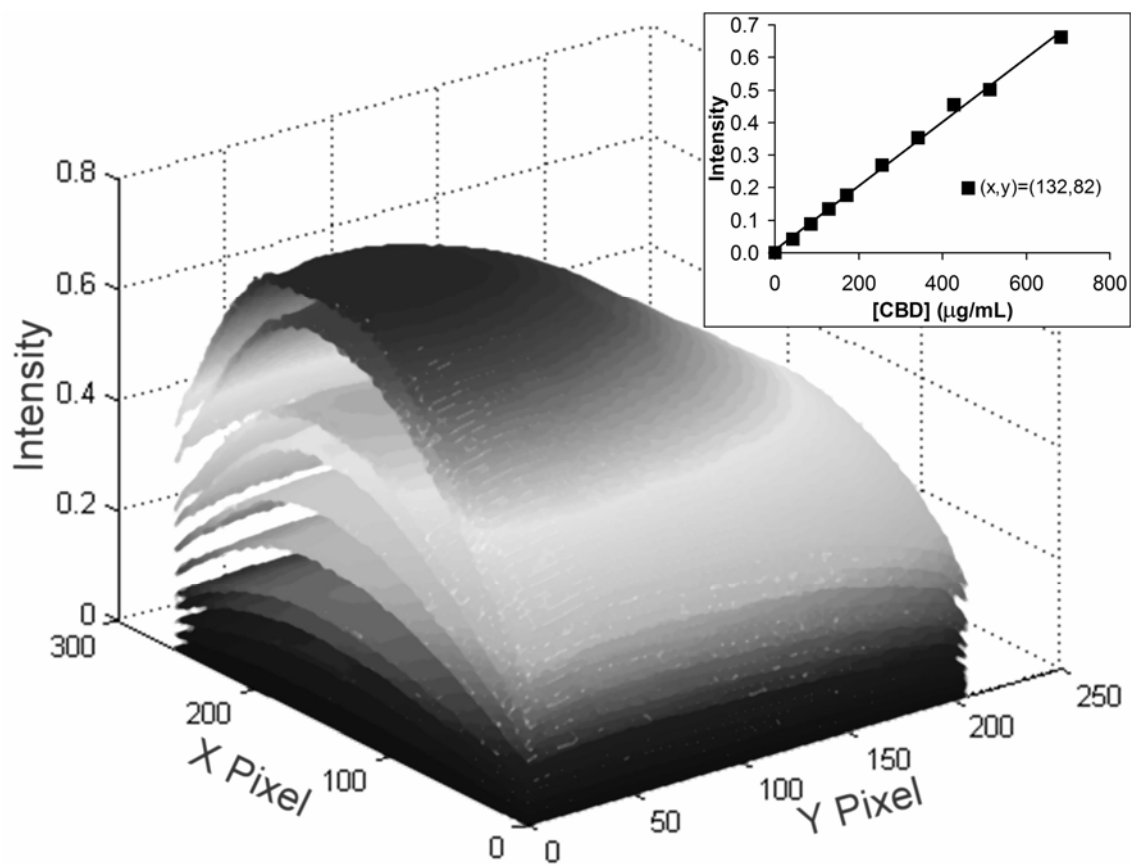


Figure M2.4. Calibration images obtained at capture time of 300 ms; each surface represents a different CBD-FITC concentration. The inset shows, as an example, the CBD concentration versus pixel intensity, obtained approximately at the center of the images.

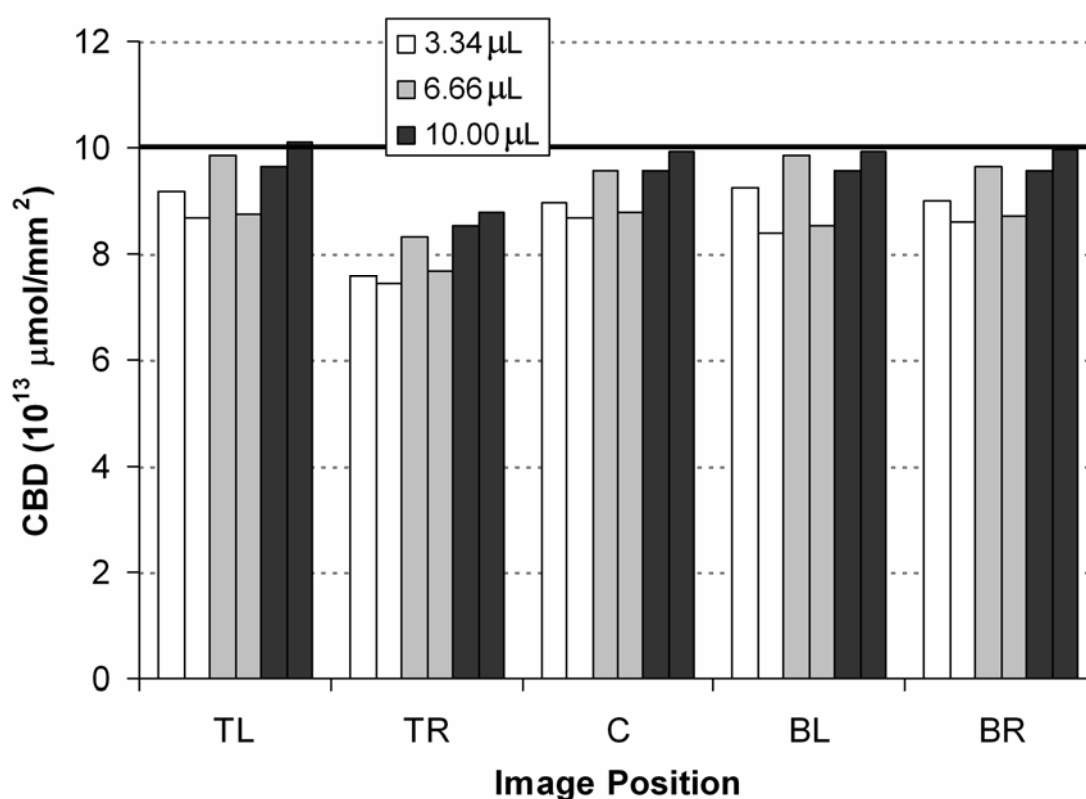


Figure M2.5. Estimated CBD-FITC per unit area, for three different protein solutions volumes. The labeling classes (TL – top left; TR – top right; C – centre; BL – bottom left; BR – bottom right) refer to average values obtained at different selected regions in the image. The black line corresponds to the expected value. Duplicate values are shown for each volume used.

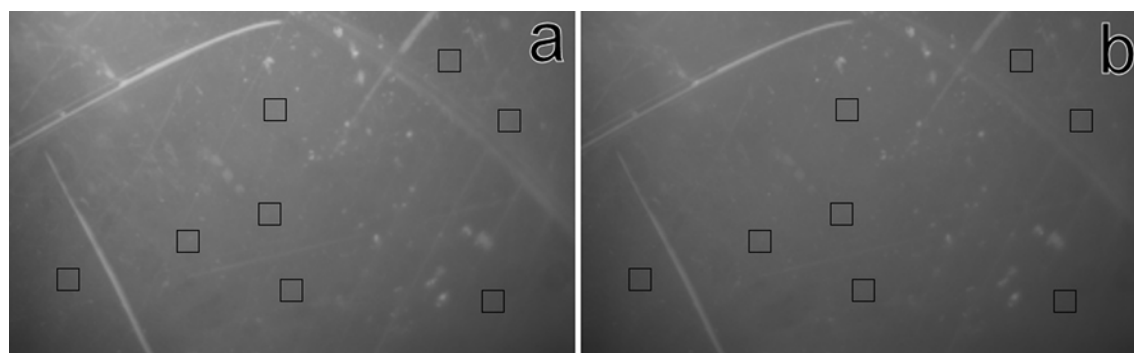


Figure M2.6. Cellulose film images obtained, for 400 ms of exposure time, at 0 (a) and 20 seconds (b) of exposure to the fluorescence light. The black squares indicate the positions where the measurements were carried out.

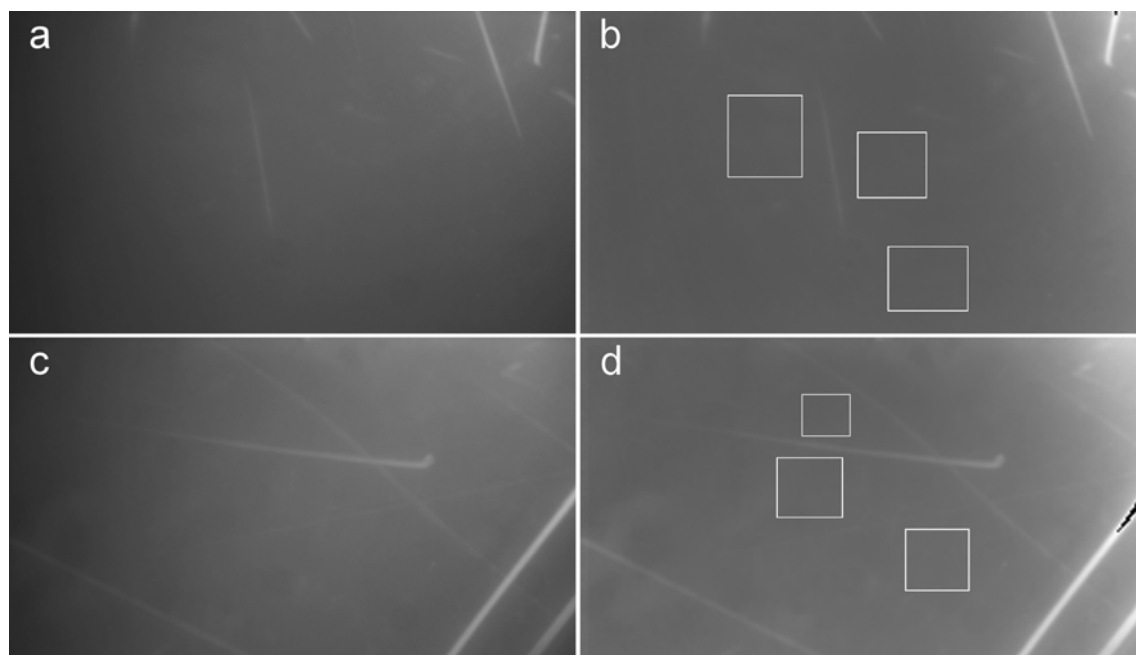


Figure M2.7. Images of cellulose films with adsorbed CBD-FITC: (a) and (c) correspond to grey scale images of the films, produced by the fluorescent light emitted by the CBD linked FITC; (b) and (d) correspond to the program treated images, where black color corresponds to $0 \mu\text{mol}\cdot\text{mm}^{-2}$ and white color to the maximum concentration used in the corresponding calibration procedure.

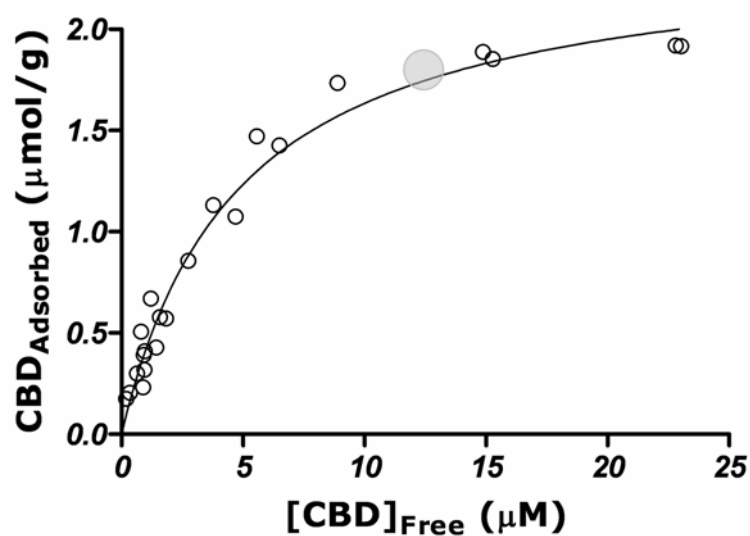


Figure M2.8. Adsorption isotherm of CBD on Whatman CF11 fibers, for 2 hours contact. The line was obtained by nonlinear regression of the Langmuir isotherm, resulting in the constants: $CBD_{Max} = 2.42 \mu\text{mol}\cdot\text{g}^{-1}$ and $k_a = 0.209 \mu\text{M}^{-1}$. The grey circle corresponds to the equilibrium position of samples put in contact with an initial CBD concentration of $400 \mu\text{g}\cdot\text{mL}^{-1}$.

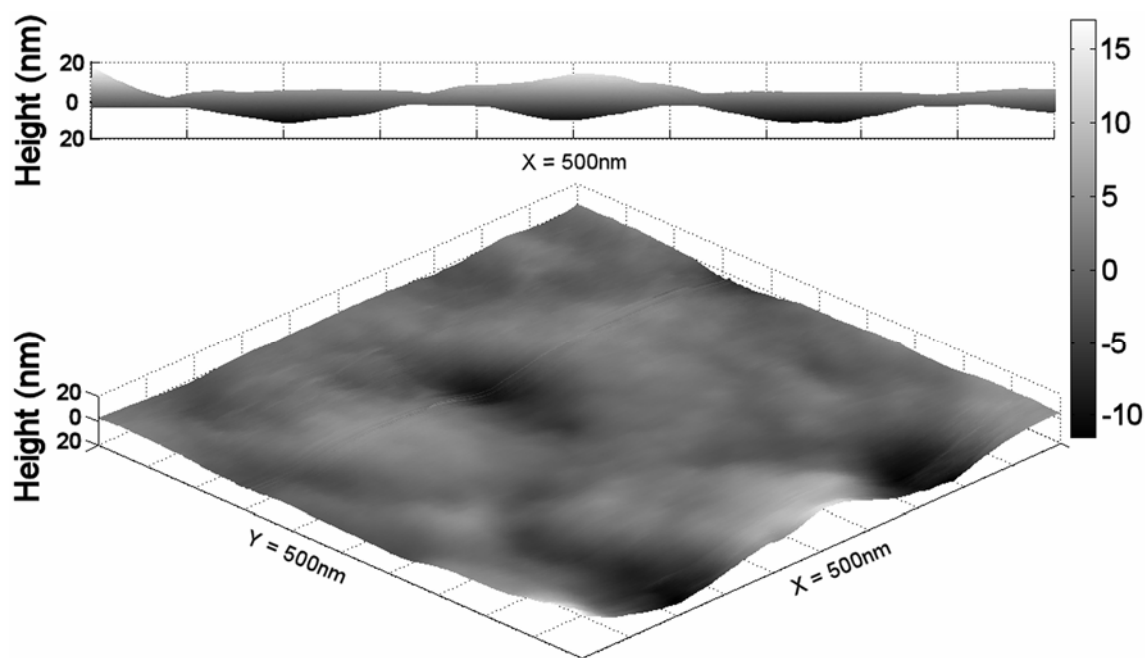


Figure M2.9. AFM surface image of cellulose film, obtained in the air. The upper image corresponds to the xx side view.

Tables

Table M2.1. Sensitivity factor values for each channel, as a function of the capture time.

Time (ms)	f_R	f_G	f_B
200	0.206	0.699	0.095
300	0.204	0.700	0.097
700	0.206	0.699	0.094
1000	0.210	0.692	0.098
2000	0.208	0.692	0.100
3000	0.215	0.690	0.095
Average	0.208	0.695	0.096

Table M2.2. Values of the fluorescence intensity at 0 (I_0) and 20 seconds (I) of continuous exposure to fluorescence light and for the calculated photobleaching constant rate.

I_0	I	k_d (s^{-1})
107.7	91.74	0.00804
99.32	83.78	0.00850
125.6	104.9	0.00904
111.5	94.58	0.00822
111.3	93.69	0.00863
98.73	83.07	0.00864
74.95	63.88	0.00799
88.15	73.95	0.00878
Average		0.00848 ± 0.00031

M3. Quantification of the CBD-FITC conjugates surface coating on cellulose fibers

(To be submitted to *BMC Biotechnology*)

Ricardo Pinto¹, António Luís Amaral^{1,2}, Eugénio Campos Ferreira¹, Manuel Mota¹, Manuel Vilanova^{3,4}, Katia Ruel⁵, Miguel Gama^{1,*}

¹Centro de Engenharia Biológica, Universidade do Minho, 4710-057 Braga, Portugal.

²Departamento de Tecnologia Química, ESTIG, IPB, Apartado 1038, 5301-854 Bragança, Portugal.

³ICBAS - Instituto de Ciências Biomédicas de Abel Salazar, Largo do Professor Abel Salazar 2, 4099-003, Porto, Portugal

⁴IBMC - Instituto de Biologia Molecular e Celular, Rua do Campo Alegre, 823, 4150-180 Porto, Portugal

⁵Centre de Recherches sur les Macromolécules Végétales (CERMAV)-UPR CNRS 5301, BP 53, 38041 Grenoble cedex 9 France

*Corresponding author

Email addresses:

RP: joaoricardo@yahoo.com

ALA: lpamaral@deb.uminho.pt

ECF: ecferreira@deb.uminho.pt

MM: mmota@deb.uminho.pt

MV: vilanova@icbas.up.pt

KR: Katia.Ruel@cermav.cnrs.fr

MG: fmgama@deb.uminho.pt

Abstract

Background

Cellulose Binding Domains (CBD) were conjugated with fluorescein isothiocyanate (FITC). The surface concentration of the Binding Domains adsorbed on cellulose fibres was determined by fluorescence image analysis.

Results

For a CBD-FITC concentration of 60 µg/mL, a coating fraction of 78% and 110% was estimated for *Portucel* and Whatman fibres, respectively. For a saturating CBD concentration, using Whatman CF11 fibres, a surface concentration of 25.2×10^{-13} mol/mm² was estimated, the equivalent to 4 protein monolayers. This result does not imply the existence of several adsorbed protein layers.

Conclusions

It was verified that CBDs were able to penetrate the fibres, according to confocal microscopy and TEM-immunolabelling analysis. The surface concentration of adsorbed CBDs was greater on amorphous fibres (phosphoric acid swollen) than on more crystalline ones (Whatman CF11 and Sigmacell 20).

Background

Due to its high sensitivity and specificity, fluorescence analysis has been extensively used in microarray technology [1], gene expression monitoring [2], protein diffusion [3] or *in vivo* chemical elements uptake and localization studies [4]. Another area to benefit from fluorescence based techniques is protein quantification. The use of either non-covalent [5] or covalent labelling [6,7] increased the detection sensitivity to as low as 40 ng/mL.

Cellulose-Binding Domains (CBD) are modules present in most celulas, being responsible for their high affinity to cellulose crystalline surfaces [8,9]. The CBD used in this work, produced by limited proteolysis, belongs to cellobiohydrolase I (CBHI) of *Trichoderma reesei*, as shown in a previous work [10]. Three tyrosine residues define a flat surface, which may be responsible for the affinity to cellulose [11]. This protein has a single amine, the N-terminal of the linker region, which allows a specific reaction with fluorescein isothiocyanate (FITC). The conjugation with FITC does not affect the CBD interaction with cellulose, since the

N-terminal is isolated from the cellulose interacting part of the protein. Indeed, the conjugation of FITC does not modify the CBD adsorption isotherms [12,13]. Since there is only one amine group present in the CBD, the stoichiometry of the conjugation reaction is 1:1. The FITC fluorophore has been attached to antibodies [14,15], to microparticles [16] or to other binding domains [12,17].

Cellulose-Binding Domains (CBD) have been used to target functional molecules to cellulose-containing materials [18], to improve pulp properties [19] or as an additive for paper recycling [20]. Bearing in mind that these applications are related to surface effects, in this work we attempted to quantify the CBD surface coverage of cellulose fibres, using the approach based on the use of CBD-FITC previously developed. Our aim was to quantify the protein adsorbed on cellulose fibres and, more specifically, the surface concentration of CBD. This value could, alternatively, be estimated by measuring the specific surface area, by means of the BET isotherm [21]. However, the BET approach is not ideal for porous materials [22]. The presence of CBDs in the interior of the fibres was also investigated.

Results and Discussion

In a previous work [20], we have shown that CBDs affect the technical properties of paper fibres (secondary fibres from the paper mill *Portucel*). The concentration of CBDs, used in those experiments, was in the range of 1-2 mg of CBD per gram of fibres. It is arguable whether this relatively low amount of protein is sufficient to cause modifications in the fibres' interfacial properties. This would probably imply a substantial coating of the fibres by CBDs. In this work, we analyzed fibres from *Portucel* treated with CBDs conjugated to FITC, and attempted to estimate the percentage of surface coverage. As may be observed in Figure 1, the fibres do not display a uniform distribution of fluorescence. This may be due to the chemical heterogeneity (lignin/hemicellulose) and/or to the variable crystallinity [23]. The regions with less intense fluorescence in the picture were selected for CBD-FITC quantification, since these regions are expected to be more crystalline (Pinto *et al.*, unpublished). The detected fluorescence is produced by CBDs adsorbed on both sides of the fibres (top and bottom). Indeed, the fluorescent radiation crosses the fibres with just a slight reduction in intensity (results to be published). Figure 2 shows a Whatman CF11 fibre, both on bright field and fluorescence microscopy. As it can be observed in the circled area, this cellulose has a rather smooth surface. The extremities of the fibres are expected to have a higher number of fissures and loosen microfibrils, increasing the available area, and consequently the adsorbing sites for CBDs [12], as indicated by the higher

fluorescence emission (Fig. 2). The adsorption of CBDs on Whatman CF11 fibres was analyzed, using a protein concentration of 2 mg/g_{fibras}. The estimated surface concentrations of CBDs adsorbed on Portucel and Whatman CF11 fibres (Fig. 1) are shown in Figure 3.

In another experiment, Whatman CF11, amorphous cellulose and Sigmacell 20 fibres were allowed to adsorb CBDs from a much more concentrated CBD solution (400 µg/mL), corresponding to 20 mg/g_{Fibras} (Fig. 4). This concentration is expected to saturate the fibres according to the adsorption isotherm.

Considering the size [24] of a cellobiohydrolase I CBD (3.0×1.8 nm), the density of a CBD monolayer corresponds to 3.08×10^{-13} mol/mm². It is also considered that the fluorescent signal is produced by CBDs adsorbed on the two sides of the fibres' external surface. Indeed, the accessible area may be much larger than the one corresponding to a flat, impenetrable fibre. Therefore, an estimate of about 4 layers of CBDs adsorbed in the Whatman CF11 surface results from this reasoning, when the larger concentration of CBDs is used; for a lower CBD concentration, a surface coverage of 77% and 110% is estimated, respectively, for Portucel and Whatman fibres (Fig. 3), dividing the calculated surface concentration by the theoretical monolayer of CBDs. This is much higher than the expected maximum of one layer of adsorbed CBD, at saturation. Although the surface is apparently smooth, the fibres may have irregularities, such as microfissures or holes created by CBDs [25]. The presence of more or less loose microfibrils, large pores or fissures may substantially increase the surface area and the amount of bound proteins, thus leading to a higher fluorescence emission than the theorized monolayer. Indeed, confocal microscopy reveals that the surface has many irregularities (Fig. 5-c), while the inner region presents a homogeneous structure (Fig. 5-a). Another important observation provided by confocal microscopy was that fluorescence in the inner core of the fibres was always superior to the background intensity (Fig. 5-d and Fig. 5-e), indicating that CBDs may have penetrated into the fibre. As a matter of fact, as shown in Figure 5-d, fluorescent material (CBD-FITC) was detected at all depths of the fibre. This observation is supported by immunolabelling of CBD-treated CF11 fibres (Fig. 6). This analysis revealed the presence of CBDs (black spots) in the interior of the fibre. Considering this, we may now explain that the surface concentration of CBDs in Figure 3 arises from the CBDs penetration deep inside the fibres. Another aspect to take into account is that CBDs may not adsorb as a single and well ordered monolayer, but rather as agglomerates [26], thereby increasing the average fluorescence per unit area. Nevertheless, it is quite probable that the CBD coating of the external surface is rather significant.

Amorphous cellulose was prepared, by treating Whatman CF11 with phosphoric acid, which induces the swelling of fibres. As it can be seen in Figure 4, the fibres are larger than the

original ones (amorphous Whatman *versus* Whatman CF11). This swelling effect is due to the disruption or loosening of the microfibrils, thus increasing the volume occupied by the total fibre. As a result, the total surface area available for CBD adsorption increases. Consequently, it is expected that the measured CBD fluorescence would be higher than the one obtained for CF11 fibres, mostly due to an easier penetration of CBD into the fibres structure. This was confirmed, as can be seen in Figure 3. The surface coverage increases about 50% (4 versus 6 layers, respectively for Whatman CF11 and amorphous cellulose). This result can arise either from increased CBD affinity for the more amorphous fibres, or to easier penetration, and hence higher concentration in the fibres. Due to the higher fluorescence obtained with these fibres, the majority of the image exceeded the maximum concentration used in the calibration and it had to be excluded in the image analysis (Fig. 4).

Sigmacell 20 is obtained by the separation of crushed cellulose fibres, with an average size of 20 μm . This mechanical treatment expectedly leads to broken ends or loosen fibrils (amorphous material). Then, the adsorption of CBD is expected to be higher than with CF11 and comparable to the amorphous cellulose (see Figure 3). Again, the fibres present a high fluorescence emission corresponding to a high amount of adsorbed CBD: about 5 layers.

Conclusions

In this work, the surface concentration of CBD adsorbed on cellulose fibres was estimated. The coating values obtained were higher than expected, corresponding in theory to several layers (4 to 6) of CBDs adsorbed on the external surface. However, it has been demonstrated that the CBDs penetrate the fibres. An important amount of CBDs was detected inside the fibres by immunolabelling and confocal microscopy. It seems that a large fraction of the adsorbed CBDs actually penetrate the fibres. The surface coverage values are, undoubtedly, high enough to justify a change in the fibres' surface properties. CBDs may therefore be used as powerful tools to modulate the fibres' surface properties.

Methods

Chemicals

Fluorescein isothiocyanate (FITC), SigmaCell Type 20 and Whatman CF11 were obtained from Sigma. Secondary fibres were kindly supplied by *Portucel Viana*. All chemicals were of the highest purity available in the market.

Amorphous Cellulose Preparation

Amorphous cellulose was prepared by treating Whatman CF11 fibres with phosphoric acid. Briefly, 0.17 g of Whatman CF11 were slowly mixed with 10 mL of cold (4 °C) phosphoric acid (85%), and left in contact for 5 minutes. Then, 600 mL of cold water were added and the suspension was filtered through a test sieve (mesh width 71 µm, according to DIN 4188). Finally, the fibres were extensively washed first in tap water and afterwards with distilled water. The obtained material was lyophilized and stored.

CBD Production

The CBDs were prepared according to the following methodology: the Celluclast[®] commercial enzymatic preparation (Novozymes A/S, Denmark) was digested with Papain (1:1200, protein basis). The CBDs were separated by ultrafiltration through a 10 kDa membrane (Pellicon 2 TFF System from Millipore, USA) and concentrated by precipitation with ammonium sulphate (Merck, Darmstadt, Germany). After dialysis, the protein was injected on a Sepharose Fast-Flow gel (Amersham Pharmacia Biotech AB, Sweden), and the non-adsorbed protein was collected and lyophilized. The purity and identity (CBD from *T. reesei* CBH I) of this protein has been demonstrated by N-terminal sequencing and MALDI-TOF [10].

CBD-FITC production

The conjugation of CBD with the labelling probe was carried out by mixing 20 µg of FITC per mg of CBD (2 mg protein/mL in 0.1 M HEPES buffer, pH 9.0). This solution was incubated overnight in the dark, at room temperature, with magnetic stirring. To eliminate the unbound FITC, the labelled CBD mixture was filtered through a BIO-GEL P-4 (BIO-RAD, Hercules, USA) column, previously equilibrated with 50 mM sodium acetate buffer (Panreac, Barcelona, Spain).

CBD-FITC Adsorption

Adsorption assays of FITC-labelled CBD were carried out at 4 °C. The conjugates were allowed to adsorb on cellulose fibres (20 g/L, in 50 mM sodium acetate buffer, pH 5.0), with continuous magnetic stirring, in the dark, for 2 hours. The supernatant with unbound CBD was removed by centrifugation at 3219 RCF for 10 minutes (Heraeus Megafuge 1.0R). The fibres were washed with acetate buffer to remove the non-adsorbed CBD-FITC.

Image Acquisition

Fluorescence microscopy observations were performed in a Zeiss Axioskop microscope (Zeiss, Oberkochen, Germany) equipped with a Zeiss AxioCam HRc attached camera (Zeiss, Oberkochen, Germany) and using the AxioVision 3.1 software (Zeiss, Oberkochen, Germany). All images were acquired at 1300x1030 pixels and 24 bits colour depths (8 bits per channel). The FITC-CBD quantification was performed as described elsewhere (Pinto *et al.*, unpublished).

Confocal observation was performed in an Olympus (Tokyo, Japan) Fluoview 1000 in Laser Scanning mode equipped with a 60× UPLSAPO lens.

Antiserum preparation

CBD-specific antibodies were produced in a rabbit (*Oryctolagus cuniculus*) maintained under standard conditions of housing with unrestricted access to food and water; these conditions followed European Union Directive no. 86/609/CEE. Briefly, the rabbit was immunized intradermally (i.d.) with a 1:1 suspension of Phosphate Buffered saline (PBS) / Complete Freund's adjuvant containing 500 µg CBD and boosted two weeks later i.d. with a 1:1 suspension of PBS / Incomplete Freund's adjuvant containing 500 µg CBD. Blood was collected three weeks after the second immunization for the preparation of immune serum. Purification of IgG antibodies from this serum sample was performed as follows: the serum sample was equilibrated in a binding buffer (20 mM sodium phosphate, pH 7.0) by overnight dialysis and 3 ml of this preparation was applied to a Protein G HP affinity column (HiTrap, Amersham Biosciences, UK). Bound antibodies were eluted with Glycine -HCl buffer, pH 2.7 and recovered in 50 µl of 1M Tris-HCl pH 9.0 per ml of eluent, according to the manufacturer's instructions. Recovered IgG antibodies were further equilibrated in PBS in a VIVAPORE concentrator with a 7.5 kDa cutoff membrane (Vivascience, Hanover, Germany) and stored at -80°C in frozen aliquots. The anti-CBD antibody titre of this preparation was determined by ELISA. Specific anti-Sap2 or anti CaS antibodies in mice sera collected by retroorbital bleeding were quantified by ELISA. Polystyrene microtitre plates (Nunc, Roskilde, Denmark) were coated with 20 µg/ml of CBD and incubated o.n. at 4° C. Wells were then saturated for 1h at room temperature with 1% BSA in PBS. Serial dilutions of the serum samples were then plated and incubated for 2h at room temperature. After washing, bound antibodies were detected by adding alkaline phosphatase-coupled monoclonal goat anti-rabbit-IgG antibody (Southern Biotechnology Associates, Birmingham, ALA, USA) for 30 min at room temperature. Substrate solution containing p-nitrophenyl phosphate (Sigma, St. Louis, USA) was then added after washing and the reaction was stopped by adding 0.1 M EDTA pH 8.0. The absorbance was

measured at 405 nm. The ELISA antibody titres were expressed as the reciprocal of the highest dilution giving an absorbance of 0.1 above that of the control (no serum added). The titre of anti CBD antibodies in the purified IgG preparation was of 4014. No antibodies with this specificity were detected in the control sera from non-immunized rabbits.

Immunolabelling in Transmission Electron Microscopy

The CBD-treated Whatman CF11 fibres were fixed in a freshly prepared mixture of 0.2% glutaraldehyde (v/v), 2% paraformaldehyde (w/v) in 0.05 M phosphate buffer (pH 7-7.2). Successive periods of vacuum (5 to 10 min) and air inlet were carried out, up to two hours. Afterwards, the fibres were washed 3×10 minutes with 0.05 M phosphate buffer. The samples were then dehydrated through a graded series of ethanol and embedded in London Resin White (hard mixture) polymerized for 24 h at 50°C.

Immunolabelling was done on ultrathin transverse sections (500 Å) floating on plastic rings [27]. The sections were floated on several dilutions of the antiserum in 10 mM Tris buffered saline (500 mM NaCl) to determine the optimal ratio of labelling and background [28]. The secondary marker was Protein A-gold (pA G5, BioCell). The gold particles were further enhanced using a silver enhancing Amersham kit. Finally, the thin-sections were transferred on copper-grids, post-stained with 2.5% aqueous uranyl acetate and examined with a Philips CM 200 Cryo-TEM at an accelerating voltage of 80 kV.

To guarantee semi-quantitative comparative labelling, experiments were carried out in parallel on treated and non-treated samples of CBD. Therefore, the exposure to the antibody was identical.

Authors' contributions

RP carried out the amorphous cellulose, CBD and CBD-FITC production, made the adsorption assays and the image acquisition, participated in the conception of this work and manuscript writing. ALA and ECF helped conceiving the image analysis system. MV produced the antiserum. KR was responsible for the TEM-immunolabeling experiments. MM is the director of the research unit and helped to draft the manuscript. MG participated in the conception and supervision of the work and contributed to the manuscript preparation. All authors read and approved the final manuscript.

Acknowledgements

Ricardo Pinto was supported by a grant from the Fundação para a Ciência e a Tecnologia (FCT) SFRH/BD/6934/2001.

References

1. Nagl S, Schaeferling M, Wolfbeis OS: **Fluorescence analysis in microarray technology.** *Microchimica Acta* 2005, **151**: 1-21.
2. Stewart CN, Millwood RJ, Halfhill MD, Ayalew M, Cardoza V, Kooshki M *et al.*: **Laser-induced fluorescence imaging and spectroscopy of GFP transgenic plants.** *Journal of Fluorescence* 2005, **15**: 697-705.
3. Sonesson AW, Callisen TH, Brismar H, Elofsson UM: **Lipase surface diffusion studied by fluorescence recovery after photobleaching.** *Langmuir* 2005, **21**: 11949-11956.
4. Plant AL, Benson DM, Smith LC: **Cellular Uptake and Intracellular-Localization of Benzo(A)Pyrene by Digital Fluorescence Imaging Microscopy.** *Journal of Cell Biology* 1985, **100**: 1295-1308.
5. Guttman A, Ronai Z, Csapo Z, Gerstner A, Sasvari-Szekely M: **Rapid analysis of covalently and non-covalently fluorophore-labeled proteins using ultra-thin-layer sodium dodecylsulfate gel electrophoresis.** *Journal of Chromatography A* 2000, **894**: 329-335.
6. Mackintosh JA, Veal DA, Karuso P: **Fluoroprofile, a fluorescence-based assay for rapid and sensitive quantitation of proteins in solution.** *Proteomics* 2005, **5**: 4673-4677.
7. Zhang XW, Zhao FL, Li KA: **Fluorometric method for the microdetermination of protein using indigo carmine.** *Microchemical Journal* 2001, **68**: 53-59.
8. Limon MC, Margolles-Clark E, Benitez T, Penttila M: **Addition of substrate-binding domains increases substrate-binding capacity and specific activity of a chitinase from *Trichoderma harzianum*.** *Fems Microbiology Letters* 2001, **198**: 57-63.

9. Srisodsuk M: *Mode of action of Trichoderma reesei cellobiohydrolase I on crystalline cellulose*. VTT Publications 188; 1994. PhD.
10. Pinto R, Carvalho J, Mota M, Gama M. **Large-scale production of cellulose-binding domains. Adsorption studies using CBD-FITC conjugates.** *Cellulose* 2006, **13**: 557-569.
11. Mattinen ML, Linder M, Teleman A, Annala A: **Interaction between cellohexaose and cellulose binding domains from Trichoderma reesei cellulases.** *Febs Letters* 1997, **407**: 291-296.
12. Hilden L, Daniel G, Johansson G: **Use of a fluorescence labelled, carbohydrate-binding module from Phanerochaete chrysosporium Cel7D for studying wood cell wall ultrastructure.** *Biotechnology Letters* 2003, **25**: 553-558.
13. Jervis EJ, Haynes CA, Kilburn DG: **Surface diffusion of cellulases and their isolated binding domains on cellulose.** *Journal of Biological Chemistry* 1997, **272**: 24016-24023.
14. Bossowski A, Stasiak-Barmuta A, Czarnocka B, Urban M, Dadan J: **Application of mouse monoclonal antibodies for identification of antigen regions of human thyroid peroxidase in adolescents with Graves' disease and non-toxic multinodular goiter by flow cytometry.** *Autoimmunity* 2005, **38**: 605-611.
15. Lenkei R, Andersson B: **Determination of the Antibody-Binding Capacity of Lymphocyte Membrane-Antigens by Flow-Cytometry in 58 Blood-Donors.** *Journal of Immunological Methods* 1995, **183**: 267-277.
16. Maculotti K, Genta I, Perugini P, Imam M, Bernkop-Schnurch A, Pavanetto F: **Preparation and in vitro evaluation of thiolated chitosan microparticles.** *Journal of Microencapsulation* 2005, **22**: 459-470.
17. Zeltins A, Schrempf H: **Visualization of Alpha-Chitin with A Specific Chitin-Binding Protein (Chb1) from Streptomyces-Olivaceoviridis.** *Analytical Biochemistry* 1995, **231**: 287-294.
18. Levy I, Shani Z, Shoseyov O: **Modification of polysaccharides and plant cell wall by endo-1,4-beta-glucanase and cellulose-binding domains.** *Biomolecular Engineering* 2002, **19**: 17-30.

19. Suurnakki A, Tenkanen M, Siika-aho M, Niku-Paavola ML, Viikari L, Buchert J: **Trichoderma reesei cellulases and their core domains in the hydrolysis and modification of chemical pulp.** *Cellulose* 2000, **7**: 189-209.
20. Pala H, Lemos MA, Mota M, Gama FM: **Enzymatic upgrade of old paperboard containers.** *Enzyme and Microbial Technology* 2001, **29**: 274-279.
21. Brunauer S, Emmett PH, Teller E: **Adsorption of Gases in Multimolecular Layers.** *Journal of the American Chemical Society* 1938, **60**: 309-319.
22. Sing K: **The use of nitrogen adsorption for the characterisation of porous materials.** *Colloids and Surfaces A-Physicochemical and Engineering Aspects* 2001, **187**: 3-9.
23. Teeri TT: **Crystalline cellulose degradation: New insight into the function of cellobiohydrolases.** *Trends in Biotechnology* 1997, **15**: 160-167.
24. Kraulis PJ, Clore GM, Nilges M, Jones TA, Pettersson G, Knowles J *et al.*: **Determination of the 3-Dimensional Solution Structure of the C-Terminal Domain of Cellobiohydrolase-I from Trichoderma-Reesei - A Study Using Nuclear Magnetic-Resonance and Hybrid Distance Geometry Dynamical Simulated Annealing.** *Biochemistry* 1989, **28**: 7241-7257.
25. Gao PJ, Chen GJ, Wang TH, Zhang YS, Liu J: **Non-hydrolytic disruption of crystalline structure of cellulose by cellulose binding domain and linker sequence of cellobiohydrolase I from Penicillium janthinellum.** *Acta Biochimica et Biophysica Sinica* 2001, **33**: 13-18.
26. Nigmatullin R, Lovitt R, Wright C, Linder M, Nakari-Setälä T, Gama A: **Atomic force microscopy study of cellulose surface interaction controlled by cellulose binding domains.** *Colloids and Surfaces B-Biointerfaces* 2004, **35**: 125-135.
27. Ruel K, Ambert K, Joseleau JP: **Influence of the enzyme equipment of white-rot fungi on the patterns of wood degradation.** *Fems Microbiology Reviews* 1994, **13**: 241-254.
28. Ruel K, Faix O, Joseleau J-P: **New immunogold probes for studying the distribution of the different lignin types during plant cell wall biogenesis.** *Journal of Trace and Microprobe Techniques* 1994, **12**: 247-265.

Figures

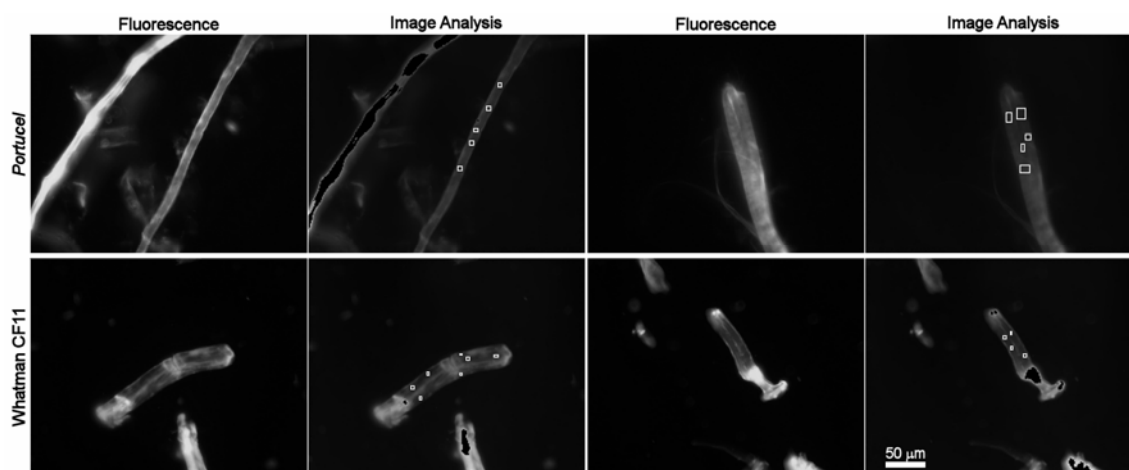


Figure M3.1. Portucel and Whatman CF11 fibres treated with CBD-FITC. The fibres treated with a concentration of $60 \mu\text{g/mL}$ (or $2 \text{ mg}_{\text{CBD}}/\text{g}_{\text{fibres}}$). The images were acquired with an exposure time of 600 ms. The white squares identify the areas selected for analysis. The more fluorescent parts (black regions on the analyzed images) are out of range (calibration shown elsewhere), and were therefore excluded from the analysis.

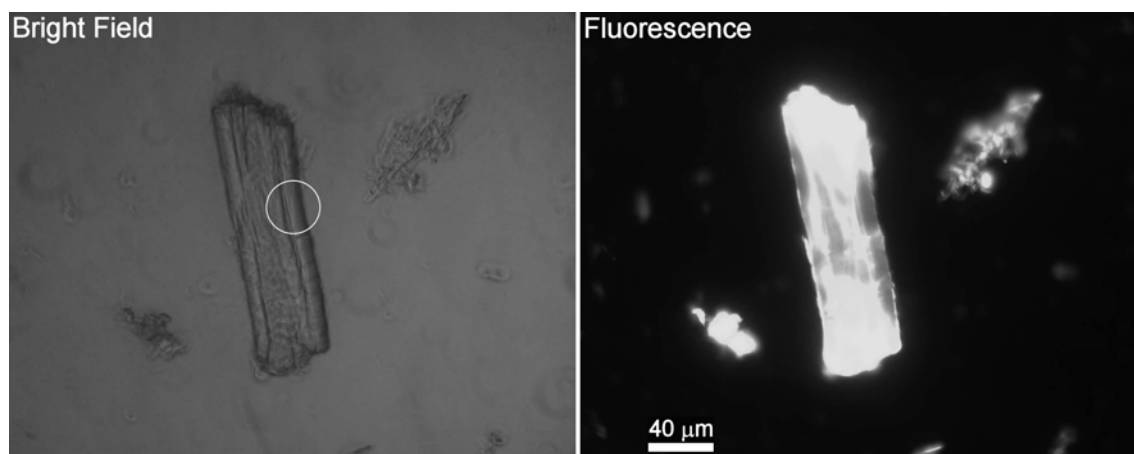


Figure M3.2. Whatman CF11 images. The characteristic curled structure of the fibres (circle).

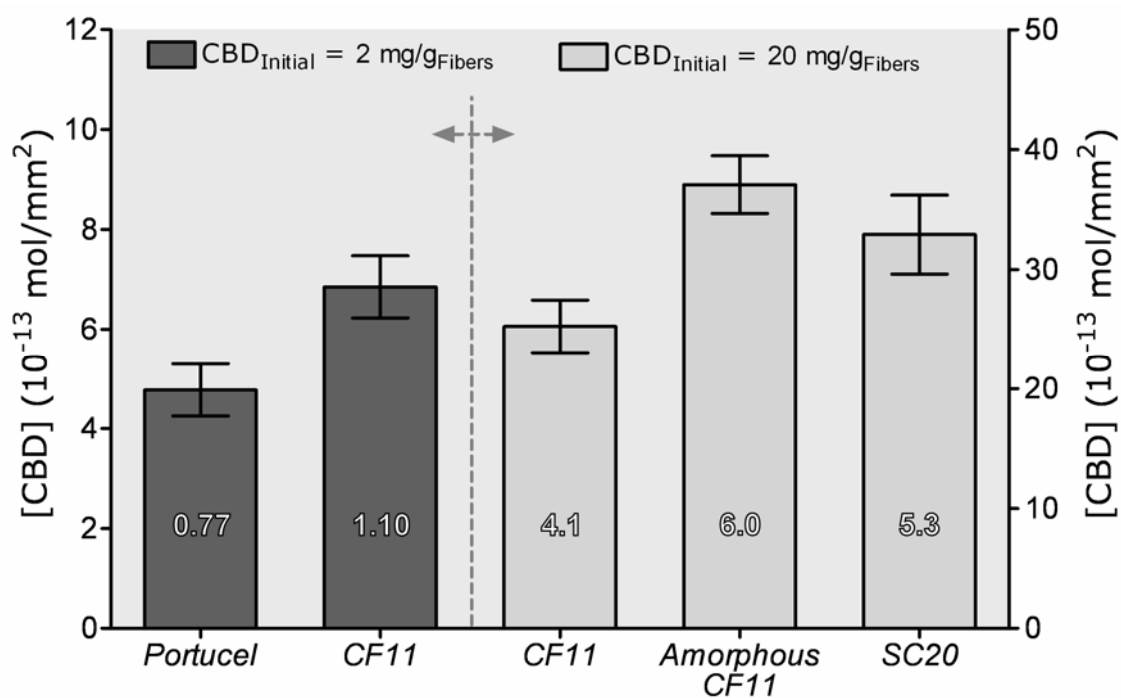


Figure M3.3. Estimated surface concentration of adsorbed CBD. The estimated fraction of surface coverage is indicated in the figure bars. The values shown are based on the assumption that the protein is adsorbed on the external surface of the fibres only. The values are shown with 95% confidence intervals error bars.

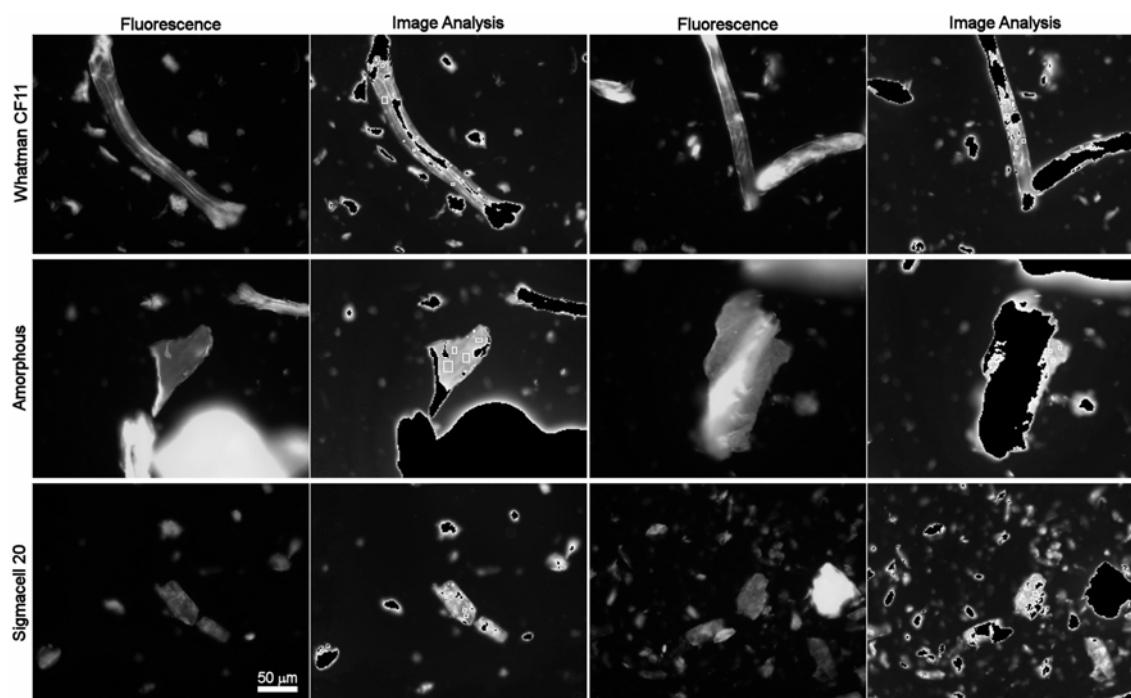


Figure M3.4. Images obtained by fluorescence microscopy of Whatman CF11, amorphous and Sigmacell 20 fibres. The images were obtained before – 1st and 3rd column – and after – 2nd and 4th column – the image analysis of fibres treated with a CBD-FITC concentration of 400 $\mu\text{g}/\text{mL}$. The black areas on the treated images correspond to the fluorescence emission, which is higher than the one used in the calibration. Fluorescence images acquired for 100 ms (CF11) and 80 ms (Amorphous and Sigmacell).

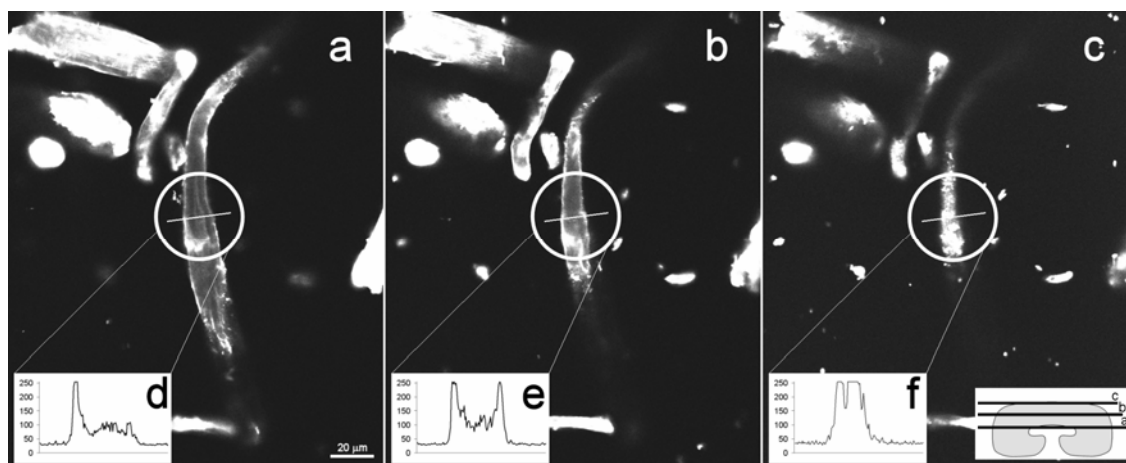


Figure M3.5. Images from confocal microscopy. Three plans of a CF11 fibre are presented, as schematized in the right insertion of figure *c*. The insertions *d*, *e* and *f* correspond to the pixels intensity (256 grey levels) obtained at the position indicated by the line (white circle), at different depths. The adsorption conditions were $20 \text{ mg}_{\text{CBD}}/\text{g}_{\text{Fibre}}$, for 30 minutes of contact. Each image corresponds to an acquisition thickness of $1 \mu\text{m}$.

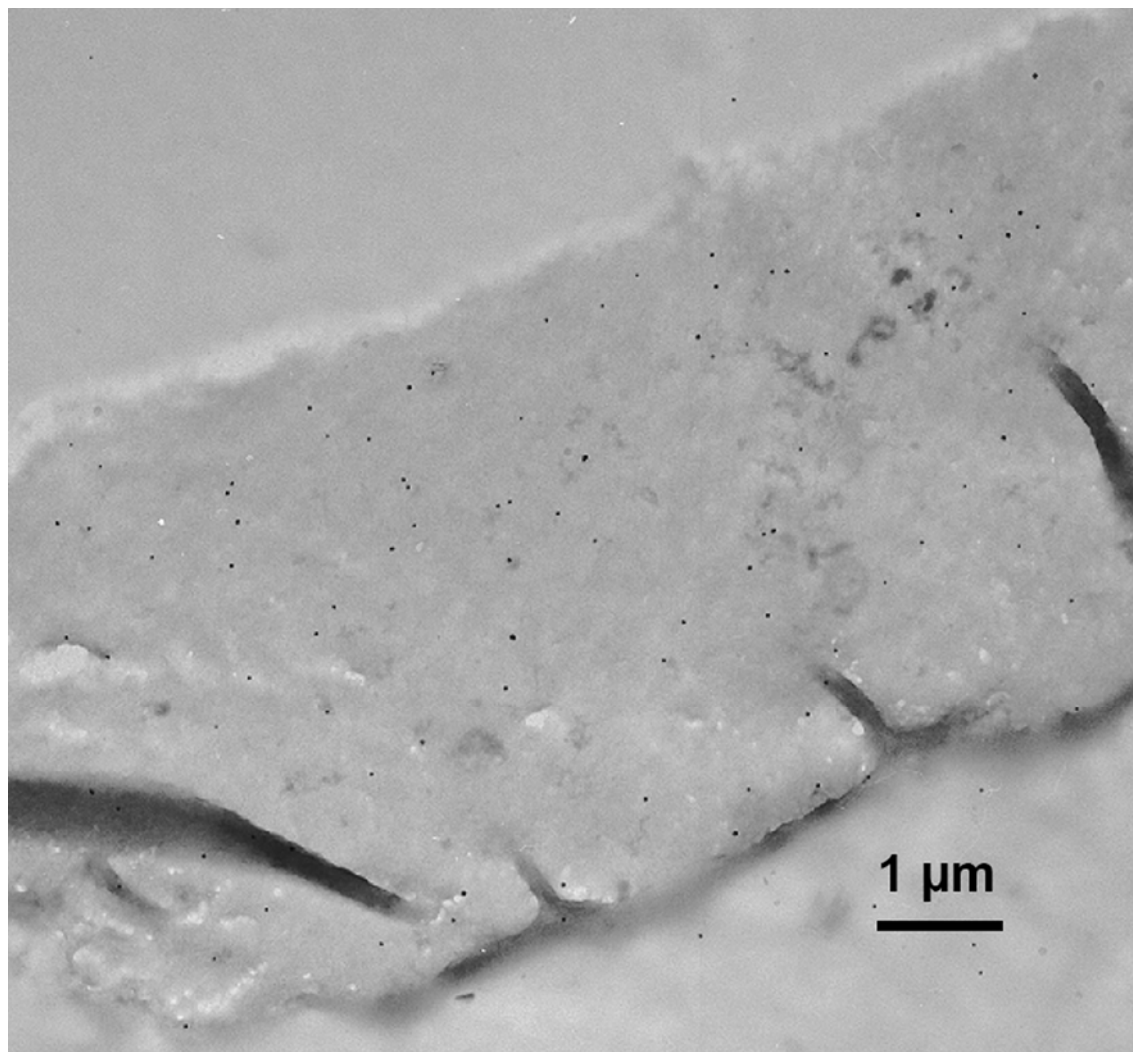


Figure M3.6. Electron microscopy image of immunolabeling of CBD-treated Whatman CF11 fibers.

M4. Effect of Cellulose-Binding Domains on Pulp Paper Properties

(Submitted to *Journal of Biotechnology*)

Ricardo Pinto¹, Ana Paula Duarte², Manuel Mota¹, Miguel Gama^{1,*}

¹Centro de Engenharia Biológica, Universidade do Minho
4710-057 Braga, Portugal.

²Departamento de Ciências e Tecnologia Papel, Universidade da Beira Interior
Rua Marquês d'Ávila e Bolama, 6201-001 Covilhã

*e-mail: fmgama@deb.uminho.pt; phone: +351253604400; fax: +351253678986.

Abstract

The effect of Cellulose-Binding Domains (CBD) on the properties of different kinds of paper fibers is analyzed. Eucalyptus, pine and secondary fibers, submitted to different degrees of refining, were treated with CBDs. The pulp and paper properties were analyzed. CBDs conjugated chemically with Lysozyme were also used, to study the effect of the adsorbed protein electric charge on the fibers modification. The surface properties of paper and fibers were also analyzed by ZETA-potential and contact angle measurements. Both CBDs and CBD-Lysozyme conjugates improve the pulp drainability and air permeability of the papersheets. The use of CBD conjugates allows the control of the cellulosic fibers surface properties, such as hydrophobicity and electric charge.

Keywords: Cellulose-binding domain, fiber properties, ZETA-potential, contact angle

Abbreviations: BSA, bovine serum albumin; CBD, cellulose-binding domains; DMSO, dimethyl sulfoxide; DNS, dinitro-salicylic acid; FPU, filter paper units; HSAB, N-hydroxysuccinimidyl 4-azidobenzoate; MALDI-TOF, Matrix-assisted laser desorption/ionisation-time of flight; pI, isoelectric point; °SR, Schopper-Riegler degree; UV, ultraviolet radiation; WRV, water retention value; ΔG^T_{cwc} , variation of the total free energy; γ^{LW} , surface tension apolar component (Lifshitz-van der Waals interaction); γ^+ and γ^- , positive and negative surface tension components; θ , contact angle

Introduction

Enzymes have been applied in paper production, for the modification of fiber/paper properties. Xylanases have been used in the treatment of softwood kraft pulps, allowing the reduction of bleaching chemical requirements (Suurnäkki et al., 1994; Senior and Hamilton, 1993). Endo-glucanases have been used in deinking of recycled paper (Geng and Li, 2003). Cellulases and hemicellulases have been used to improve fibers refining (Seo et al., 2000) and freeness/drainage (Jackson et al., 1993; Pala et al., 2001; Stork et al., 1995). Enzymes hydrolyze the polysaccharides, leading to reduction of both fiber strength and mass.

Cellulose-binding domains (CBDs) are proteins that exhibit high cellulose affinity (Black et al., 1997). They are produced by a large number of fungi and bacteria, associated to the cellulases catalytic modules (Irwin et al., 1998; Mattinen et al., 1998). DNA recombinant technology may be used to fuse CBDs with other proteins with different size, charge, hydrophobicity, catalytic activity, bioactivity, etc (Reinikainen et al., 1997). CBDs are, therefore, potentially very useful in the activation and modification of cellulosic fibers (Kitaoka and Tanaka, 2001).

In a previous work we have shown that CBDs, obtained by proteolysis of *Trichoderma reesei* cellulases, have the ability to modify the drainability of recycled paper pulps (Pala et al., 2001). In the present work, we analyze the potential of CBDs to modify different types of fibers, submitted to various degrees of refining. Fibers from Eucalyptus and Pine, as well as secondary fibers, were used. Furthermore, CBDs were chemically conjugated with lysozyme, as this protein has a pI of 11.4, hence being expected to positively charge the fibers. The surface and technical properties of the fibers, treated with the lysozyme conjugated CBDs, were also analyzed..

Materials and Methods

Chemicals

Sodium acetate was obtained from Panreac (Barcelona, Spain), ammonium sulphate from Merck (Darmstadt, Germany), and the other from Sigma-Aldrich (St. Louis, USA). Primary fibers were from industrial bleached kraft pulp of *Eucalyptus globulus* and industrial unbleached kraft pulp of *Pinus pinaster* (Pine). Secondary fibers were gently supplied by *Portucel Viana* (Kraftliner paper) and *Nisa* companies (tissue paper). All chemicals were of the highest purity available.

CBD Production

The CBDs were prepared according to the following methodology: the commercial enzymatic preparation Celluclast[®] (Novozymes A/S, Denmark) was digested with Papain (1:1200, protein basis). CBDs were separated by ultrafiltration through a 10 kDa membrane (Pellicon 2 TFF System from Millipore, USA) and concentrated by precipitation with ammonium sulphate. After dialysis, the protein was injected in a Sepharose Fast-Flow gel (Amersham Pharmacia Biotech AB, Sweden), and the non-adsorbed protein was collected and lyophilized. The purity of this protein was demonstrated by N-terminal sequencing and MALDI-TOF, as described in Pinto et al. (2006).

Protein Conjugation

The chemical N-hydroxysuccinimidyl 4-azidobenzoate (HSAB) was used to conjugate CBD with lysozyme. This molecule is a well known heterobifunctional reticulating agent (Johnson et al., 1981). One of its structural groups reacts with a free amine, and the other is, under UV irradiation, highly reactive, preferably also with a free amine. HSAB was dissolved in dry DMSO (150 mg·mL⁻¹). Then it was added (10×8 μL aliquots, with 20 minutes interval) to 40 mg of CBD in 4 mL phosphate buffer (20 mM, pH 7.5), and the mixture was kept at room temperature in the dark, for 20 hours. The unreacted HSAB was separated by thoroughly dialyzing the reaction mixture in a 1 kDa Cellu-Sep H1 membrane (Membrane Filtration Products, Inc., Texas, USA), against acetate buffer (50 mM, pH 5.0), always in the dark. The activated CBD was then mixed with lysozyme (at a molar ratio of 3 to 1 mol, respectively) and

photo-conjugated for 30 minutes, on ice, by direct exposure to an 8W UV lamp (254 nm), in a Camag UV-Cabinet II (Muttentz, Switzerland).

The conjugate obtained was analyzed by size exclusion chromatography, using a Bio-Gel P-60 (Bio-Rad, California, USA) column, packed according to the manufacture instructions, using acetate buffer (50 mM, pH 5.0) as eluent.

Adsorption assays, using Whatman CF11 cellulose, were carried out by mixing the CBDs and lysozyme, conjugated or not (at a molar ratio of 3 to 1 mol, respectively), in acetate buffer (50 mM, pH 5.0), at 5°C. After 2 hours, the supernatants were separated by centrifugation (12225 RCF, Sigma 4K10, B. Braun) and the protein content in the supernatant was assessed by spectrofluorimetry (model FP6200, Jasco Corporation, Japan).

Treatment with CBD and CBD-lysozyme conjugates

Cellulose fibers, at 10% (w/w) consistency, were beaten in a PFI mill for 0, 1000 or 3000 revolutions. Afterwards, CBDs were adsorbed by mixing the protein (2 mg per gram of fibers, dry weight) with 30 g of fibers (dry weight) in acetate buffer (50 mM, pH 5.0 and final volume of 2 L) for 30 minutes at 22-25°C. Control experiments were performed by adding buffer without the protein. Fibers were filtered and the fines were recovered by re-filtering the permeate through the fibers cake. The fibers were finally re-suspended with demineralized water to 2% (w/v) consistency.

Fibers were also treated with 4 mg of CBD-lysozyme or 2.24 mg of CBDs (equivalent to the amount of CBD present in the conjugates), per gram of cellulose, in the same conditions as stated above for CBDs adsorption.

Analysis of the Pulp and Paper Properties

The pulp and handsheet properties were analyzed using standard procedures: ISO 5267/1 (Schopper-Riegler); ISO 5636/3 1992(F) (permeability); ISO 1924/2 1985(F) (tensile strength and break length); ISO 1974(F) (tearing); ISO 2758 1983(E) (bursting strength). The water retention value (WRV) was determined according to the method reported by Silvy et al. (1968).

Contact Angle Measurement

Sigmacell 20 fibers (pure cellulose), after CBD or CBD-lysozyme conjugates adsorption (10 mg per gram of fiber, for 30 minutes at 5°C), were filtered on a 0.45 µm membrane and air dried. The Sigmacell 20 membrane film obtained, and stripes of *Portucel* papersheets, were analyzed by contact angle measurements. The samples were held in an OCA20 apparatus

(Dataphysics, Filderstadt, Germany), using a double coated tape. The contact angles were measured with the SCA20 software (Dataphysics, Filderstadt, Germany), using 3 μL of each liquid probe (water, 1-bromonaphthalene and formamide). The surface tension components (γ_c^{LW} , γ_c^+ and γ_c^- , $\text{mJ}\cdot\text{m}^{-2}$) of cellulose fibers were obtained by resolving the Good-van Oss-Chaudhury equation for each liquid (van Oss et al., 1988a):

$$(1 + \cos \theta) \cdot \gamma_L = 2 \cdot \left(\sqrt{\gamma_c^{LW} \cdot \gamma_L^{LW}} + \sqrt{\gamma_c^+ \cdot \gamma_L^-} + \sqrt{\gamma_c^- \cdot \gamma_L^+} \right) \quad (1)$$

Where γ_L , γ_L^{LW} , γ_L^+ and γ_L^- are the surface tension, Lifshitz-van der Waals interaction (apolar component) and the positive and negative surface tension components, respectively, of the liquid (L). The degree of hydrophobicity can be assessed by calculating the variation of the total free energy (ΔG_{cwc}^T , $\text{mJ}\cdot\text{m}^{-2}$) between two moieties of cellulose immersed in water (van Oss et al., 1988a):

$$\Delta G_{cwc}^T = -2 \cdot \left(\sqrt{\gamma_c^{LW}} - \sqrt{\gamma_w^{LW}} \right)^2 + 4 \cdot \left(\sqrt{\gamma_c^+ \cdot \gamma_w^-} + \sqrt{\gamma_c^- \cdot \gamma_w^+} - \sqrt{\gamma_c^+ \cdot \gamma_c^-} - \sqrt{\gamma_w^+ \cdot \gamma_w^-} \right) \quad (2)$$

Where the subscripts c and w stand for cellulose and water, respectively.

ZETA-Potential

The ZETA-potential of *Portucel* and Eucalyptus fibers was assessed by measuring the streaming potential across a fiber pad, by Müttek SZP-06 (Herrsching, Germany) apparatus, according to the device instructions.

The Sigmacell 20 fibers were allowed to adsorb either CBDs or conjugates (13 mg per gram of dry fibers) at 5°C in acetate buffer (20 mM, pH 5.0). After 2 hours of contact, the fibers were centrifuged and the supernatant discarded. The fibers were then diluted in 30mL of ultrapure water and the ZETA-potential was measured by electrophoretic mobility, in a Zeta-Meter 3.0+ apparatus.

Results and Discussion

CBD Treatment of Paper Fibers

The pulp drainability is the capacity of the pulp for water drainage and is measured by the Schopper-Riegler degree ($^\circ\text{SR}$). The effect of CBD treatment on the drainability of different pulps was analyzed (Figure M4.1). As can be seen, pulp drainability decreases with the refining process ($^\circ\text{SR}$ increases), because the fiber becomes more hydrated and fibrillated. The adsorption of CBD implied a reduction of the $^\circ\text{SR}$ values, as compared to the blank samples, to a maximum

of 15%, for each of the pulps used. This result has been described in a previous paper (Pala et al., 2001) for secondary fibers. The drainage improvement has also been observed when using cellulases (Oksanen et al., 2000; Pala et al., 2001; Stork et al., 1995). It has been theorized that this improvement, when obtained with cellulases, is due to the hydrolysis of the amorphous cellulose on the fibers surface and/or of the fines in the solution. The CBD sample used in this work has a reduced ability to hydrolyze cellulose (as estimated by FPU measurement). As a matter of fact, the release of sugars is not detected by DNS method, after the CBD treatment, since the CBD used is almost pure, as shown elsewhere (Pinto et al., 2006). In this case, the improved drainability may be explained by dispersion of fines, which allows the water to flow more freely between the fibers. The stabilization of fines/fibers in aqueous medium has been observed (Pinto et al., 2004) by SEM analysis of Whatman CF11 fibers with and without adsorbed CBD. The stabilization may be the result of either (or both) improved fibers hydration and steric effects.

Table M4.1 presents the water retention values (WRV) for the four kinds of fibers used. As can be seen, the CBD adsorption increases, in most cases, the WRV value. As expected, refining also increases WRV. It can also be seen that secondary fibers have higher WRV. These values are in agreement with differential scanning calorimetry results, reported by Dourado et al. (1999). In that work, it was shown that CBD adsorption increases both the bound water and the specific heat of dehydration. In our view, the higher WRV is due to the presence of oligosaccharides (30%, w/w) attached to the CBDs (Pinto et al., 2006), with high water affinity. This value has been related to the fibers ability to form hydrogen bonds during paper making, and thus, to paper strength. However, it is probable that the CBDs with linked oligosaccharides will stabilize the fibers due to steric effects and thus reduce the interfiber interactions, in water suspensions.

Table M4.2 presents the air permeability of the papersheets. As a general trend, the CBDs treatment increases the air permeability. The increase is more significant for the secondary fibers, not refined, and for the Pine fibers, at the highest refinement. The air permeability is an important parameter, since it is related to the ability to remove water during the paper drying step. A higher permeability implies lower drying times, thus lower heat consumption and a faster production rate.

Figure M4.2 and Figure M4.3 show the variation induced by the CBDs adsorptions on the physical parameters of the handsheets prepared with each kind of fiber. As can be observed, the variation is less favorable with increasing refining. Another aspect to be retained is that for the non-refined virgin fibers, the CBDs slightly increase the paper strength. This effect is statistically

significant for the Eucalyptus fibers. This improvement may be explained by variations on the surface properties induced by adsorbed CBDs. The non-refined fibers have a lower overall surface area, and hence the effect of CBD is expected to be more important in this case, since the specific coverage of the fibers must be higher. On the other hand, by increasing the water retention value, CBDs stabilizes the fibers, allowing for a better water drainage, hence lower Schopper-Riegler values.

CBD Conjugation with Lysozyme

Figure M4.4 presents the size exclusion chromatogram of the obtained conjugates. As can be observed, after the conjugation reaction, the lysozyme peak (elution time ~150 minutes) is much lower. Moreover, the reaction leads to the appearance of higher molecular weight peaks, which should correspond to conjugates of one molecule of lysozyme with one or more CBDs. The CBDs obtained by proteolysis are a module from the *Trichoderma reesei* cellobiohydrolase I enzyme (Pinto et al., 2006), and have only one free amine, the N-terminal one. Thus, a single connection between each CBD and lysozyme molecules is possible. This conjugation induces a higher cellulose affinity of the protein, as shown in Figure M4.5. The conjugates adsorption reveals higher affinity than the one exhibited by a mixture of CBD and lysozyme, at the same molar ratio as the conjugates. The higher affinity may result from both the presence of multimeric proteins with several CBDs and to the lysozyme positive charge: the cellulose fibers, being negatively charged, induce an electrostatic favorable interaction with the conjugates.

Table M4.3 shows that the conjugates do not reduce the Schopper-Riegler index as much as CBD. In turn, the permeability is enhanced by the conjugates adsorption (Table M4.3), maybe due to the fact that lysozyme as a high isoelectric point, and thus a high positive charge at the used pH. Consequently, an electrostatic repulsion may yield more porous paper sheets. In terms of the paper strength parameters, a reduction is observed, although not statistically significant ($p > 0.05$). Probably, the presence of the protein on the fibers/fines surface impairs the interfiber hydrogen bonding.

Surface Properties

Table M4.4 present the ZETA-potential values, measured for the Eucalyptus and *Portu cel* fibers. With adsorbed CBDs ($2.24 \text{ mg} \cdot \text{g}_{\text{cellulose}}^{-1}$) or conjugates ($4 \text{ mg} \cdot \text{g}_{\text{cellulose}}^{-1}$), only the unrefined Eucalyptus fibers present a significant variation of the measured ZETA-potential, probably due to its lower surface area and fines content, as compared to the refined fibers. Paquot et al. (1994) have shown that the ZETA-potential of cellulose fibers treated with proteins (BSA and

lysozyme) only for high protein surface coverage varies significantly. This may explain the negligible ZETA-potential variation observed with the refined pulps. Due to high fines content, thus high surface area, the ZETA-potential values of *Portucel* remain invariable. With Sigmacell fibers, a much higher concentration of protein was used ($13 \text{ mg}\cdot\text{g}^{-1}$ versus $2 \text{ mg}\cdot\text{g}^{-1}$ used with the paper fibers) and, consequently, the values of ZETA-potential vary significantly as expected, exhibiting a much higher positive value when conjugates are used.

Table M4.5 shows the apolar (γ^{LW}) and polar (γ^+ and γ^-) surface tension components, along with the variation of the total free energy for the interaction of fibers in water (ΔG_{cwc}). The ΔG_{cwc} is a parameter indicative of the hydrophilicity (positive values) or hydrophobicity (negative values) of the fibers (van Oss et al., 1988a). The adsorption of CBD slightly increased the hydrophilicity of pure cellulose (Sigmacell) and of primary fibers (Eucalyptus), despite the ZETA-potential (determined by electrophoretic mobility) increased for Sigmacell fibers after adsorption of CBDs (Table M4.4), shifting from negative to positive values. The surface properties of virgin Eucalyptus fibers and of Sigmacell (pure cellulose) are quite similar. The secondary fibers (*Portucel*) contain print pigments, glues, etc. This may explain the different values obtained for the polar surface tension components of the untreated fibers (higher γ^+ and a significantly lower γ^-) and hydrophobic paper surface (negative ΔG_{cwc}). Thus, a different effect of the CBD adsorption may be expected. As seen in Table M4.5, the CBD adsorption reduces the negative component (γ^-), an effect not observed with the other studied fibers (virgin Eucalyptus fibers and the pure cellulose Sigmacell). The ΔG_{cwc} does not account for steric and hydration forces, that may be quite relevant when analyzing the effect of adsorbed proteins on the surface properties. The results (Table M4.5) show that CBDs adsorption did not change the polar and apolar surface properties dramatically. Nevertheless, the effect in the hydration and interfiber interaction is relevant, as revealed by WRV and the higher value of ΔG_{cwc} .

The adsorption of conjugates to pure cellulose (Sigmacell) increased the ZETA potential more than the CBDs (Table M4.4), as expected from their positive charge at pH 5.0. The adsorption of the positively charged conjugates strongly reduces the fibers γ^- (negative polar component), as may be observed on Table M4.5. Consequently, due to the reduction of polarity, the fibers surface becomes hydrophobic (negative ΔG_{cwc}). This effect is also a consequence of the properties of dry lysozyme, which has a hydrophobic character (Van Oss et al., 1988b). It should be mentioned that even after 10 seconds of the first contact of the water drop with the Sigmacell with adsorbed conjugates, virtually no absorption of water was observed, as opposed to the other fibers. Since the *Portucel* fibers are hydrophobic, the conjugate adsorption did not produce any major modification of the surface tension components. Due to the much higher

protein concentration (13 mg/g_{cellulose}) used in the assays with Sigmacell, a dramatic effect is observed; in the case of *Portucel* fibers, the protein concentration (2 mg/g_{cellulose}) was insufficient to induce a similar effect.

Conclusion

The CBD adsorption leads to a change on the surface properties of fibers, as revealed by the change in the pulp drainage and air permeability of the papersheets. When conjugated to other proteins, CBDs may be used to drive other proteins/molecules, with different properties, to the fibers surface, enhancing the paper functionality. It is possible, with this strategy, to modify both the technical properties of pulp and paper and the fibers surface properties, such as electric charge and hydrophobicity.

Acknowledgments

Ricardo Pinto was supported by Fundação para a Ciência e a Tecnologia (FCT) grant SFRH/BD/6934/2001.

Bibliography

- Black, G.W., Rixon, J.E., Clarke, J.H., Hazlewood, G.P., Ferreira, L.M. A., Bolam, D.N., Gilbert, H.J., 1997. Cellulose binding domains and linker sequences potentiate the activity of hemicellulases against complex substrates. *J. Biotechnol.* 57, 59-69.
- Dourado, F., Mota, M., Pala, H., Gama, F.M., 1999. Effect of cellulase adsorption on the surface and interfacial properties of cellulose. *Cellulose* 6, 265-282.
- Geng, X., Li, K., 2003. Deinking of recycled mixed office paper using two endo-glucanases, CelB and CelE, from the anaerobic fungus *Orpinomyces* PC-2. *TAPPI J.* 2, 29-32.

Irwin, D., Shin, D.-H., Zhang, S., Barr, B.K., Sakon, J., Karplus, P.A., Wilson, D.B., 1998. Roles of the Catalytic Domain and Two Cellulose Binding Domains of *Thermomonospora fusca* E4 in Cellulose Hydrolysis. *J. Bacteriol.* 180, 1709-1714.

Jackson, L.S., Heitmann, J.A., Joyce, T.W., 1993. Enzymatic modifications of secondary fiber. *TAPPI J.* 76, 147-154.

Johnson, G.L., Macandrew, V.I., Pilch, P.F., 1981. Identification of the glucagon receptor in rat liver membranes by photoaffinity crosslinking. *Proc. Natl. Acad. Sci. USA* 78, 875-878.

Kitaoka, T., Tanaka, H., 2001. Novel paper strength additive containing cellulose-binding domain of cellulose. *J. Wood Sci.* 47, 322-324.

Mattinen, M.-L., Linder, M., Drakenberg, T., Annala, A., 1998. Solution structure of the cellulose-binding domain of endoglucanase I from *Trichoderma reesei* and its interaction with cello-oligosaccharides. *Eur. J. Biochem.* 256, 279-286.

Oksanen, T., Pere, J., Paavilainen, L., Buchert, J., Viikari, L., 2000. Treatment of recycled kraft pulps with *Trichoderma reesei* hemicellulases and cellulases. *J. Biotechnol.* 78, 39-48.

Paquot, M., Godin, F., Dumont de Chassart, Q., 1994. Effects of electrokinetic characteristics on the formation of a protein-microcrystalline cellulose complex. *Lebensm. Wiss. u. Technol.* 27, 11-15.

Pala, H., Lemos, M.A., Mota, M., Gama, F.M., 2001. Enzymatic upgrade of old paperboard containers. *Enzyme Microb. Technol.* 29, 274-279.

Pinto, R., Moreira, S., Mota, M., Gama, M., 2004. Studies on the Cellulose-Binding Domains Adsorption to Cellulose. *Langmuir* 20, 1409-1413.

Pinto, R., Carvalho, J., Mota, M., Gama, M., 2006. Large Scale Production of Cellulose-Binding Domains. Adsorption Studies Using CBD-FITC Conjugates. *Cellulose* (Accepted for publication), (Available: <http://www.springerlink.com/link.asp?id=6107175714463362>).

Reinikainen, T., Takkinen, K., Teeri, T.T., 1997. Comparison of the adsorption properties of a single-chain antibody fragment fused to a fungal or bacterial cellulose-binding domain. *Enzyme Microb. Technol.* 20, 143-149.

Senior, D.J., Hamilton, J., 1993. Xylanase treatment for the bleaching of softwood kraft pulps: the effect of chlorine dioxide substitution. *TAPPI J.* 76, 200-206.

Seo, Y.B., Shin, Y.C., Jeon, Y., 2000. Enzymatic and mechanical treatment on chemical pulp. *TAPPI J.* 83, 1-9.

Silvy, J., Romatier, G., Chiodi, R., 1968. Méthodes pratiques de contrôle du raffinage. *Revue A.T.I.P.* 22, 31-53.

Stork, G., Pereira, H., Wood, T.M., Düsterhöft, E.M., Toft, A., Puls, J., 1995. Upgrading recycled pulps using enzymatic treatment. *TAPPI J.* 78, 79-88.

Suurnäkki, A., Kantelinen, A., Buchert, J., Viikari, L., 1994. Enzyme-aided bleaching of industrial softwood kraft pulps. *TAPPI J.* 77, 111-116.

van Oss, C.J., Chaudhury, M.K., Good, R.J., 1988a. Interfacial Lifshitz-van der Waals and Polar Interactions in Macroscopic Systems. *Chem. Rev.* 88, 927-941.

van Oss, C.J., Good, R.J., Chaudhury, M.K., 1988b. Additive and nonadditive surface tension components and the interpretation of contact angles. *Langmuir* 4, 884-891.

Figures

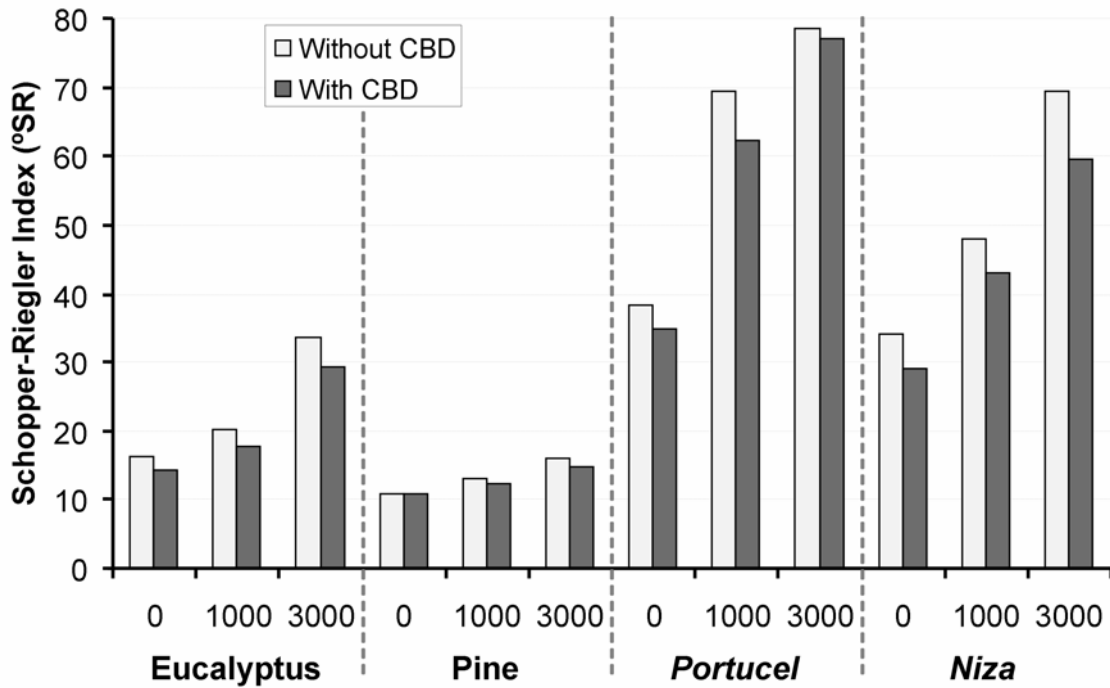


Figure M4.1. Schopper-Riegler index obtained for the several paper fibers studied.

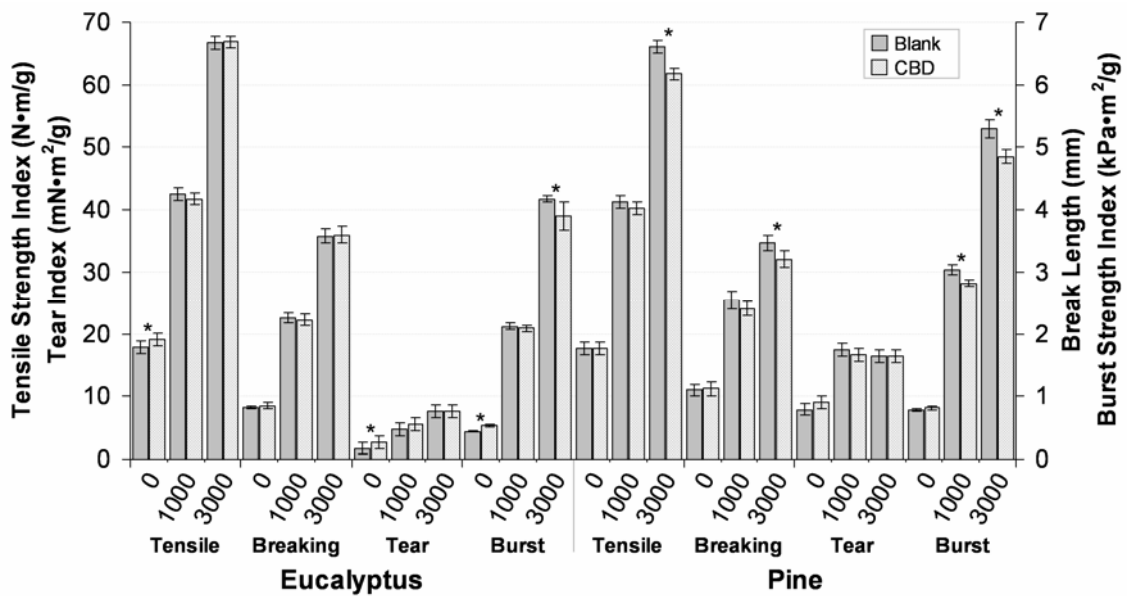


Figure M4.2. Physical properties variation between the CBD treated and untreated (control), at three different beating revolutions (0, 1000 and 3000), of virgin (primary) fibers, with the respective confidence interval at 95%. The stars (*) indicates a statistic meaningful variation ($p < 0.05$).

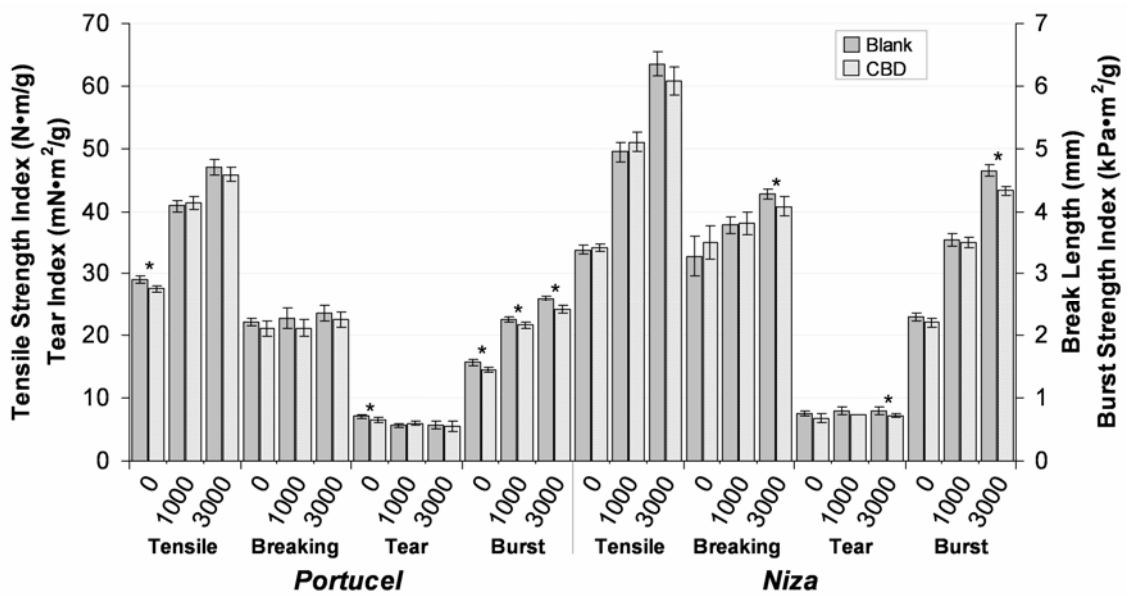


Figure M4.3. Physical properties variation between the CBD treated and untreated (control), at three different beating revolutions (0, 1000 and 3000), of recycled (secondary) fibers, with the respective confidence interval at 95%. The stars (*) indicates a statistic meaningful variation ($p < 0.05$).

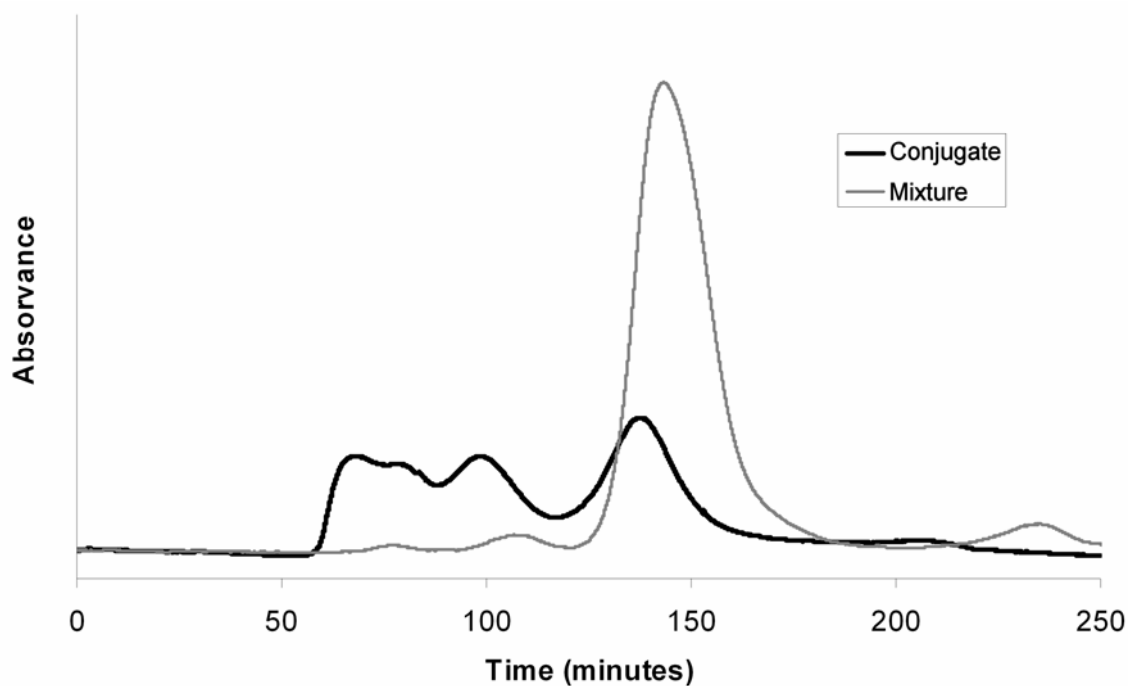


Figure M4.4. Size exclusion chromatography of the CBD-lysozyme conjugate and of a mixture of the two proteins.

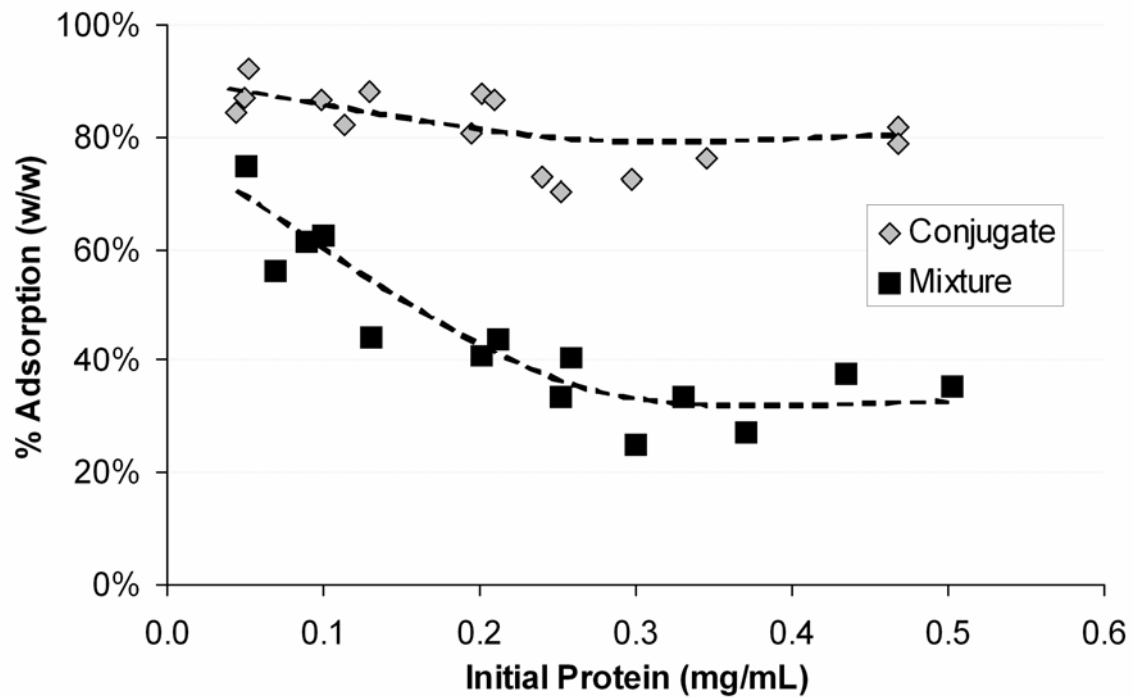


Figure M4.5. Adsorption, on Whatman CF11, of CBD in mixture or conjugated with lysozyme, using the same CBD to lysozyme molar ratio.

Tables

Table M4.1. Water retention value (WRV) obtained for the fibers used (\pm confidence interval at 95%).

		WRV (g/g)		
		0	1000	3000
Eucalyptus	Blank	0.78 \pm 0.01	1.12 \pm 0.02	1.38 \pm 0.02 ^a
	CBD	0.78 \pm 0.01	1.14 \pm 0.01	1.44 \pm 0.02 ^a
Pine	Blank	0.91 \pm 0.01 ^a	1.21 \pm 0.01 ^a	1.46 \pm 0.01
	CBD	0.93 \pm 0.01 ^a	1.24 \pm 0.01 ^a	1.47 \pm 0.02
Portucel	Blank	1.19 \pm 0.01 ^a	1.41 \pm 0.02	1.55 \pm 0.01 ^a
	CBD	1.22 \pm 0.01 ^a	1.40 \pm 0.02	1.62 \pm 0.01 ^a
Niza	Blank	1.08 \pm 0.02 ^a	1.30 \pm 0.02 ^a	1.59 \pm 0.02 ^a
	CBD	1.11 \pm 0.01 ^a	1.33 \pm 0.01 ^a	1.49 \pm 0.01 ^a

^a Means statistically different ($p < 0.05$)

Table M4.2. Permeability of papersheets obtained for the cellulose types used (\pm confidence interval at 95%).

		Permeability ($\mu\text{m}/\text{Pa}/\text{s}$)		
		0	1000	3000
Eucalyptus	Blank	53.4 \pm 0.7 ^a	40.4 \pm 1.2 ^a	12.3 \pm 1.4
	CBD	54.4 \pm 0.4 ^a	43.7 \pm 1.9 ^a	12.2 \pm 1.3
Pine	Blank	60.9 \pm 0.2 ^a	54.5 \pm 1.0	32.4 \pm 1.5 ^a
	CBD	60.4 \pm 0.1 ^a	54.1 \pm 0.6	37.0 \pm 1.8 ^a
Portucel	Blank	10.7 \pm 0.5 ^a	1.88 \pm 0.12	0.62 \pm 0.02 ^a
	CBD	16.2 \pm 1.4 ^a	1.80 \pm 0.10	0.43 \pm 0.03 ^a
Niza	Blank	11.6 \pm 0.3 ^a	3.18 \pm 0.10 ^a	1.16 \pm 0.02 ^b
	CBD	13.6 \pm 0.3 ^a	3.53 \pm 0.12 ^a	1.94 \pm 0.09 ^b

^a Means statistically different ($p < 0.05$); ^b Means with different variances

Table M4.3. Physical properties of the Portucel fibers without treatment (Blank) and CBD or conjugate treated (\pm confidence interval at 95%).

	Blank	CBD	Conjugate
Schopper-Riegler Index (°SR)	48.4 \pm 5.1 ^a	40.5 \pm 5.1 ^a	43.6 \pm 5.7 ^a
Permeability ($\mu\text{m}/\text{Pa}/\text{s}$)	6.78 \pm 0.25 ^a	8.12 \pm 0.19 ^a	9.27 \pm 0.29 ^a
Tensile Strength Index (N·m/g)	38.1 \pm 0.9	38.3 \pm 0.7	36.7 \pm 0.6
Breaking Length (mm)	2.49 \pm 0.13	2.42 \pm 0.11	2.36 \pm 0.12
Tear Index (mN·m ² /g)	2.78 \pm 0.37	2.56 \pm 0.38	2.94 \pm 0.46






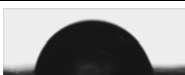
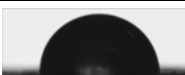
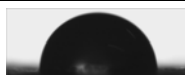
^a Means statically different ($p < 0.05$)

Table M4.4. ZETA-potential measurements (mV), by streaming potential, of *Portucel* and *Eucalyptus* (two different refinement conditions) fibers, without treatment (Blank) and CBD or conjugate treated, and of *Sigmacell* fibers made by electrophoretic mobility (\pm confidence interval at 95%).

		Fiber batch 1		Fiber batch 2		
		Blank	CBD	Blank	CBD	Conjugate
<i>Portucel</i>	0 PFI	-60.3 \pm 0.5	-58.5 \pm 0.8 ^(a)	-40.5 \pm 1.1	-38.3 \pm 0.5 ^(b)	-38.1 \pm 0.5 ^(c)
<i>Eucalyptus</i>	0 PFI	-81.2 \pm 1.2	-59.7 \pm 0.6 ^(a)	-71.3 \pm 1.0	-65.2 \pm 0.6 ^(b)	-57.8 \pm 0.7 ^(c)
	3000 PFI	—	—	-52.7 \pm 0.6	-53.6 \pm 1.0 ^(b)	-54.3 \pm 0.2 ^(c)
<i>Sigmacell</i>	—	—	—	-11 \pm 1	10 \pm 1 ^(d)	40 \pm 1 ^(d)

Assays made with a mass of protein per gram of dry cellulose of (a) 2 mg, (b) 2.24 mg, (c) 4 mg and (d) 13 mg.

Table M4.5. Surface tension components (γ^{LW} , γ^+ and γ^- , mJ/m²) and degree of hydrophobicity (ΔG_{cwc} , mJ/m²) for cellulose fibers without treatment (Blank) and CBD or conjugate treated, obtained by contact angle. Examples of contact images of water drops are also shown. The protein concentration used are as referred in Table M4.4.

		Blank	CBD	Conjugate
Eucalyptus	γ^{LW}	39.8	39.8	–
	γ^+	0.82	0.83	–
	γ^-	44.3	46.5	–
	ΔG_{cwc}	 21.2	 23.9	–
Sigmacell	γ^{LW}	38.7	39.7	40.0
	γ^+	0.91	0.69	1.10
	γ^-	45.5	49.4	11.9
	ΔG_{cwc}	 22.9	 28.0	 -31.1
Portucel	γ^{LW}	41.3	41.7	41.2
	γ^+	3.03	4.61	3.90
	γ^-	1.52	0.04	0.23
	ΔG_{cwc}	 -56.7	 -62.7	 -62.3